May 2017

Functional Roles of Matrix Metalloproteinases in Bone Metastatic Prostate Cancer

Jeremy S. Frieling
University of South Florida, jeremy.frieling@ncf.edu

Functional Roles of Matrix Metalloproteinases in Bone Metastatic Prostate Cancer

by

Jeremy S. Frieling

A dissertation submitted in partial fulfillment
of the requirements for the degree of
Doctor of Philosophy
with a concentration in Cancer Biology
Department of Cell Biology, Microbiology, and Molecular Biology
College of Arts and Sciences
University of South Florida

Major Professor: Conor C. Lynch, Ph.D.
Wenlong Bai, Ph.D.
Srikumar Chellappan, Ph.D.
John M. Koomen, Ph.D.

Date of Approval:
May 22, 2017

Keywords: PTHrP, IGF, osteoblast, osteoclast, skeletal malignancy, MMP

Dedication

Dedicated to Friends and Family:

I would especially like to thank my parents, Steve and Brandy Frieling, for their unyielding love and support and for always convincing me to stay the course. Next I must thank my sister, Daiquiri, who has been a best friend to me for as long as I can remember. I would also like to thank my grandparents, Joyce and Claude Massett, and my aunt Sherri. You have all inspired me and helped along this journey. And I could never forget to mention two gentle and loving Great Danes, Noah and Moses, and their rambunctious successor, Zorro. Thanks for the hugs, the laughter, and the broken bones and bruises….Zorro. Finally, I would like to dedicate this work to the Moffitt patients who bravely fight this terrible disease day in and day out. Your courage keeps me motivated even on the most trying of days.

Thank You.

Acknowledgement

First, I owe immense thanks to my mentor, Dr. Conor Lynch, for his incredible guidance and training. His attitude, understanding, and respect for others creates an environment that I look forward to being a part of every day, and his patience and sincere dedication to training have allowed me to grow and advance as a scientist and a person. I am also grateful to my past and present committee members: Dr. Wenlong Bai, Dr. Srikumar Chellappan, Dr. John Koomen, and Dr. Lori Hazlehurst. Your thoughtful suggestions and assistance have helped advance both the project and my education. I would also like to thank Dr. Florent Elefteriou for generously offering his time to serve as the external committee chair.

Next, I would like to acknowledge my "lab family:" Sinéad Aherne, Arturo Araujo, Lizzie Atomi Pamen, Leah Cook, Chen Hao Lo, Jeremy McGuire, Gemma Shay, Marilena Tauro, and T.J. Utset-Ward. Your suggestions, critiques, and friendships are priceless. I absolutely must thank Maria Hernandez for helping schedule meetings, finding lost orders, listening to my problems, providing brownies, and offering her advice. I would also like thank my fellow Cancer Biology students and the Cancer Biology Student Organization for your support over the years.

The expertise of the Moffitt Core Facilities was essential to these studies and furthering my knowledge of valuable technologies. I would especially like to acknowledge Victoria Izumi of the Proteomics Core, Mikalai Budzevich of the Small Animal Imaging Lab, and Aga Kasprzak, Joe Johnson, and Jonathan Nguyen of the Microscopy Core for routinely going above and beyond expectations.

Finally, I will be forever grateful to the Cancer Biology PhD Program and the opportunities it has provided me. In addition to program director, Dr. Ken Wright has been a fantastic adviser since I entered the program, and Cathy Gaffney is surely one the hardest working people at Moffitt keeping all the graduate students in good standing. Without your assistance, this day would not be possible. Thank You!

Table of Contents

List of Tables

List of Figures

Abstract

Skeletal metastasis is a lethal component of many advanced cancers including prostate, the second most common cancer among men. Patients whose prostate cancer is localized and detected early benefit from multiple treatment options ranging from active surveillance to radiation and surgery, resulting in a 5-year survival rate of nearly 100%. Unfortunately, the prognosis and survival for patients with advanced metastatic disease is much worse due to the highly aggressive nature of the disease and a paucity of treatment options. Understanding the mechanisms and interactions that occur between metastatic cancer cells and the bone will enable the future treatment landscape for bone metastatic prostate cancer to expand, thereby improving patient outcomes. Our current knowledge of how metastatic prostate cancer cells interact with the bone is summarized in a model known as the "vicious cycle." Numerous fundamental vicious cycle factors have been identified, including parathyroid hormone-related protein (PTHrP), while additional elements, such as matrix metalloproteinases (MMPs), are progressively being discovered and added to the model.

PTHrP is a critical regulator of bone resorption and augments osteolysis in skeletal malignancies. In Chapter 2, we report that the *mature $PTHrP_{1-36}$ hormone is processed by MMPs to yield a stable product, $PTHrP_{1-17}$*. $PTHrP_{1-17}$ retains the ability to signal through PTH1R to induce calcium flux and ERK phosphorylation but not cyclic AMP production or CREB phosphorylation. Notably, $PTHrP_{1-17}$ promotes osteoblast migration and mineralization *in vitro*, and systemic administration of $PTHrP_{1-17}$

augments ectopic bone formation *in vivo*. Further, in contrast to $PTHrP_{1-36}$, $PTHrP_{1-17}$ does not affect osteoclast formation/function *in vitro* or *in vivo*. Finally, immunoprecipitation-mass spectrometry analyses using $PTHrP_{1-17}$-specific antibodies establish that $PTHrP_{1-17}$ is indeed generated by cancer cells. Thus, MMP-directed processing of PTHrP disables the osteolytic functions of the mature hormone to promote osteogenesis, indicating important roles for this mechanism in bone remodeling in normal and disease contexts.

MMPs have traditionally been associated with cancer progression based on their extracellular matrix degrading activities. However, it has become evident that their regulation of non-extracellular matrix substrates can exert both contributive and protective effects during tumorigenesis. Previous studies of matrix metalloproteinase-3 (MMP-3) have demonstrated tissue dependent pro- and anti-tumorigenic effects, but despite elevated expression, its roles have not been explored in bone metastatic prostate cancer. In Chapter 3, we show that *tumor-derived MMP-3 contributes to prostate tumor growth in bone*. *In vitro*, we observe that silencing *MMP-3* reduces prostate cancer cell proliferation. Further, we found increased levels of IGFBP3, a known MMP-3 substrate, and decreased IGF-1R, ERK, and AKT phosphorylation in the *MMP-3* silenced cells. Notably, we also observe reduced tumor growth and proliferation in *in vivo* intratibial models when tumor-derived MMP-3 expression is silenced. These data suggest that increased MMP-3 expression by prostate cancer cells contributes to their proliferation in bone by regulating the activity of the IGF/IGF-1R signaling axis.

Taken together, our studies indicate that MMPs possess important functional roles in bone metastatic prostate cancer. We believe that elucidation of these mechanisms and their contributions to the vicious cycle of bone metastasis will offer novel opportunities to design effective therapeutic treatment options.

Chapter 1. Clinical and Biological Understanding and Study of Bone Metastatic Prostate Cancers

1.1 Prostate Cancer and Bone Metastasis

Prostate cancer is the second most common cancer in American men with approximately 1 in 7 men being diagnosed during their lifetimes [1]. With an aging population, the incidence of prostate cancer is forecasted to continue rising. The majority of prostate cancers are adenocarcinomas. These cancers originate from the prostate epithelia-comprising basal cells or luminal cells. In addition, some prostate cancers arise from the neuroendocrine cells of the prostate [2]. Though rare, neuroendocrine prostate cancers are more aggressive and challenging to treat than adenocarcinomas. It is also possible for one patient to have more than one type of prostate cancer [2]. Patients whose disease is detected at an early stage benefit from a range of treatment strategies including radiotherapy and prostatectomy, resulting in 5 year survival rates near 100% [3, 4]. However, the clinical reality is that many men present with advanced stages of the disease where 5 year survival rates are only 28% [4]. Currently, the main treatment option for men with metastatic cancer is hormone therapy. Historic contributions from Charles Huggins and Clarence Hodges in 1941 revealed that prostate cancer progression could be inhibited by removal of androgens [5]. These early observations paved the way for the development of androgen

Portions of this chapter have been previously published (Frieling et al., Cancer Control, 2015 Jan; 22(1): 109-20) and are utilized with permission of the publisher, CCJ (p 147).

deprivation therapy, either surgically through castration or chemically through the use of androgen inhibitors, which has remained the standard treatment for men with advanced disease for the past 70 years. Despite the remarkable initial response to androgen deprivation for men with advanced disease, it almost invariably progresses to a castration resistant state within 18-24 months [6].

1.1.1 **Castration Resistant Prostate Cancer (CRPC)**

Castration resistant prostate cancer (CRPC) is defined by disease progression that, despite androgen deprivation, is often indicated by rising levels of prostate specific antigen (PSA), an androgen receptor target [7]. The development of resistance to hormonal intervention and the causes of disease progression are not fully understood, though a number of mechanisms have been demonstrated, with the majority focusing on continued AR activity caused by AR variants. In addition, numerous mechanisms contributing to tumorigenesis including TMPRSS2/ERG fusion, PTEN mutation and loss, Nkx3.1 expression loss, and enhanced Egr1 activity have been described [8].

1.1.2 **Metastatic Castration Resistant Prostate Cancer (mCRPC)**

As the disease progresses, CRPC ultimately advances to metastatic castration resistant prostate cancer (mCRPC). Prostate cancer preferentially metastasizes to bone [9]. As the disease transitions from castration sensitive to castration resistant, the incidence of bone metastases increases, with more than 90% of mCRPC patients developing bone lesions [10, 11]. Patients with mCRPC have a poor prognosis and a predicted survival of less than 2 years from the initial time of diagnosis. Consequently, mCRPC is responsible for a significant portion of the 30,000 prostate cancer related deaths every year [1, 12]. Furthermore, symptomatic mCRPC patients are at a high risk

for skeletal related events (SRE) including spontaneous fracture, spinal cord compression, and hypercalcemia that are a source of significant pain and decreased quality of life [13]. Currently mCRPC is an incurable disease of major clinical significance.

1.2 Organotropism and Outgrowth of Metastases in Bone

1.2.1 The Metastatic Cascade

Metastasis from the primary site to a secondary site is a multi-step process, with each step presenting a unique hurdle for the disseminated cells to overcome. This series of events is termed the metastatic cascade [14]. Although it is technically an inefficient process with low probability of success, metastasis is a primary cause of cancer mortality. The process begins with tumor growth at the primary site. As the primary tumor expands and becomes vascularized, tumor cells begin to locally invade by adopting a more mesenchymal phenotype and breaching the basement membrane into the stroma. Following local invasion, tumor cells gain access to the vasculature and intravasate into the bloodstream or lymphatic system. Although the bloodstream provides a route by which the disseminated cells can travel to secondary organs and tissues, shear forces and susceptibility to anoikis create a hostile environment for circulating tumor cells. Tumor cells that survive in circulation will become lodged in capillaries, frequently in the lung, due to being significantly larger than erythrocytes and other blood cells (most cancer cells are >20 μm in diameter whereas the capillaries are 3 μm to 8 μm in inner diameter). Although it is poorly understood, some of these cells reach other organs such as the bone, with certain cancers metastasizing to secondary

sites more frequently than others [15]. To establish at the secondary site, the tumor cells must extravasate and form micrometastases. Micrometastases can be widely distributed, and recent evidence suggests that they occur early in tumor progression but may remain clinically undetectable [16]. Colonization and outgrowth of clinically detectable macrometastases is considered the final step in the metastatic cascade (reviewed by [14]).

1.2.2 **What is Bone?**

Bone is comprised of osteoblast-derived type I collagen that is mineralized by deposition of hydroxyapatite, a combination of magnesium, calcium, and phosphate ions. The resulting extracellular mineralized matrix is an extremely strong substance, with the collagen fibers imparting a degree of flexibility to avoid brittleness and fracture. Two major types of ossification (bone production) contribute to building the human skeleton. Intramembranous ossification and bone development originates from fibrous membranes and is responsible for producing flat bones like the skull and clavicle whereas endochondral ossification originates from hyaline cartilage and generates long bones such as the femur and tibia [17]. There are also two primary types of bone tissue, both of which are incorporated during intramembranous and endochondral ossification. Cortical bone (sometimes called compact bone) is dense and primarily structural or mechanical in nature while trabecular bone (sometimes referred to as cancellous or spongy bone) is metabolically active and is located within the bone marrow compartment.

The combination of 206 bones in our skeleton constitutes a framework for the other organs and tissues that make up the human body. Bone plays an important role

in organ protection, provides for the attachment of ligaments and tendons to yield locomotion, and acts as a reservoir for most of the body's calcium, magnesium, and phosphate. The bone marrow is also the primary site for hematopoiesis.

1.2.3 **Bone Stroma and Remodeling**

Given the crucial functions that the skeleton provides, remodeling and homeostasis are critical. Bone is continually remodeled at a rate of about ten percent per year [18]. Bone metabolism is part of routine skeleton maintenance, but the activity can also occur in response to a fracture or to meet the demands of mechanical loading and stimuli. Bone remodeling occurs in localized regions called basic multicellular units (BMU) [19]. Within the BMU exists a remarkable microcosm of specialized cells: osteoclasts, osteoblasts, and osteocytes. These cells reside beneath a bone remodeling compartment (BRC) canopy and must collaborate with each other to preserve the tightly regulated balance of bone destruction and formation during bone metabolism. If the balance is perturbed, the overall health of the skeleton is compromised and can result in diseases such as osteoporosis, Paget's disease, or cancer associated bone destruction/formation observed in bone metastatic carcinomas like breast and prostate, respectively.

Osteoclasts are the cells responsible for resorption of existing bone tissue. These cells form when three or more monocytic precursor cells fuse in response to macrophage colony-stimulating factor (M-CSF) and receptor activator of nuclear kappa B ligand (RANKL) cytokines secreted by neighboring osteoblasts [20]. Mature osteoclasts are defined as giant, multi-nucleated bone resorbing cells (approximately 50-100 μM in diameter), and express high levels tartrate-resistant acid phosphatase

(TRAcP) [21]. Osteoclasts that are recruited to the bone surface polarize to form a ruffled border, which increases the cytoplasmic interface with the bone, and an F-actin rich sealing zone. Within the sealing zone, an ATP dependent proton pump creates an acidic environment, and enzymes including MMPs and cathepsin K are secreted to facilitate localized degradation of the underlying bone matrix [21, 22]. The bi-products of degradation include cleaved collagen fragments along with latent growth factors released from the matrix. The duration of the bone resorption phase is approximately 3 weeks [23].

Osteoblasts function to produce new bone matrix in the areas of previous resorption. They are derived from mesenchymal stem cells and differentiate in response to bone morphogenetic proteins (BMPs), Wnt/β-catenin signaling cues, and parathyroid hormone-related protein (PTHrP) [24-26]. During bone resorption, osteoblasts are recruited to the BMU where they secrete type I collagen and other matrix proteins to form a non-mineralized layer of osteoid, the first step in synthesizing new bone. As the layers of osteoid accumulate, increased expression of osteopontin is observed concomitantly with mineralization [25, 27]. Comprising about 90% of adult bone, type I collagen fibrils contribute to the strength and integrity of the bone. Complete mineralization occurs over a 3-4 month period [23]. Subsequent to bone formation, or apposition, some osteoblasts become bone lining cells, where they acquire a more flattened shape to permanently reside on the bone surface, mostly on trabeculae. Bone lining cells possess important functions such as controlling calcium levels, generating signals to osteoclasts, and forming the BRC during remodeling processes [22, 28]. Other osteoblasts are retained within the bone matrix where they

terminally differentiate into mechanosensory osteocytes [22]. Osteocytes are multifunctional cells that constitute up to 95% of all bone cells. Though isolated within the bone, osteocytes communicate efficiently with osteoblasts and osteoclasts via to a sophisticated network of canaliculi. This network allows osteocytes to serve as sentinels of the bone, detecting fractures or changes in mechanical loading to regulate bone metabolism. As the skeleton ages, there is an increase in osteocyte apoptosis, possibly induced by hypermineralization of the perilacunar matrix, leading fewer viable osteocytes. This reduction in viable osteocytes is believed to contribute to age-related skeletal disorders such as osteoporosis [29].

1.2.4 **Osteotropism**

An unsolved question surrounding metastasis is why prostate cancer has such a predilection for the bone microenvironment. More than a century ago, Stephen Paget formulated the “seed and soil” hypothesis to address this question based on his studies of breast cancer patient case histories [30]. The hypothesis suggested that metastasis requires “fertile soil” for outgrowth and that metastasis is a challenging process that begins long before the “seed” meets the “soil.” Paget’s hypothesis was challenged by James Ewing in the 1920s, proposing that metastasis was instead dependent on anatomy, vasculature, and lymphatics [31]. Metastasis by anatomy would become the accepted model until the 1970s when modern experiments rekindled interest in the “seed and soil” hypothesis, notably observations that circulating tumor cells reach the vasculature of all organs, but only certain organs are receptive for metastasis [14, 32]. In reality, prostate to bone metastasis occurs by a blend of both hypotheses, metastasizing first to the pelvic lymph node and then to sites in the bone including iliac

crests, sacrum wings, L1-L5 vertebrae, T8-T12 vertebrae, ribs, manubrium, humeral heads, and femoral necks [33]. While 15-30% of prostate to bone metastases are due to cells traveling through the Batson's plexus to the lumbar spine, it is clear that molecular factors such as chemokines and integrins underpin the propensity for prostate cancer cells to metastasize to the skeleton [13].

1.2.5 **Osteomimicry**

A recurring theme in bone metastasis is the hijacking of normal bone mechanisms by tumor cells. The concept of "osteomimicry" is one where bone metastatic prostate cells acquire the ability to produce proteins that are normally restricted to bone cells, such as osteoblasts, in order to survive and proliferate in the otherwise restrictive bone microenvironment [34]. A number of genes normally expressed in bone have been detected in prostate cells including osteocalcin, osteopontin, bone sialoprotein, osteonectin, RANK, RANKL, and PTHrP [34-37]. Interestingly, the expression of these genes seems to be associated with the metastatic capacity of the cells. Studies in both PC3 and LNCaP have shown that osteonectin expression is highest in more invasive and metastatic sublines including the LNCaP metastatic variant, C4-2B. Immunohistochemical analyses of patient-derived specimens support these findings, indicating that osteonectin protein levels were elevated in metastatic foci from bone compared to soft tissue prostate metastases including the bladder and liver [35]. In addition to changes in gene expression, prostate tumor cells may adopt biological activities specific to bone cells. *In vitro* studies indicate that human C4-2B prostate tumor cells are capable of depositing hydroxyapatite and contributing to mineralization, a common feature of the sclerotic lesions observed *in vivo* [36].

1.2.6 **Understanding the Tumor Microenvironment**

1.2.6.1 ***Pre-Metastatic Niche and Exosomes***

Primary tumor derived factors have been implicated in the development of pre-metastatic niches in distant organs [38]. Through a series of *in vivo* experiments, it was illustrated that conditioned media derived from highly metastatic cancer cell lines such as B-16 melanoma cell lines could stimulate the mobilization of bone marrow derived VEGFR-1+ VLA4+ Id3+ hematopoietic precursor cells (HPCs) from the bone marrow to developing pre-metastatic niche sites including lung, liver, spleen, kidney, and testis [38]. Recently, cancer derived exosomes have been implicated as the mechanism facilitating long distance tumor-stroma interactions and initiating the pre-metastatic niche [39]. Exosomes are a micro-vesicle measuring 30-100nm and known to carry a variety of cargo including functional proteins, mRNA, and miRNA [40]. In the context of pre-metastatic niche formation, B16-F10 derived exosomes have been labeled and shown to “home” to common sites of melanoma metastasis. Further, in the pre-metastatic niche, exosomes can educate bone marrow derived cells to support metastatic tumor growth via the horizontal transfer of the c-MET protein [41].

Exosome shedding has also been demonstrated in prostate cancer with studies demonstrating the presence of microvesicles termed “oncosomes” (0.5-5μm) in prostate cancer conditioned media. Oncosomes contain a variety of signal transduction proteins including Akt and Src, as well as miRNAs, and can interact with both tumor and stromal cells to elicit disease promoting responses [42, 43]. Additionally, there is a correlation between a Gleason score higher than 7 and the number of oncosomes present in patient plasma [44]. Based on these findings it is plausible that prostate cancer derived

exosomes can play a role in the formation of pre-metastatic niches in the bone microenvironment, and emerging evidence suggests that prostate cancer cells homing to the bone microenvironment can occupy the endosteal and/or vascular niches.

1.2.6.2 ***SDF-1(CXCL12)/CXCR4 and similar signaling axes***

Bone is the home of regulatory sites for hematopoietic stem cells (HSCs); these cells are localized to the vascular (inner bone marrow) and endosteal (outer bone marrow) niches where they either await hematopoietic demand or reside in a quiescent state [45]. Disseminated tumor cells (DTCs) have been found in the bone marrow niches where they either form metastases or remain dormant. One well defined signaling axis implicated in metastasis and homing to the niche is that between stromal cell-derived factor-1 (SDF-1)/C-X-C chemokine motif 12 (CXCL12) and its receptor C-X-C chemokine receptor type 4 (CXCR4), a system normally utilized by HSCs [46]. CXCL12 expression is increased in the pre-metastatic niche, and studies in prostate cancer have demonstrated that tumor cells with high bone homing capacity express CXCR4 and CXCR7 to parasitize the HSC niche (Figure 1A-B). Furthermore, the expression of CXCR4 and CXCR7 correlates with poor prognosis [38, 47, 48]. Additional axes including MCP-1/CCR2 and CXCL16/CXCR6 have also been found to contribute to prostate cancer progression through increases in proliferation, migration, and invasion [49, 50].

1.2.7 **The Vicious Cycle**

Once the tumor cells have disseminated and homed to the bone, their survival and growth are largely dependent on a permissive microenvironment. Exosomes and other signaling cues from the primary tumor can help “prepare the soil” prior to

colonizing the bone, however metastatic tumor cells can also directly impact the bone stroma to facilitate invasion and proliferation via the secretion of various growth factors, cytokines, and hormones. In turn, osteoblasts and osteoclasts can interact with the tumor cells. These interactions between the tumor cells, osteoblasts, and osteoclasts are summarized in a classic mechanism called the “vicious cycle.”

1.2.7.1 *Classical Explanation of Tumor-Bone Cellular Interactions*

Prostate to bone metastases are characterized by areas of mixed osteogenesis and osteolysis that give rise to painful lesions [51]. Numerous factors including PTHrP, IL-1, IL-6, and IL-11 are highly expressed by tumor cells and have been shown to interact with osteoblasts. Aside from their osteogenic activities, osteoblasts are stimulated by these tumor-derived factors to produce the cytokine RANKL. It is well known that RANKL is a crucial molecule for osteoclast differentiation and therefore contributes to the extensive bone remodeling seen in skeletal malignancies. Besides destruction of the bone, osteoclast mediated bone resorption releases a multitude of bone derived factors such as TGF-β, insulin growth factor (IGF), platelet derived growth factor (PDGF), and fibroblast growth factor (FGF) from the bone matrix. These factors are subject to regulation in the local tumor microenvironment where they can provide positive feedback via interaction with their respective receptors on the surface of tumor cells. These interactions contribute to tumor cell proliferation and continued production of tumor derived factors allowing the cycle to repeat [52].

1.2.7.2 *Integrating New Discoveries into the Vicious Cycle*

The vicious cycle is continually evolving to include additional cell types, cytokines, proteases, and new therapies (Figure 1-1 C) [53-56]. Several studies from

our group have shown contributory roles for highly expressed host matrix metalloproteinases (MMPs) in the vicious cycle, including the regulation of bone-derived latent TGF-β and VEGF-A bioavailability by MMP-2 and MMP-9, and the generation of a soluble form of RANKL by MMP-7 which promotes osteoclastogenesis and mammary tumor induced osteolysis *in vivo* [57-59]. In recent years, the interactions with immune cells have become an appreciated component of the metastatic cascade and an integral part of the vicious cycle. Bone marrow is a reservoir for a wide range of immune cells including macrophages, myeloid-derived suppressor cells (MDSCs), dendritic cells, and T-cells. Interestingly, T-cells have been shown to both stimulate and inhibit osteoclast formation, but the recruitment of T-regs to the bone marrow may actually inhibit osteoclastogenesis. MDSCs within the tumor-bone microenvironment suppress T-cells, release angiogenic, tumor promoting factors, and secrete TGF-β to promote tumor growth [60, 61]. It has also been shown that recruited MDSCs can differentiate into osteoclasts [62, 63]. Through these mechanisms, MDSCs can play major roles in the vicious cycle and promote tumor induced bone disease. Similarly, macrophages can polarize based on cues from the microenvironment leading to anti (M1) and pro (M2) tumorigenic phenotypes [64]. M2 polarized macrophages have been shown to assist in immune evasion and tumor promotion by secreting anti-inflammatory cytokines and proteinases including MMP-9 [64, 65].

1.3 Approved Therapies for Bone Metastatic Prostate Cancer

Despite remaining incurable with most treatment options being palliative, recent discoveries and improved understanding of the molecular mechanisms underlying mCRPC have allowed the therapeutic landscape for mCRPC treatment to rapidly

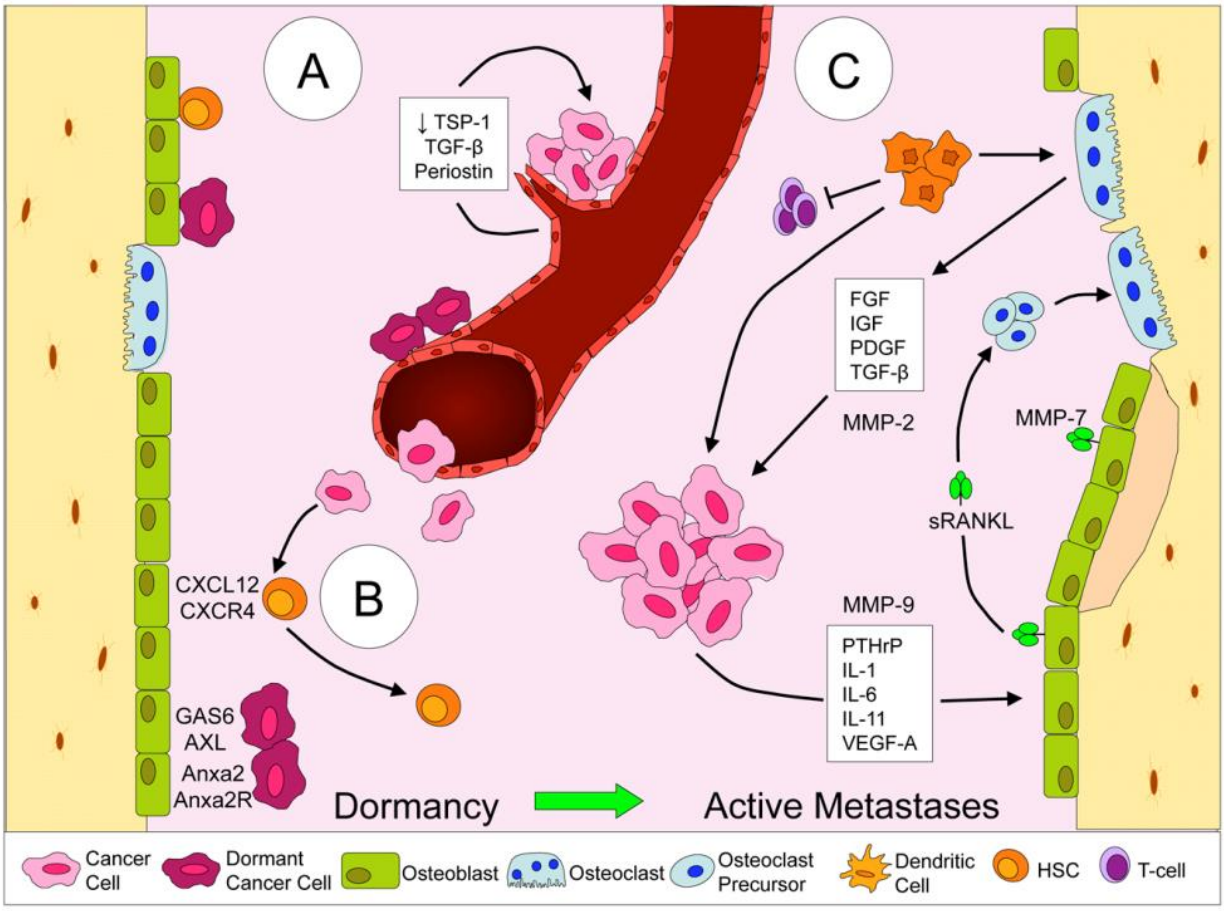

Figure 1-1. Dormancy and the "Vicious Cycle" of Bone Metastasis

*(**A**) Disseminated tumor cells can home to the vascular niche and cluster on stable endothelium. Decreased expression of thrombospondin-1 combined with activation of transforming growth factor β and periostin in areas of "sprouting" vasculature can result in the outgrowth of tumor cells. (**B**) Cancer cells may also home to the endosteal niche via mechanisms such as chemokine motif 12/chemokine receptor 4 where they compete with quiescent hematopoietic stem cells for osteoblast interaction. Subsequently, the cancer cells can be maintained in a dormant state via interactions with GAS6 and ANXA-2 expressing niche osteoblasts or proliferate into metastases. (**C**) A "vicious cycle" occurs between tumor cells and other cells of the bone microenvironment. Factors secreted by the tumor cells act on osteoblasts, leading to the increased production of additional factors into the microenvironment, providing positive feedback to the cancer cells. Matrix metalloproteinases 2, 7, and 9 contribute to the vicious cycle by regulating factors such as vascular endothelial growth factor A, RANKL, and transforming growth factor β, whereas myeloid-derived suppressor cells contribute by releasing pro-tumorigenic factors, suppressing T-cells, and differentiating into osteoclasts.*

expand. These new therapeutic strategies include both broad spectrum and targeted therapies that will ultimately have a positive impact on overall survival for these patients within the next decade (Table 1-1). The expansion began with docetaxel in 2004, which at the time was the first therapy to provide improved survival to mCRPC patients [66, 67]. However, many patients develop resistance to this chemotherapy. To combat this

issue, five new agents have received FDA approval to treat mCRPC since April 2010: abiraterone acetate, enzalutamide, cabazitaxel, radium-223, and sipuleucel-T [68]. Below is a discussion of these newly approved agents that target the cancer and host compartments.

1.3.1 **Hormone Therapies**

One of the defining measures of mCRPC is resistance to androgen deprivation therapy. The mechanism of castration resistance is not fully understood, but significant inroads have been made. For example, prostate cancer cells circumvent castration by overexpressing and increasing the sensitivity of the AR to residual androgens, acquiring AR gene mutations leading to gain of function or promiscuous ligand interactions, splice variants resulting in constitutive AR activation or ligand independent receptors, and post-translational modifications affecting the stability, localization, and activity of the receptor [69]. Alternative methods utilized by prostate cancer cells to synthesize dihydrotestosterone (DHT) have also been shown to circumvent androgen deprivation methods [70-72]. Efforts to target these mechanisms have resulted in newly FDA approved androgen deprivation therapy (ADT) options such as abiraterone acetate that inhibits the activity of the CYP17A1 enzyme, thereby preventing androgen synthesis. Abiraterone has been successful in improving the overall survival and radiographic progression free survival of men with mCRPC [73, 74]. Another therapeutic strategy for preventing androgen utilization by the mCRPC cells is by targeting the AR directly with reagents such as flutamide, nilutamide, and bicalutamide. Recently, enzalutamide was approved for the treatment of mCRPC in a post-docetaxel setting [75, 76]. Enzalutamide has a superior affinity to the AR compared to other AR antagonists and

works by preventing nuclear translocation of the receptor, DNA binding, and recruitment of co-activators of the AR to not only increase overall survival but also delay the onset of SREs [77-79]. Recent results from an ongoing phase III trial demonstrated impressive activity of enzalutamide in chemotherapy naïve patients, potentially leading to future FDA approval of enzalutamide for this subset of mCRPC patients (NCT01212991) [80, 81].

1.3.2 **Chemotherapies**

In addition to ADT strategies, taxane derived chemotherapies are a mainstay treatment for mCRPC. Docetaxel has remained the standard therapy for mCRPC since 2004 [66, 67]. Cabazitaxel is a more recent derivative of the taxoid family that has shown increases in overall survival, improvements in progression free survival, and improved PSA response rates in men with mCRPC [82, 83]. Cabazitaxel was approved for the treatment of post-docetaxel mCRPC patients by the FDA in 2010 [84]. Additional clinical trials studying the effectiveness of cabazitaxel as first-line therapy and in combination with ADT agents like enzalutamide are ongoing (NCT02254785, NCT02522715).

1.3.3 **Microenvironment Targeted Therapies**

Given the heterogeneity of mCRPCs and likelihood of ADT/chemotherapy resistance, targeting the genetically stable host microenvironments that support the mCRPC instead of the cancer cells themselves represents an attractive treatment approach. Immune evasion is a hallmark of cancer progression and the goal of recently approved sipuleucel-T is to make mCRPCs more visible to cytotoxic T-cells [85, 86] Sipuleucel-T is an autologous immunotherapy approved for treatment of asymptomatic

or minimally symptomatic mCRPC due to a lack of evidence showing that it directly impacts the cancer [87]. Sipuleucel-T harnesses the properties of the patient's own immune system by collecting peripheral blood mononuclear cells and activating them *ex vivo* by exposure to a fusion protein consisting of prostatic acid phosphatase (PAP) and GM-CSF with PAP being a protein commonly expressed by prostate cancer cells. Patients receive three separate infusions of the activated cells at two-week intervals to generate PAP expressing dendritic cells that in turn activate T-cells to recognize and eliminate PAP expressing prostate cancer cells [85]. Sipuleucel-T is the only FDA approved immunotherapy to improve survival in prostate cancer, however increasing concern over a lack of anti-tumor responses in clinical practice suggests that additional studies to identify patients best suited for Sipuleucel-T may be needed [88, 89].

The majority of mCRPCs arise in the bone matrix where they induce extensive bone remodeling by stimulating osteoblasts and osteoclasts. The process not only promotes the growth of the mCRPCs via the solubilization of bone matrix sequestered growth factors but also causes the patient significant pain and SREs such as pathological fracture. Therefore, preventing cancer-bone interaction has been a major focus for several decades. Bisphosphonates such as zoledronic acid, are reagents that can "stick" to bones undergoing remodeling and upon resorption by osteoclasts induce apoptosis thereby limiting the amount of cancer induced bone disease [90]. In the clinic, zoledronic acid has demonstrated a benefit for mCRPC patients by decreasing the time to SRE incidence [91]. However, although zoledronic acid lowered disease morbidity, no increase in overall survival has been demonstrated. Receptor activator of nuclear kappa B ligand (RANKL) is a molecule that is critical for the maturation and

activation of bone resorbing osteoclasts. Denosumab is a fully humanized monoclonal antibody that prevents RANKL interaction with the RANK receptor [92]. For patients with bone mCRPCs, clinical trials demonstrated a significant delay in the time to first SRE compared to zoledronic acid [93]. There is additional evidence that Denosumab may have direct effects on tumor burden, particularly tumor cells expressing the RANKL receptor, RANK [94, 95]. Further, pre-clinical *in vivo* animal studies have highlighted the efficacy of docetaxel/Denosumab combination treatment in increasing median survival times, suggesting that combinatorial approaches with Denosumab could significantly enhance the overall survival of men with mCRPC [96].

The most recent agent to receive FDA approval for mCRPC is radium-223 [97]. The bone seeking properties of radium-223 as well as other radiopharmaceuticals make them particularly useful in the treatment of bone metastases. Whereas most radiopharmaceuticals emit beta particles, radium-223 emits alpha particles to deliver more localized radiation (<100 μm distance) to induce localized cell death via DNA damage [98]. In a study of men with mCRPC previously treated with radiotherapy, radium-223 showed improved overall survival, time to PSA progression, and reduced alkaline phosphatase levels (measure of bone remodeling). In addition, radium-223 delays the time to first SRE [99], whereas previous radiopharmaceuticals used to treat mCRPC were only effective at reducing pain. Therefore, radium-223 represents an important step forward for the field [97].

1.3.4 **Ongoing Clinical Challenges**

Although several new cancer and microenvironment specific therapies are under development to treat prostate cancers, there are areas for improvement, particularly

with screening and the detection of metastases. While early detection is clearly the best scenario for successful treatment, a significant number of men will initially present with advanced prostate cancer harboring occult metastases. As we learn more about the disease, additional challenges are also emerging such as the discovery of disseminated tumor cells (DTCs) that have developed mechanisms to metastasize and remain dormant in the bone as well as the heterogeneous composition of most cancers.

Table 1-1. Approved Therapies for the Treatment of mCRPC

Drug	Target	Effect
Abiraterone acetate	CYP17A1	Reduces circulating testosterone levels
Cabazitaxel	Microtubules	Microtubule stabililzation, interrupts cell cycle
Denosumab	RANKL	Decreases bone resorption
Docetaxel	Microtubules	Microtubule stabilization, interrupts cell cycle
Enzalutamide	Androgen Receptor	Androgen receptor antagonism, prevents signaling
Radium-223	Bone	Localized radiation
Sipuleucel-T	Ex vivo activation of peripheral blood mononuclear cells	T-cell activation
Zoledronic Acid	Osteoclasts	Decreases bone resorption

1.3.4.1 *Detection of Bone Metastases*

Since prostate to bone metastases are primarily bone forming sclerotic lesions, bone scanning using technetium-99m-methyl diphosphonate is often used for diagnosis. Technetium-99m-methyl diphosphonate is particularly useful for detecting osteogenic

lesions due to the incorporation of the radionuclide tracer into regions of new bone formation by osteoblasts [100]. MRI and PET/CT are also used for detection. A recent trial comparing 18F-NaF PET/CT, 18F-FDG PET/CT, MRI, and technetium-99m-methyl diphosphonate identified strengths for each modality [101]. New approaches of combining modalities help to compensate for each method's weaknesses and increase sensitivity and accuracy. However, the ability to detect occult or micrometastases less than 5mm remains a limitation for all current methodologies [102]. Ongoing experimental imaging may yield improved imaging options. One such approach relies on dynamic contrast-enhanced (DCE) MRI or CT scans to visualize the vasculature of bone metastases. In addition to detecting metastases, this approach shows promise for measuring treatment responses before changes in tumor volume are noted [102].

1.3.4.2 ***Disseminated Tumor Cells and Dormancy***

Increasing evidence suggests that tumor cells disseminated from the prostate localize to the bone marrow niche and displace the resident hematopoietic stem cells (HSCs), where they either proliferate to form metastases or enter a state of dormancy [103]. Tumor cell dissemination appears to be an early event in prostate cancer, since patients who undergo prostatectomy may present with metastases many years later [104, 105]. DTCs reside in the bone marrow niche where they can remain dormant and resistant to chemotherapy for long time periods (>10 years) before emerging to form metastatic outgrowths [104]. Although most prostate cancer patients harbor DTCs, not all will develop metastases, suggesting that mechanisms exist to maintain DTC dormancy as well as promote awakening [105].

Recent work has identified several bone marrow dependent mechanisms as modulators of prostate cancer DTC dormancy. In the endosteal (outer bone marrow) niche, osteoblast expression of Annexin II (Anxa2) combined with expression of the Anxa2 receptor, Anxa2R, by HSCs is important in regulating HSC homing to the niche (Figure 1-1 A and B). Interestingly, Anxa2R expression is elevated in metastatic prostate tumor cells and as such, the Anxa2/Anxa2R axis can be hijacked to promote the homing of prostate tumor cells to the niche. Interrupting the interaction between Anxa2 and Anxa2R is sufficient to reduce tumor burden in the niche [106]. Continued studies have revealed that the ligation of Anxa2 with Anxa2R stimulates expression of the Axl receptor tyrosine kinase [107]. Axl, along with Tyro3 and Mer, are receptors for osteoblast expressed Growth arrest-specific 6 (GAS6) [108]. As was the case with Anxa2/Anxa2R, the GAS6/Axl interaction normally occurs between HSC and osteoblasts and is one mechanism of controlling HSC dormancy [109]. Interestingly, engagement of osteoblast expressed GAS6 and tumor cell expressed Axl yields a similar result including growth arrest and enhanced drug resistance in prostate cancer cells [107]. Following up on these observations, recently published data show that these activities may be specific to the Axl receptor compared to other GAS6 receptors, where a high ratio of Axl to Tyro3 expression encourages maintenance of a dormant state compared to reducing expression of Axl and increasing expression of Tyro3 which promoted awakening and outgrowth [108].

Interactions between osteoblasts and tumor cells are also important to DTC dormancy. Prostate cancer cells that bind with osteoblasts also upregulate expression of TANK binding kinase 1 (TBK1). *In vitro* and *in vivo* knockdown of TBK1 resulted in

decreased drug resistance, suggesting that TBK1 may also play a role in these processes [110]. A high p38/ERK ratio has been shown to maintain dormancy of squamous carcinoma cells derived from bone marrow, however interactions with microenvironment proteins such as fibrillar collagen can stimulate a switch to high ERK/p38 ratio and reverses dormancy [111]. Interestingly, bone marrow derived TGF-β2 has been implicated in maintaining dormancy of DTCs by p38 activation, and inhibiting either TGF-β receptor-1 (TGFBR1) or p38 leads to DTC proliferation and metastasis [112]. Similarly, bone morphogenetic protein 7 (BMP-7) was recently shown to trigger prostate cancer DTC dormancy in part by activation of p38 [113]. While much focus has been placed on the endosteal niche, the vascular niche also has implications for DTC dormancy. Using advanced imaging techniques, it has been shown that dormant DTCs also home to perivascular niches in the bone marrow and lung. These niches promote dormancy through thrombospondin-1 (TSP-1) expression, but dormancy is lost in regions of sprouting vasculature, due to a loss of TSP-1 and activation of TGF-β and periostin [114]. *In vivo* experiments in mice receiving bone marrow transplants revealed that fewer HSCs successfully engrafted in tumor bearing mice, suggesting that the tumor cells occupying the niche outcompete HSCs for residence. In addition, expansion of the endosteal osteoblast niche with parathyroid hormone (PTH) promotes metastasis, whereas decreasing the size of the niche using conditional osteoblast knockout models reduces dissemination [115]. Importantly, it was demonstrated that tumor cells can be forced out of the niche by using established HSC mobilization approaches, perhaps offering an opportunity for therapeutic intervention [115].

1.3.4.3 ***Heterogeneity***

Cancer cell heterogeneity is a challenging clinical component in many cancers including prostate cancer [116-118]. Greater heterogeneity not only facilitates the evolution of cancer's resistance to treatment but also gives the cancer a number of phenotypic strategies that allow for growth in a variety of microenvironments such as the bone. The question then arises as to how to treat heterogeneous cancers? Emerging studies suggest that most patients would be best served by therapies tailored not only towards cancer cells harboring common aberrations but also by therapies geared towards smaller clonal populations that could ultimately become dominant and resistant. Current National Comprehensive Cancer Network (NCCN) guidelines provide recommendations as to how to apply the sequence of existing therapies to mCRPC patients based on individual patient parameters. Recent studies suggest that altering the sequence or combination of existing therapies can have a profound impact on overall survival [119]. In order circumvent costly and time-consuming clinical trials assessing the combination and sequence alterations of the new line of targeted therapies currently in clinical trials, alternative approaches are required. The use of patient derived xenograft (PDX) models has been useful for translational studies in other diseases such as breast cancer [120]. PDX models are preferable to cell lines or organoid based models as these are subject to selective pressure during *in vitro* culturing and often correlate poorly with clinical outcome. However, difficulties encountered with the take rates of prostate cancer xenografts has traditionally resulted in a lack of available PDX models for prostate cancer research. Recently, a series of 21 prostate cancer PDXs were generated from numerous organ sites including primary,

adrenal, bladder, lymph node, liver, and bone [121]. These PDXs are serially passaged in mice and retain key histologic and molecular features of clinical disease. As a result, a better representation of clinical responses can be obtained. With regards to bone metastatic prostate cancer, 2 PDXs from bone metastases were established, but these do not spontaneously metastasize to the bone and varied take rates were observed with intratibial injections. Those that did successfully grow in bone recapitulated the clinical scenario by generating metastatic lesions that were osteoblastic, mixed, and/or osteolytic. The establishment of multiple prostate cancer PDXs will also make it possible to conduct “PDX Clinical Trials” which utilize multiple PDXs to test promising therapies or combinations of therapies in a format similar to a phase II clinical trial [121]. Outside of the wet lab, the integration of *in silico* computational models and genetic algorithms with individual patient derived biological data can also lead to the rapid optimization of therapy choice and sequence as well. Such computational models have been applied to bone metastatic prostate cancer and have been particularly useful at evaluating and predicting the responses for both existing and experimental therapies [56, 122].

1.4 Discussion

While there is emphasis on the need for therapies aimed at initiation of metastasis or eradication of DTCs, many patients will still present with active metastases. Therefore improved therapies for these patients via continued understanding of the vicious cycle should remain a priority, as the interactions between tumor and stromal cells in the vicious cycle offer many opportunities to intervene.

Present therapies like zoledronic acid and Denosumab interfere with the osteolytic component of the vicious cycle, however *there is a lack of therapies to inhibit the unique osteosclerotic component of prostate to bone metastases*. Many roles for specific MMPs have also been elucidated in the vicious cycle [53, 58, 59], and the development of MMP inhibitors with improved specificity is one promising strategy that could be used to modulate the vicious cycle [123, 124].

From these discoveries, it is also becoming evident that prostate cancer metastasis is not a linear, stepwise procedure. Defining the mechanisms that control CRPC metastasis and outgrowth and the mechanisms that lead to the unique osteogenic lesions can elucidate new therapeutic targets that not only impact the cancer cells directly but also the processes that facilitate the formation of a pre-metastatic niche, niche seeding, dormancy, and the vicious cycle [125]. These new discoveries will ultimately impact how mCRPCs are treated clinically.

Chapter 2. MMP Processing of PTHrP Yields a Selective Regulator of Osteogenesis, $PTHrP_{1-17}$

2.1 Introduction

In addition to elevated risk for spontaneous fractures, intense pain, and increased morbidity, patients with skeletal malignancy frequently present with humoral hypercalcemia of malignancy (HHM), a condition resulting in elevated blood calcium levels due increased osteoclast mediated bone resorption driven by their cancer [126]. The precise mechanisms and factors responsible for HHM have long been topics of interest for researchers, with multiple hypotheses having been generated over the years. In 1941, Dr. Fuller Albright posited that parathyroid hormone (PTH) or a factor similar to PTH might be secreted by tumors to cause the hypercalcemia observed in cancer patients [127, 128]. Alternative factors such as vitamin D sterols, prostaglandins, and transforming growth factors (TGFs) were also proposed, but these have not been consistently observed at increased levels in patients with HHM [129]. Nearly 50 years later, Dr. Albright's hypothesis was validated with the discovery of PTHrP [130-132]. In the 30 years since its discovery, our knowledge of PTHrP has expanded from viewing it as an HHM causing, cancer derived hormone, to a cytokine expressed in numerous tissues with abundant functions occurring throughout our lifespans [128].

Portions of this chapter have been previously published (Frieling et al., Oncogene, 2017 April 3) and are utilized with permission of the publisher (p148-149).

2.1.1 **PTHrP in Cancer**

Since it was discovered in a cancer setting, a substantial number of studies have focused on roles for PTHrP in malignancy. PTHrP is overexpressed in numerous cancers and involved in several steps of cancer progression [133]. Analyses of PTHrP expression in breast cancer specimens indicate that 60% of primary breast tumors and 90% of bone metastatic breast cancers express PTHrP, suggesting that it is important for tumor growth in bone [134, 135]. Breast cancer metastases generate osteolytic lesions that are a product of increased osteoclast formation and activity. Traditionally, PTHrP has been associated with driving the osteolytic phenotype by mediating the expression of RANKL by osteoblasts, which can drive the fusion of osteoclast precursors into mature bone resorbing osteoclasts via interactions with RANKL [20]. For example, the administration of monoclonal PTHrP neutralizing antibodies in mice inoculated with MDA-MB-231 cells led to a significant reduction in osteolytic bone lesions as well as a decrease in tumor size, demonstrating the potent effects of PTHrP in osteolytic breast cancer bone metastases [136]. Intriguingly, Ras driven PTHrP overexpression has also been noted in prostate cancers which form predominantly osteogenic metastatic bone lesions [137]. Despite this key difference, PTHrP has been shown to be a vital factor in this process as well, where it was shown to contribute to pathological bone remodeling and facilitate tumor growth *in vivo* after inoculation of PTHrP overexpressing ACE-1 prostate cancer cells [138]. The methods by which PTHrP activity is regulated to contribute to the development of both osteogenic and osteolytic lesions are not well understood and may be related to the presence of additional factors, such as Wnts, present in the tumor-bone microenvironment.

2.1.2 **PTHrP in Development and Normal Physiology**

While significant attention has been placed on understanding the effects of PTHrP in the context of skeletal malignancy, it also possesses very important roles throughout development and during normal physiology. Unlike PTH, whose expression is restricted to the parathyroid glands, PTHrP is ubiquitously expressed in tissues including heart, skin, bone marrow, fetal liver, gastric mucosa, adrenal, thyroid, breast, and parathyroid glands, and it has been shown to signal in paracrine, autocrine, and intracrine manners [139, 140]. *In vivo* gene ablation studies resulted in phenotypes that reveal particular importance for PTHrP in skeletal and mammary gland development. Systemic deletion of PTHrP (*Pthlh*$^{-/-}$) produces a neonatal lethal phenotype, with the pups dying less than 24 hours after birth due to respiratory failure attributed to defective rib cage formation [141]. These mice also develop domed skulls, shortened snouts and mandibles, and short limbs, suggesting special importance in endochondral bone formation. Non-skeletal organs and tissues appeared normal [141]. Expression of PTHrP in chondrocytes alone rescues the phenotype and allows the mice to survive to 4-months [142, 143]. Studying the phenotype of these rescued mice has revealed a failure of early ductal development and provides evidence of a role for PTHrP in branching morphogenesis [144]. These mice also display dwarfing and failed tooth eruption [142, 143, 145]. Consistent with these findings, PTHrP haploinsufficiency produces mice that appear normal at birth but show low bone mass, decreased trabecular thickness and connectivity, and increased adiposity as they approach 3 months of age. In accord with these *in vivo* phenotypes, it has since been established that PTHrP is critical for regulating growth plate development by controlling the

proliferation and differentiation of chondrocytes [146]. Additional observations have shown that the recruitment of bone marrow precursors is compromised and osteoblast apoptosis is increased in PTHrP heterozygous animal models [26].

Throughout adult life, PTHrP remains an important mediator of skeletal remodeling. It is important to note that PTHrP has a bimodal effect on the skeleton, acting primarily on osteoblasts while indirectly influencing osteoclast activity via cytokines such as RANKL [147]. As a potent mediator of bone metabolism, PTHrP has been the focus for potential therapeutic agents for disorders such as osteoporosis [128]. These studies have shown that the dosing and level of exposure are critical to the balance between anabolic and catabolic activity, with intermittent dosing regiments being key to generating an osteogenic response [148-150]. Recently, an anabolic PTHrP analog called abaloparatide underwent clinical investigation for osteoporosis, including via transdermal delivery (NCT01343004, NCT0167462, NCT00542425). The results of phase III clinical trials showed that treatment of postmenopausal women with abaloparatide for 24 weeks with 40 or 80 µg/kg/day resulted in increases in bone mineral density compared to placebo [128, 151, 152].

2.1.3 **PTHrP Gene, Protein Structure, and Susceptibility to Proteolysis**

Parathyroid hormone-related protein is a member of the parathyroid family of hormones. The PTHrP gene, *PTHLH,* is located on the short arm of chromosome 12 whereas PTH is found on chromosome 11, reinforcing the view that PTHrP likely arose from gene duplication at some point in evolution [129, 133]. The resulting protein is highly conserved among species, however alternative splicing produces three unique protein isoforms (139, 141, or 173 amino acids). Alternative splicing is unique to human

PTHrP, and certain isoforms appear to be preferentially expressed in specific tissues. The reasons for this have not been elucidated, however the presence of instability motifs that vary between the mRNA of the isoforms suggests the possibility of distinct half-lives and may also facilitate the paracrine/autocrine roles for PTHrP as opposed to the endocrine activities associated with PTH [133].

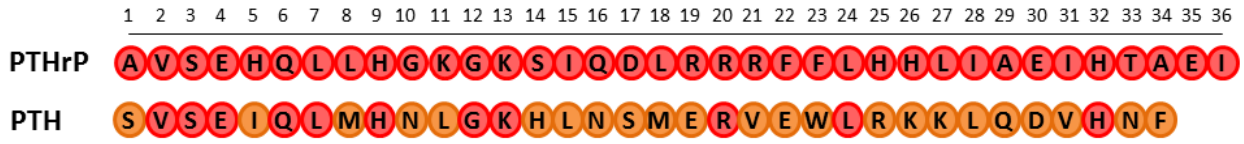

Figure 2-1. Comparison of PTHrP and PTH Amino Acid Sequences

Most homology between $PTHrP_{1-36}$ and PTH_{1-34} (biologically active forms) is within the N-terminal residues, where 8 of the first 13 amino acids are common. Despite noteworthy differences within the 15-34 sequence, which is involved with receptor ligation, both PTHrP and PTH signal through the same receptor, PTH1R.

The PTHrP protein shares homology with PTH, primarily in the N-terminal region where 8 of the first 13 amino acid residues are identical (Figure 2-1). The remainder of the amino acid sequences show minimal homology, but they share a common G-protein coupled receptor (GPCR) for signaling, the type I PTH receptor (PTH1R) [129]. Upon ligation, a series of conformational changes in PTH1R lead to a shift of transmembrane domain 3 away from transmembrane domain 6, permitting access to the cytoplasmic loops by G proteins that are associated with the adenylyl cyclase and phospholipase C pathways [153]. Through these signaling pathways, PTHrP stimulates the accumulation of intracellular second messengers such as cAMP, DAG, and inositol triphosphate (IP3) which subsequently leads to activation of protein kinase A (PKA), protein kinase C (PKC), and release of intracellular Ca2+ respectively (Figure 2-2) [154]. This can have

further downstream effects including CREB and ERK phosphorylation [128, 155, 156]. Following ligation and signal transduction, the receptor is negatively regulated by desensitization, internalization, and down-regulation. However, some studies have demonstrated that internalization may not necessarily terminate signaling as the authors observed that internalized PTH1R could still regulate cAMP for PTH_{1-34}, although $PTHrP_{1-36}$ was restricted to the cell surface, perhaps offering some degree of regulation between PTH and PTHrP [157].

Traditionally, most if not all known PTHrP activities have been associated with PTH1R, and extensive studies have attempted to determine the minimum amino acid sequence able to stimulate PTH1R. PTHrP binds to the receptor via the "two site model," where an interaction between the C-terminal domain of active PTHrP (amino acids 15-34) and the N-terminal region of the receptor contributes to binding affinity. Despite differing in amino acid sequences beyond amino acid 13, both PTH and PTHrP contain a crucial alpha-helical binding motif within the amino acids 15-34 sequence [158]. The second interaction occurs between the N-terminal domain of PTHrP and the juxtamembrane region of the PTH1R. This interaction is believed to contribute to the induction of signaling [159]. Although the C-terminal region of the protein appears to be important for the "two site model," [155], multiple studies suggest that it is not a necessity for PTH1R activation. This is supported by studies showing that both PTH 1-14 and 1-15 are capable of stimulating cAMP but at doses 5 to 6 orders of magnitude higher than that of PTH 1-34 [160]. Further studies have pinpointed that residues 1-6 play a critical role in eliciting an adenylyl cyclase response. N-terminal deleted analogs such as 3-34 or 7-34 bind PTH1R, but these are unable to completely stimulate adenylyl

cyclase and in some instances may act as competitive PTH1R antagonists [161, 162]. Whereas N-terminal residues are more commonly associated with mediating adenylyl cyclase/PKA/cAMP signaling, the C-terminal portion of $PTH_{1\text{-}34}$ including 29-32 has often been associated with mediating PKC [163]. However, modifying the first residue of PTH led to diminished IP production via PLC, suggesting that PKC activity might also be dependent to some degree on the N-terminal region of PTH [162].

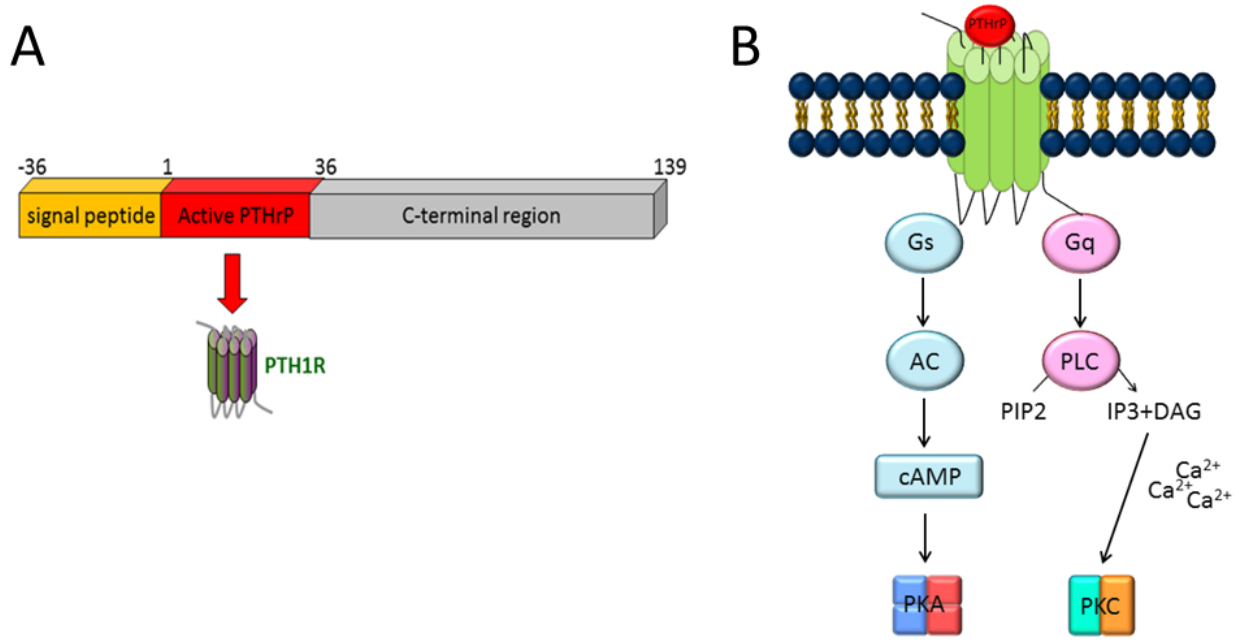

Figure 2-2. Active PTHrP Signals via PTH1R to Induce Downstream Effects

*(**A**) PTHrP is produced as a 139, 141, or 173 amino acid protein with a 36 amino acid signal peptide requiring further processing for activation. Amino acids 1-36 constitute active PTHrP which signals through PTH1R. (**B**) PTHrP (and PTH) activities are mediated via signaling through a G-protein coupled receptor called PTH1R. In skeletal tissue, PTH1R is expressed on the surface of osteoblasts, osteocytes, and chondrocytes. The pathway consists of two signaling arms resulting in the activation of protein kinase A (PKA) or protein kinase C (PKC).*

2.1.4 **PTHrP Processing**

The PTHrP protein has leader sequence of 36 amino acids (-36 to -1 signal peptide) utilized for intracellular trafficking and secretion. The leader sequence is

typically removed as the nascent peptide enters the rough endoplasmic reticulum [164]. After removal of the leader sequence, the resulting product is considered “pro-PTHrP” and is subject to further modification by proteolytic cleavage. Multiple predicted mono- and multi-basic cleavage sites suggest that much of the protein sequence is highly susceptible to proteolytic cleavage, and it has long been thought that full length PTHrP is a precursor protein that gets processed into smaller, active peptides [165]. The susceptibility to proteolysis may also serve as a mechanism that allows PTHrP to act locally compared to PTH which predominantly behaves as a hormone. Peptide fragments generated by proteolysis have been detected from several scenarios including bench-top test tube reactions, cell culture conditioned media, and even patient serum (Table 2-1). However, the functions, mechanisms, and proteases responsible for the generation of these fragments currently represent a major gap in our knowledge.

2.1.5 **Products Generated by PTHrP Proteolysis**

Many experts in the field have speculated that the full length PTHrP protein in fact serves as a pro-hormone that is subject to post-translational proteolytic processing based on the numerous dibasic residues such as arginines and lysines found in its sequence [165]. As was noted above, continuous administration of $PTHrP_{1\text{-}36}$ has been shown to induce systemic osteolysis while intermittent application of the hormone promotes bone formation [26, 166, 167]. The reason for these differential effects has been potentially ascribed to the labile nature of mature PTHrP [133], and the generation of multiple protein products by post-translational proteolysis may contribute to its numerous biological functions in a diverse range of tissues.

Table 2-1. Previously Identified PTHrP Cleavage Products

Previous studies have identified multiple PTHrP products resulting from proteolysis, however the activities of these products and the proteases that generate them are largely unknown.

Fragment	Proteases Involved	Known Activities	Reference
1-23	PSA, Neprilysin	Unknown (Loss of cAMP stimulation)	[168, 169]
1-26	Neprilysin	Unknown	[169]
1-36	Prohormone thiol protease; Furin; Others unknown	Mature PTHrP	[170-173]
1-86	Unknown	Osteogenic MSC Differentiation	[174]
12-48	Unknown	Unknown (prognostic marker for bone metastases in breast cancer)	[175]
38-64	Unknown	Cell growth and lung repair	[176]
38-94	Unknown	Inhibition of breast cancer cell growth and invasion, promotion of apoptosis	[177, 178]
38-111	Unknown	Unknown	[179]
67-86	Unknown	Inhibition of growth and invasion of breast cancer cells	[180]
107-111	Unknown	Inhibition of osteoclast resorption	[181]
107-139	Unknown	Inhibition of osteoclast resorption	[182]

2.1.5.1 *PTHrP$_{1-36}$ as the Predominant, Active Protein*

Evidence of post-translational PTHrP processing raises questions about what amino acid sequence range comprises the active species of the protein responsible for classic PTH1R mediated functions, such as those in bone development. Traditionally it is thought that PTHrP$_{1-36}$ represents the mature form of PTHrP, with an arginine residue at amino acid position 37 serving as the preferred cleavage site [171]. This region is also relatively homoglogous to PTH (Figure 2-1) [170]. Indeed most of the classic

biological activities attributed to PTHrP such as regulating osteoblast differentiation [26, 183] and stimulating osteoclast formation through osteoblast secretion of RANKL [20, 26] are recapitulated with this 36 amino acid form (occasionally $PTHrP_{1-34}$). It has also been shown that administering $PTHrP_{1-34}$ to PTHrP heterozygous mice improves the skeletal deficits associated with this phenotype [26]. Similarly, $PTHrP_{1-36}$ given by subcutaneous injection to post-menopausal osteoporotic women in clinical trials yields anabolic effects demonstrated by increases in bone mineral density after 3 months of daily treatment [149]. Despite this knowledge, the exact proteases involved in the generation of $PTHrP_{1-36}$ have not been defined and could vary depending on tissue.

2.1.5.2 ***N-terminal Derived Peptides***

Numerous peptides besides $PTHrP_{1-36}$ are generated by both identified and unidentified proteases. For example, kallikrein3/prostate specific antigen (PSA) has been shown to generate a $PTHrP_{1-23}$ peptide from $PTHrP_{1-141}$ [168]. Studies with the resulting 23 amino acid protein revealed that PSA cleavage abolishes PTHrP induced cAMP activity in MC3T3E1 cells, potentially representing a tissue (prostate) specific mechanism of regulation PTHrP activity. $PTHrP_{1-23/1-26}$ is also generated by neprilysin, a membrane bound member of the metalloproteainse family [169]. The fact that multiple proteases generate the same protein would suggest there is a potential fundamental role, but further studies are required to identify activity for $PTHrP_{1-23}$.

2.1.5.3 ***C-terminal Derived Peptides***

Several mid-region PTHrP products have been detected and studied including $PTHrP_{38-94}$, $PTHrP_{38-111}$, and $PTHrP_{67-86}$. Roles in regulating cellular behaviors including growth, invasion, apoptosis have been ascribed to many of these peptides (Table 2-1),

however to date it is unclear how these fragments are generated. An exciting recent study has explored the utility of $PTHrP_{12-48}$ as a prognostic marker for bone metastatic breast cancer [175]. Using SELDI-TOF MS, the plasma proteome of 36 breast cancer patients was interrogated and determined that $PTHrP_{12-48}$ could identify patients at risk when combined with serum N-terminal telopeptide (NTX) measurements. It has been suggested by other researchers that dipeptidyl peptidase (DPP) may be able to cleave between amino acids 48 and 49 of PTHrP [128], but it is presently unclear which protease(s) are involved with the generation of $PTHrP_{12-48}$, or if this fragment possesses bioactivity. Regardless, given the painful and devastating clinical manifestation of bone metastases and the lack of clinically significant cancer and bone biomarkers, this discovery represents an important step forward in the field.

2.1.5.4 ***Osteostatin***

One of the best studied PTHrP products besides $PTHrP_{1-36}$ is osteostatin, a protein comprised of amino acids 107-139. Again, the proteases and processes involved in generating $PTHrP_{107-139}$ are not known, but studies focused on the activity of this peptide have consistently reported on its ability to inhibit osteoclast activity both *in vitro* and *in vivo.* The potent anti-resorptive activity of $PTHrP_{107-139}$ appears to be contained within amino acids 107 to 111. Additional studies focusing on just the $PTHrP_{107-111}$ sequence indicate that this product possesses very similar activity to $PTHrP_{107-139}$. Treating a neonatal mouse model with $PTHrP_{107-111}$ in the presence of $PTHrP_{1-34}$, which is known to induce bone resorption in this model, demonstrated that $PTHrP_{107-111}$ in fact antagonizes the pro-resorptive effect of active PTHrP when administered daily for either 6 or 16 days [181]. Conversely, there is evidence where

$PTHrP_{107-111}$ and $PTHrP_{107-139}$ stimulate osteoclast like cell formation in an *in vitro* assay. The resulting osteoclasts were tested on dentine slices and shown to be functional [184]. It is possible that $PTHrP_{107-111}$ (like $PTHrP_{1-36}$) could have both osteogenic and osteolytic activities depending on administration and dosing. Although experiments using PKA and PKC inhibitors have suggested that osteostatin signals through PTH1R, a competitive PTH1R antagonist was unable to inhibit the induction of Ca^{2+} by osteostatin [184-189].

2.1.6 **Proteases Involved in Post-Translational PTHrP Proteolysis**

Since several PTHrP peptide products appear to possess their own unique functions, understanding PTHrP proteolysis could uncover significant new roles in skeletal physiology and malignancy. Many questions regarding PTHrP processing remain unanswered. What are the functions for these peptides? Does the processing occur intracellularly or extracellularly? Which proteases generate the known fragments, and which other proteases might be involved in generating as of yet-to-be identified peptides?

As a part of normal biology, proteases are responsible for processing of proteins by hydrolysis of peptide bonds. Evolutionarily, proteases are believed to have arisen as a mechanism to catabolize proteins to facilitate the generation of amino acids [190]. Years of protease research has provided a more complete appreciation of the vast activities of proteases. A significant discovery was their ability to regulate protein activity by activating and/or often generating unique bioactive forms of their substrates [190, 191]. A total of 588 proteases have been identified in the human degradome, and these can be classified based on their catalytic mechanisms including: aspartic,

glutamic, metalloproteases, cysteine, serine, and threonine [192, 193]. Aspartic, glutamic, and metalloproteases use an activated water molecule as the nucleophile whereas cysteine, serine, and threonine rely on the specific amino acid for which they are named in the site of proteolysis [190]. Some of these proteases have been shown to target PTHrP, while many others are predicted to do so.

2.1.6.1 ***Pro-Protein Convertases***

The proprotein convertase family of serine proteases has been identified as regulators of multiple proteins including hormones, growth factors, receptors, and enzymes via their ability to cleave intracellularly. The family consists of nine secretory serine proteases: proprotein convertase 1 (PC1/3), PC2, furin, PC4, PC5, paired basic amino acid cleaving enzyme 4 (PACE4), PC7, subtilisin kexin isozyme 1 (SKI-1), and proprotein convertase subtilisin kexin 9 (PCSK9) [194]. Except for SKI-1 and PCSK9, all of these enzymes prefer to cleave at basic residues [173], many of which occur abundantly throughout the PTHrP amino acid sequence, including an abundance of lysine and arginine residues giving rise to potential cleavage sites such as a triple-arginine motif at residues 19-21 [165].

Furin is well known for its roles in processing pro-proteins via the “constitutive pathway,” the main method by which PTHrP is secreted and has been implicated in the removal of pre-pro regions of both PTH and PTHrP. The highly conserved Arg-Leu-Lys-Arg sequence that falls between proPTHrP and PTHrP is a recognized furin cleavage site, and furin is known to generate active $PTHrP_{1-36}$ [164, 173]. This was observed by co-expressing human pre-proPTH and either furin, PC1/3, or PC2 in BSC-40 and GH4C1 cell lines. Of these 3 proteases, furin was the most effective at generating

active PTHrP [173]. This was also confirmed in assays using partially purified furin and PC1 [173]. Another study evaluated the relationship between PTHrP and furin by expressing pro-PTHrP in COS-7 cells with endogenous furin expression. Transfection of pro-PTHrP alone resulted in high levels of PTHrP being secreted into conditioned cell culture medium, whereas co-transfection of anti-sense furin cDNA and pro-PTHrP resulted in a notable decrease [164]. This provides further evidence that furin is involved in the generation of active PTHrP. Given the ubiquitous tissue distribution and subcellular localization to the Golgi, furin is likely a key enzyme involved in intracellular processing and secretion of active $PTHrP_{1-36}$.

2.1.6.2 *Prostate Specific Antigen (PSA) Serine Proteases*

Prostate specific antigen (PSA) is well-known for its expression in prostate tissue where it is found increased in prostate cancer patients and has been widely adopted as a biomarker since the 1990s [195, 196]. Functional roles for PSA in prostate cancer are not well understood [197]. The normal physiological function of PSA is to degrade semenogelin I and II in seminal fluid, however it has been shown to cleave other substrates including fibronectin and laminin [198]. Cleavage of fibronectin and laminin have been suggested to promote cell invasion [199], while processing of galectin-3, nidogen-1, and IGFBP-3 by PSA may contribute to adhesion, proliferation, apoptosis, and angiogenesis [197, 200-203].

PSA can activate latent TGFβ2 via currently unknown mechanisms, an event that might contribute to the formation of osteoblastic lesions in prostate cancer [204]. Interestingly, PSA has also been demonstrated to hydrolyze PTHrP. Separate studies have reported its ability to cleave both $PTHrP_{1-34}$ and $PTHrP_{1-141}$ resulting in 1-22/23

amino acid fragments. Functional analyses of these fragments suggest that PSA cleavage may be involved in regulating PTHrP activity since the PSA generated fragments were unable to stimulate cAMP *in vitro* [168, 205].

2.1.6.3 ***Cysteine Proteases***

Prohormone thiol protease (PTP) is a potential prohormone processing enzyme that has been found to be expressed in human PTHrP producing cancer cell lines, including lung, breast, prostate, and lymphoma [172, 206]. It is therefore conceivable that PTP might process PTHrP. *In vitro* experiments using recombinant proPTHrP$_{1\text{-}141}$ show that PTP cleaves at residue 37 to generate active PTHrP$_{1\text{-}36}$. Interestingly, they also show that the local PTP-generated PTHrP$_{1\text{-}36}$ was involved in regulating lung cancer cell growth, and lung cancer cell lines that express little PTHrP do not express PTP [172]. This also suggests that multiple proteases contribute to generating the active PTHrP$_{1\text{-}36}$ form and that it may occur differently in specific tissues.

2.1.6.4 ***Matrix Metalloproteinases***

Surprisingly, it is unknown if other proteases commonly found in skeletal tissues, such as matrix metalloproteinases (MMPs), can process or regulate PTHrP$_{1\text{-}36}$. MMPs are a large (23 member) family of enzymes that collectively control processing and turnover of the extracellular matrix (ECM) [207]. Bone is rich in type I collagen, and MMPs with type I collagenase activity, including MMP-1, -2, -8, -13, -14 and -15, have reported effects on skeletal development and homeostasis [208, 209]. Further, MMPs also function as key mediators of cell-cell communication given their ability to control the bioactivity and/or bioavailability of a wide array of growth factors and cytokines [53,

210]. This is especially true in the context of skeletal malignancies, where there is the heightened MMP expression at the tumor-bone interface (Table 2-2) [211-213].

Table 2-2. Elevated MMP Expression in the Tumor-Bone Microenvironment

Laser capture microdissection and microarray analysis were used to investigate the expression of MMPs in the tumor-bone microenvironment. Compared to normal bone, MMP expression is increased at the tumor/bone interface [211].

MMP	Percentage Increase at Tumor/Bone Interface
MMP-13	3403%
MMP-7	1311%
MMP-3	366%
MMP-9	326%
MMP-2	320%
MMP-15	179%
MMP-10	129%
MMP-19	107%
MMP-11	106%
MMP-28	97%
MMP-8	96%
MMP-12	95%
MMP-24	92%
MMP-17	88%
MMP-23	85%
MMP-14	82%

In the bone microenvironment cancers provoke aberrant bone remodeling where mixed lesions containing areas of extensive bone resorption and/or bone formation [214]. Primary and metastatic bone cancers have been shown to express PTHrP, which in turn induces RANKL expression in osteoblasts lining the bone to trigger osteoclastogenesis [215]. Osteoclasts then resorb the mineralized bone matrix,

releasing bone sequestered growth factors such as transforming growth factor β (TGFβ) that promote cancer cell survival [216]. MMPs are key regulators of RANKL and TGFβ bioavailability [58, 211], and given the enzymatic susceptibility of $PTHrP_{1-36}$, we hypothesized that PTHrP was a substrate of MMPs that are expressed in bone under normal and pathological conditions. Here we report that MMPs are indeed capable of rapidly processing $PTHrP_{1-36}$ to yield unique PTHrP peptides. Moreover, one of the identified peptides, $PTHrP_{1-17}$, is stable and retains the ability to stimulate intracellular calcium flux via PTH1R but does not trigger the production of cAMP. Additionally, $PTHrP_{1-17}$ has robust biological activity, where it selectively directs mesenchymal stem cell/osteoblast differentiation and osteogenesis without (like $PTHrP_{1-36}$) affecting osteoclastogenesis/bone resorption. Collectively these data suggest that MMPs are important regulators of PTHrP activity in the normal and pathological bone microenvironment.

2.2 Materials and Methods

2.2.1 **Cell Lines and Culture**

MC3T3-E1, HEK-293, RAW264.7, and SAOS2 cell lines were purchased from the American Tissue Culture Collection (ATCC) and grown in media recommended by the ATCC. PAIII cells [217], C4-2B [218], and PC3-2M cells (Perkin Elmer) were grown in complete Dulbecco's Modified Eagle's Medium supplemented with 10% fetal bovine serum. All cell lines were periodically tested for mycoplasma (#CUL001B, R&D Systems) and short tandem repeat (STR) verified at the Moffitt Clinical Translational Research Core. Mouse bone marrow stromal cells and co-cultures were isolated from

the tibias of C57BL/6 mice and cultured as described [219]. For PTH1R shRNA knockdown (Santa Cruz, sc-40158-V) studies in mouse cells standard lentiviral transduction protocols were used. Transient transfection (Qiagen, Superfect, 301305) for forced PTH1R expression studies (Origene #RG212841-Human, MC201102-Mouse) in HEK-293 cells were conducted according to the manufacturer's instructions. For conditioned media collection, cells were incubated in serum free conditions for 3 hours prior to the addition of a fresh aliquot of serum free media. Conditioned media was then collected after a further 24 hours of incubation. For MMP inhibition/treatment, the broad spectrum inhibitor GM6001 (Millipore, #CC1010 at a final concentration of 10 μM) or recombinant MMP-3 (Millipore, #444217 at a final concentration of 100 ng/ml) were added during the collection of the conditioned media.

2.2.2 **Gene Expression Analyses**

RNA was extracted with TRIzol® according to manufacturer's instructions (Invitrogen #15596). cDNA reverse transcription was performed using a High Capacity cDNA Reverse Transcription Kit (Applied Biosystems, #4368813). Concentrations of cDNA samples were determined by Nanodrop, and equal amounts (100ng per reaction) used for real time qPCR (RT-qPCR, ABI Prism 7900HT). Primers sequences for genes of interest are: Mouse *PTH1R* Forward 5'-AGCCAGACGATGTCTTTACCAA-3'; mouse *PTH1R* Reverse 5'-GATGCTG GCGTCCACCCTT-3.' Human *PTH1R* Forward 5'-AGAGAAGAAGTACCTGTGGGG-3'; human *PTH1R* Reverse 5'-GATGATCCACTTTTTGTTCCC-3.' *PTHrP* Forward 5'-GCAGTGGAGTGTCCTGGTATTC-3'; *PTHrP* Reverse 5'-TTGGATGGACTTGCCCTTGT-3.' *RANKL* Forward 5'-ACGCCAACATTTGCTTTCGG-

3'; *RANKL* Reverse 5'-GACC AGTTTTTCGTGCTCCCT-3.' *OPG* Forward 5'-CCTTGCCCTGACCACTCTTA-3'; *OPG* Reverse 5'-CCTCACACTCACACACTCGGT-3.' *Osteocalcin* Forward 5'-GCAGCTTGGCC CAGACCTA-3'; *Osteocalcin* Reverse 5'-GGGTCAGCAGAGTGAGCAGAA-3.' *Type I Collagen* Forward 5'-ACAGACGAACAACCCAAACT-3'; *Type I Collagen* Reverse 5'-GGTTTTTGGTCACGTTCAGT-3.' *18S* Forward 5'-GTAACCCGTTGAACCCCATT-3'; *18S* Reverse 5'-CCATCCAATCGGTAGTAGCG-3.' *GAPDH* Forward 5'-CCTGCACCACCAACTGCTTA-3'; *GAPDH* Reverse 5'- CCACGATGCCAAAGTTGTCA-3.' All samples were run in triplicate and normalized to 18S or GAPDH. A panel of 84 osteogenic genes was studied using a mouse specific osteogenesis RT^2 Profiler™ Assay (Qiagen, PAMM-026ZA-12). RNA was extracted by Trizol® and subsequently purified using an RNeasy MinElute Cleanup kit (Qiagen, #74204). Reverse transcription was performed using an RT^2 First Strand Kit (Qiagen, #330401). PCR array plates were run on standard qPCR instruments (ABI Prism 7900HT) and analyzed with online software (http://www.SABiosciences.com/pcrarraydataanalysis.php). Fold change for all qPCR experiments was calculated using delta delta CT method [220].

2.2.3 **MMP Processing and Identification of Cleavage Sites**

MMP cleavage assays used recombinant PTHrP (1-86; Abcam, ab50228). 100ng of recombinant of PTHrP was incubated for 1 hour in MMP digestion buffer (0.15 M NaCl, 50 mM Tris pH 7.6) in the presence of 100 ng active MMP-2, -3, -7, -9, or -13 (Millipore). Processing was confirmed by SDS-PAGE Coomassie Brilliant Blue staining and Western blotting. For *N*-terminal amino acid sequencing (Pro-Seq, Boxford, MA), 2 µg of $PTHrP_{1-86}$ was incubated with MMP-3 (100 ng/ml) for 1 hour, separated by SDS-

PAGE, and transferred to polyvinylidine fluoride (PVDF) membranes. Subsequent to Coomassie staining/destaining, bands of interest were excised, dried, and sequenced. Matrix assisted laser desorption time-of-flight mass spectrometry (MALDI-TOF MS) analyses were performed at the Moffitt Proteomics Core. Briefly, peptides from MMP cleavage reactions were extracted using C18 ZipTips (Millipore ZTC18S096) and dried in a vacuum concentrator. Samples were resuspended in a mix of 5 µL of aqueous 2% acetonitrile, 1% acetic acid plus 5 µL of α-cyano-4-hydoxycinnamic acid (CHCA) dissolved at 5 mg/ml in 50% H_2O/50% acetonitrile.

$PTHrP_{1-36}$ (ProImmune) and the major MMP generated fragments ($PTHrP_{1-17}$, $PTHrP_{18-26}$ and $PTHrP_{27-36}$) were synthesized via standard FMOC chemistry (Symphony, PTI) and characterized as previously described prior to use for *in vitro* and *in vivo* analyses [221].

2.2.4 **Immunoblotting and Immunoprecipitation-Mass Spectrometry**

Cells were lysed with cold RIPA buffer (150 mM NaCl, 1mM EDTA, 1% Triton X-100, 1% sodium deoxycholate, 0.1% SDS, 20 mM Tris, pH 8) containing protease and phosphatase inhibitors (Thermo Scientific, #78442) using standard procedures. Total protein concentration was determined using BCA (Pierce, #23225) and 10 µg of protein loaded in 10% SDS-PAGE gels. Blots were blocked in 5% BSA for 1 hour followed by primary antibody for phospho-ERK (Cell Signaling Technology #9101; diluted 1:1000 in blocking solution + 0.1% Tween-20), ERK (Cell Signaling Technology #4695; diluted 1:1000 in blocking solution + 0.1% Tween-20), phospho-CREB (Cell Signaling Technology #9198, diluted 1:1000 in blocking solution + 0.1% Tween-20), CREB (Cell Signaling Technology #9197, diluted 1:1000 in blocking solution + 0.1% Tween-20), or

PTHrP (Santa Cruz sc20728; diluted 1:1000 in blocking solution + 0.1% Tween-20) overnight at 4°C. The blots were washed 3 x 10 minutes in 1X TBST and incubated with HRP-conjugated anti-species secondary (Cell Signaling Technology, Rabbit #7074/Mouse #7076, diluted 1:1000 in blocking solution). Blots were developed using enhanced chemiluminescence (Pierce 32106) and exposed to film. Actin (Santa Cruz sc-1615; diluted 1:1000 in blocking solution + 0.1% Tween-20) was used as a loading control.

Antibodies reactive to $PTHrP_{1-17}$, but not $PTHrP_{18-26}$ or $PTHrP_{27-36}$, were developed by the NCI Office of Cancer Clinical Proteomics Research (https://antibodies.cancer.gov) and evaluated by ELISA and spotting various amounts of PTHrP peptide (1, 10, 50, and 100ng) onto nitrocellulose membranes. Top candidates were selected and evaluated by immunoprecipitation mass spectrometry assays. Conditioned cell culture media were collected from 90% confluent cells and divided into 1 mL aliquots. 1 µg of anti-$PTHrP_{1-17}$ antibody was added per reaction and incubated for 1 hour at 4°C at which point 15 µL of Protein G beads (Ultralink, Pierce) were added and incubated at 4°C overnight. Beads were washed 3 times with IP wash buffer (100 mM NaCl 50 mM Tris HCl, 0.1% NP-40), followed by 3 washes with nanopure water (18 MΩ) and pooled. Peptide was eluted from the beads with 0.1% trifluoroacetic acid, dried, and resuspended in chromatography buffer containing 4 fmol/µL of stable isotope labeled standard (SIS) PTHrP peptides, which incorporate $^{13}C_6{}^{15}N$ lysine (residue #13 of $PTHrP_{1-17}$). Samples were analyzed using liquid chromatography-parallel reaction monitoring mass spectrometry (LC-PRM; nanoRSLC and QExactive Plus, Thermo [222]). Raw data were imported into Skyline software (https://skyline.gs.washington.edu

[223]), and PTHrP peptides were quantified using selected transitions. Quantification of peak areas for those specific fragment ions was used to determine the ratio of endogenous $PTHrP_{1-17}$ to the $PTHrP_{1-17}$ SIS.

2.2.5 **PTH1R Signaling Assays**

A cAMP-Glo™ Assay (Promega, #V1501) was used to assess cAMP production. MC3T3 and PTH1R-expressing HEK cells (2.5×10^4 cells/well, 384-well plate) were treated with varying concentrations of PTHrP peptides (1-100 nM, 15 min) and luminescence was measured on a Victor plate reader. The forskolin analog NKH 477 (Tocris, 10 µM, 15 min) was used as a positive control for cAMP assays. Calcium flux was determined by loading cells with Fluo-4 Direct™ calcium reagent + Probenecid (Invitrogen, #F10471, 1×10^5 cells, 48-well plate) and incubated for 30 minutes at 37°C followed by 30 minutes at room temperature. Increases in fluorescence were measured by time-lapse microscopy. Using this approach, the change in fluorescence intensity over time for individual cells in 3 fields of view per condition was quantified (Definiens) and graphed.

2.2.6 **MTS Proliferation Assay**

All cell types were seeded at 5×10^4 cells/well in 96-well plate and treated for 24 hours in 5% serum (MSC, Raw 264.7) or serum free (MC3T3, PAIII, PC3-2M, C4-2B, SAOS-2) containing media. CellTiter 96 (Promega, #G5421) was used to determine metabolic activity as a surrogate of proliferation, by measuring absorbance at 490nm.

2.2.7 **Morphology and Migration Assays**

For immunofluorescence studies, MC3T3 were seeded at 5 x 10^4 cells per well in 8-well glass chamber slides and treated with 10 nM of $PTHrP_{1-17}$ or $PTHrP_{1-36}$ in serum free media for 1 hour. Cells were fixed with 4% paraformaldehyde for 20 min, washed 3x with PBS, and blocked in antibody diluting buffer (2% BSA, 0.1% Triton x100) for 30 minutes at room temperature. Actin filaments were stained using Alexa Fluor 488-Phalloidin for 30 minutes at room temperature (Invitrogen A12379, diluted 1:1000 in antibody diluting buffer). Images were acquired using an upright Zeiss fluorescent microscope.

For migration assays, osteoblast (MC3T3) and MSC migration was assessed using modified Boyden chamber assay. Cells (5.0 x 10^5) were seeded in the upper chamber after 24 hour serum starvation. PTHrP peptides (10 nM in serum free media) were added to the lower chamber and incubated over a 5 hour period at 37°C. Serum free media and 1% serum media were used as negative and positive controls, respectively. Chamber filters were excised and migrated cells stained with hematoxylin. The number of migrated cells was determined by counting 3 random fields at 20x for each condition in triplicate.

2.2.8 ***In Vitro*** **Osteoblast and Osteoclast Formation Assays**

For osteoblast differentiation studies, mouse MSCs (1.2 x 10^5 cells/well in 24-well plates) were incubated for 21 days in the presence of $PTHrP_{1-17}$ or $PTHrP_{1-36}$ (10 nM, replenished every third day). Mouse osteogenic supplement (R&D, CCM009) was used as a positive control. Cells were fixed with 10% neutral buffered formalin (15 minutes, room temperature), stained with Alizarin red (2%, pH 4.1-4.3, 45 minutes, room

temperature in dark), and quantified by measuring absorbance at 405 nm. For osteoclast formation assays, adherent bone marrow macrophage precursors were cultured for 3 days in the presence of recombinant M-CSF (Preprotech, 20 ng/mL) then seeded into 48-well plates (30,000 cells/well). The cultures were expanded for an additional 2 days at which point $PTHrP_{1-17}$ or $PTHrP_{1-36}$ were added (100 nM, replenished daily). Recombinant RANKL (Oriental Yeast Company, 100 ng/mL) plus M-CSF (25 ng/mL) was used as a positive control. After 7 days, cultures were stained for tartrate-resistant acid phosphatase (TRAcP) positivity using solutions detailed below. The number of bone-lining, multi-nucleated (>3 nuclei per cell), TRAcP positive osteoclasts was quantified from multiple sections.

2.2.9 *In Vivo* Osteoclastogenesis Assays

For *in vivo* calvarial injection assays, 2 µg of $PTHrP_{1-17}$ or $PTHrP_{1-36}$ were injected subcutaneously every 6 hour for 3 days over the calvaria of 4-6 week old female *SCID-Beige* mice as reported [224, 225]. Mice were sacrificed 10 hour after the final injection and calvariae were harvested. Tissues were fixed overnight in 10% neutral buffered formalin and high resolution µCT scan analyzed (SCANCO-µCT40) as described [122]. Subsequent to reconstruction and quantitations, tissues were decalcified in 14% EDTA, pH 7.4 for 3 days. After processing, specimens were paraffin embedded and 5 µM sections prepared. The sections were stained with hematoxylin and eosin to observe gross anatomy and trichrome to measure bone formation. For TRAcP staining and osteoclast measurements, slides were deparaffinized and rehydrated to water then incubated in Basic Stock Incubation Medium (112 mM anhydrous sodium acetate, 49 mM dibasic dehydrate sodium tartrate, 0.28% glacial

acetic acid) containing 1% Naphthol-Phosphate substrate (2% Napthol AS-BI Phosphate in 2-Ethoxyethanol) for 1 hour at 37°C. Slides were then transferred to Basic Stock Incubation Medium containing 250 µL Pararosaniline dye (5% pararosaniline dye in 2N HCl) and 250 µL of sodium nitrite solution (4% sodium nitrite in distilled water) at 37°C and monitored for development of red stained osteoclasts. After developing, the slides were rinsed in distilled water and counterstained with Hematoxylin, blued, and aqueously mounted. The number of multi-nucleated, TRAcP positive osteoclasts were quantified from multiple tissue sections. Only multinucleated (>3 nuclei per cell) TRAcP positive cells were counted as osteoclasts.

2.2.10 ***In Vivo*** **Osteogenesis Assays**

For *ex vivo* calvarial organ cultures, calvariae were isolated from 4 day old *Rag2*$^{-/-}$ neonates and cultured on stainless steel wire mesh platforms in BGJb media containing 0.1% BSA as described [226]. Calvariae were treated with 10 nM of $PTHrP_{1-17}$ or $PTHrP_{1-36}$ for 14 days. Ectopic ossicle formation assays were performed by subcutaneously implanting Gelfoam sponges loaded with 1 x 10^6 mouse mesenchymal stem cells into 6 week old male *SCID*/*Beige* mice. After 1 week recovery, daily subcutaneous injections of PTHrP peptides (40 µg/kg/day) were administered for 3 weeks at which point ossicles were harvested for histology and imaging as described [227, 228]. Tibias were collected at the same time, fixed overnight, and decalcified in 14% EDTA for 3 weeks. Following processing and embedding, trichrome staining was used to identify areas of trabecular bone formation (blue/green staining of type I collagen). Bone volume to total volume (BV/TV) was calculated by measuring

trabecular bone volume within a 1.0 mm long area starting 0.5 mm from the growth plate using ImageJ software [219].

2.3 Results

2.3.1 **PTHrP is an MMP Substrate**

To test if MMPs process PTHrP, we incubated recombinant $PTHrP_{1-86}$ with MMP-3 and assessed immediate (1 hour) cleavage products (Figure 2-3 A and B). N-terminal amino acid sequencing identified that MMP-3 cleaved recombinant PTHrP to generate the mature form of the protein, $PTHrP_{1-36}$ (Figure 2-3 C). However, MALDI-TOF MS analyses demonstrated that $PTHrP_{1-36}$ was further cleaved to distinct stable peptide products, including $PTHrP_{1-17}$, $_{18-26}$ and $_{27-36}$ (Figure 2-3 D). Kinetic analyses revealed that MMP-3 generated these main PTHrP products within 1 hour, and the $PTHrP_{1-17}$ peptide was detected at timepoints as short as 1 minute, indicating rapid turnover by MMPs (Figure 2-4, Figure 2-5). We also examined the PTHrP processing activity of other MMPs present in the bone metastatic prostate cancer microenvironment and found that MMP-2, -7, -9 and -13 could generate PTHrP fragments, and that all tested, with the exception of MMP-13, consistently generated $PTHrP_{1-17}$ (Table 2-3). Thus, PTHrP is an MMP substrate.

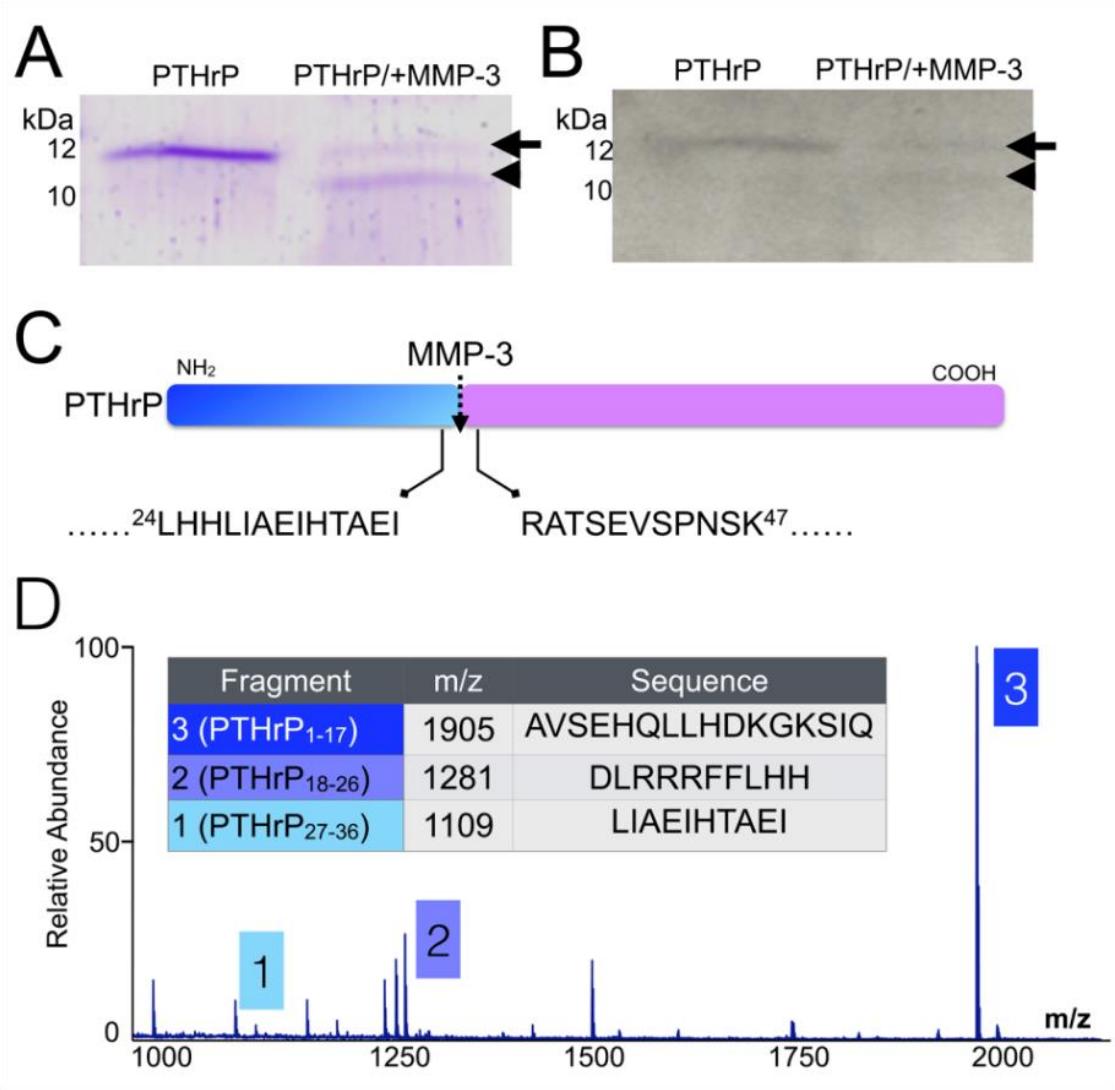

Figure 2-3. PTHrP is Processed by MMPs

*(**A** and **B**) Recombinant $PTHrP_{1-86}$ (100 ng; arrow) was incubated for 1 hour with active MMP-3 (100 ng) and products analyzed by SDS-PAGE with Coomassie blue staining (**A**) and immunoblot analysis (**B**). Arrowhead indicates cleavage product. Molecular weight markers indicated in kilodaltons (kDa). (**C**) N-terminal amino acid sequencing revealed that MMP-3 cleaved (dashed arrow) $PTHrP_{1-86}$ between amino acids 36 and 37. Arrows illustrate the amino acid sequence on either side of MMP-3 cleavage site. Amino acid position is indicated by numerical superscript. (**D**) MALDI TOF/MS analyses established that further incubation (1 hour) of PTHrP with MMP-3 yields novel, stable PTHrP fragments, $PTHrP_{1-17}$, $PTHrP_{18-26}$, and $PTHrP_{27-36}$.*

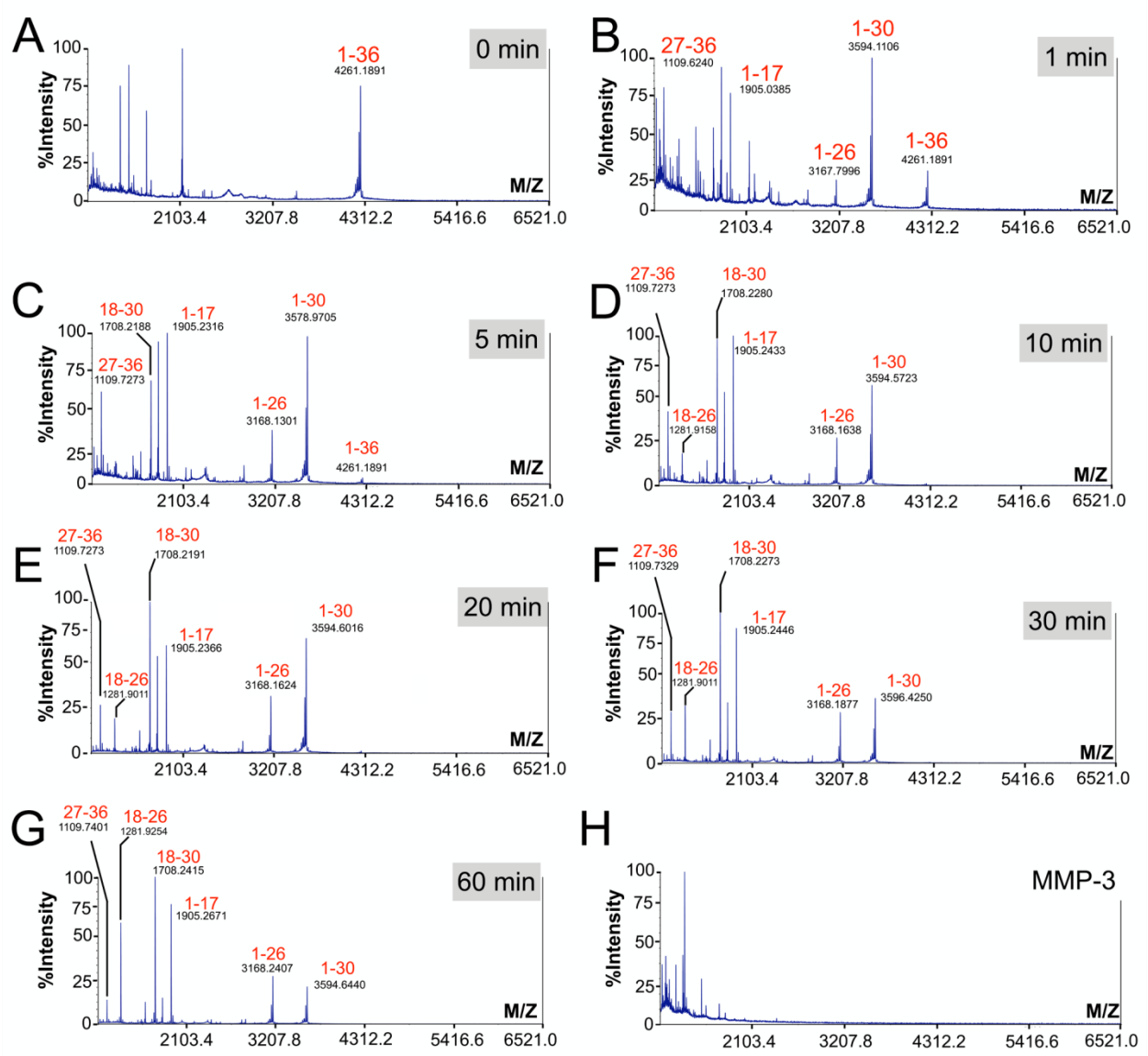

Figure 2-4. Kinetics of MMP-3 Processing of PTHrP$_{1-36}$

*(**A**) PTHrP$_{1-36}$ (500 ng) and MMP-3 (100 ng) were added together in reaction buffer in the presence of EDTA (2 mM) to prevent enzymatic activity. Mass spectrometry at the 0 minute time point shows the percent intensity (% Intensity) of the PTHrP$_{1-36}$ peak. M/Z denotes the mass to charge ratio. (**B**-**G**) EDTA was added to separate reactions at indicated time points. (**H**) Mass spectrum profile of MMP-3 enzyme (100 ng) and reaction buffer in the absence of PTHrP$_{1-36}$.*

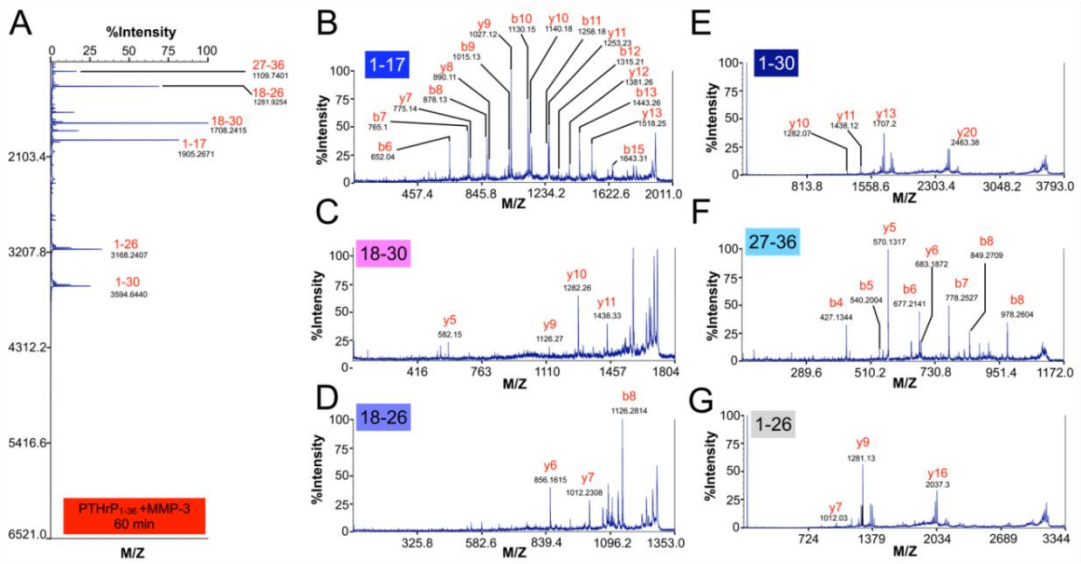

Figure 2-5. MS/MS of MMP-3 Cleaved PTHrP Peptides

*(**A**-**G**) The 60 minute $PTHrP_{1-36}$/MMP-3 reaction was analyzed by MS/MS to identify the amino acid content of the major remaining PTHrP peaks (**B**-**G**). M/Z indicates the mass/charge ratio.*

Table 2-3. MMP Generation of PTHrP Cleavage Products

A list of the PTHrP products generated by multiple MMPs over the course of 1 hour. MMPs (100 ng/ml) were incubated with $PTHrP_{1-36}$ for 1 hour at 37°C . Reactions were stopped via the addition of EDTA (2 mM). MS/MS analysis identified the major PTHrP products produced by each MMP at this time point.

PTHrP Protein Sequence	Start	End	M/Z	MMP				
				MMP-2	MMP-3	MMP-7	MMP-9	MMP-13
AVSEHQLLHDKGKSIQDLRRRFFLHHLIAEIHTAEI	1	36	4258.310838					
AVSEHQLLHDKGKSIQD	1	17	1904.982465	X	X	X	X	
AVSEHQLLHDKGKSIQDLRRRFFLHH	1	26	3167.708578	X	X	X	X	X
AVSEHQLLHDKGKSIQDLRRRFFLHHLIAE	1	30	3593.956413	X	X			X
LRRRFFLHH	18	26	1281.743954	X	X	X		
LRRRFFLHHLIAE	18	30	1706.984512		X			
LIAEIHTAEI	27	36	1109.620101	X	X	X	X	X

2.3.2 **MMP Generated PTHrP$_{1-17}$ Has Biological Activity**

To test if the MMP generated fragments of PTHrP retained biological activity, the major MMP generated PTHrP peptides, PTHrP$_{1-17}$, $_{18-26}$, and $_{27-36}$ were synthesized and assessed for their biological effects on primary mouse mesenchymal stem cells (MSCs) and osteoblasts, which express and respond to signaling from the PTHrP receptor, PTH1R (Figure 2-6 A) [147]. Low concentrations (10 nM) of PTHrP$_{1-36}$ are sufficient to activate PTH1R and promote ERK phosphorylation in these cell types [155]. Notably, treatment of MSCs and osteoblasts with 10 nM of PTHrP$_{1-36}$ or PTHrP$_{1-17}$, induced ERK phosphorylation within 5 minutes compared to control or scrambled peptide treated cells (Figure 2-6 B). Increases in response to PTHrP$_{18-26}$ and PTHrP$_{27-36}$ were noted, but these increases were very subtle and variable in repeated experiments (data not shown). We next looked at CREB phosphorylation since it is another downstream target of PTH1R signaling [229]. In contrast to our ERK analyses, we observed that phosphorylation of CREB was only induced by PTHrP$_{1-36}$ (Figure 2-6 C).

PTH1R GPCR activation also induces rapid cAMP and calcium flux responses primarily via Gs and Gq signaling respectively [230]. Again, only the addition of PTHrP$_{1-36}$ peptide induced cAMP (Figure 2-6 D), whereas both PTHrP$_{1-36}$ and PTHrP$_{1-17}$ triggered increases in calcium flux (Figure 2-6 E). No effects of the PTHrP$_{18-26}$ or PTHrP$_{27-36}$ MMP generated peptides on signaling were noted. These differential effects for PTHrP$_{1-17}$ on calcium flux versus cAMP production were recapitulated in HEK cells engineered to express the PTH1R receptor (Figure 2-7 A-C). Given the reported roles of PTHrP$_{3-34}$ and PTHrP$_{7-34}$ to act as PTH1R antagonists, we also tested multiple combinations of MMP-generated peptides in combination with PTHrP$_{1-36}$ to determine if

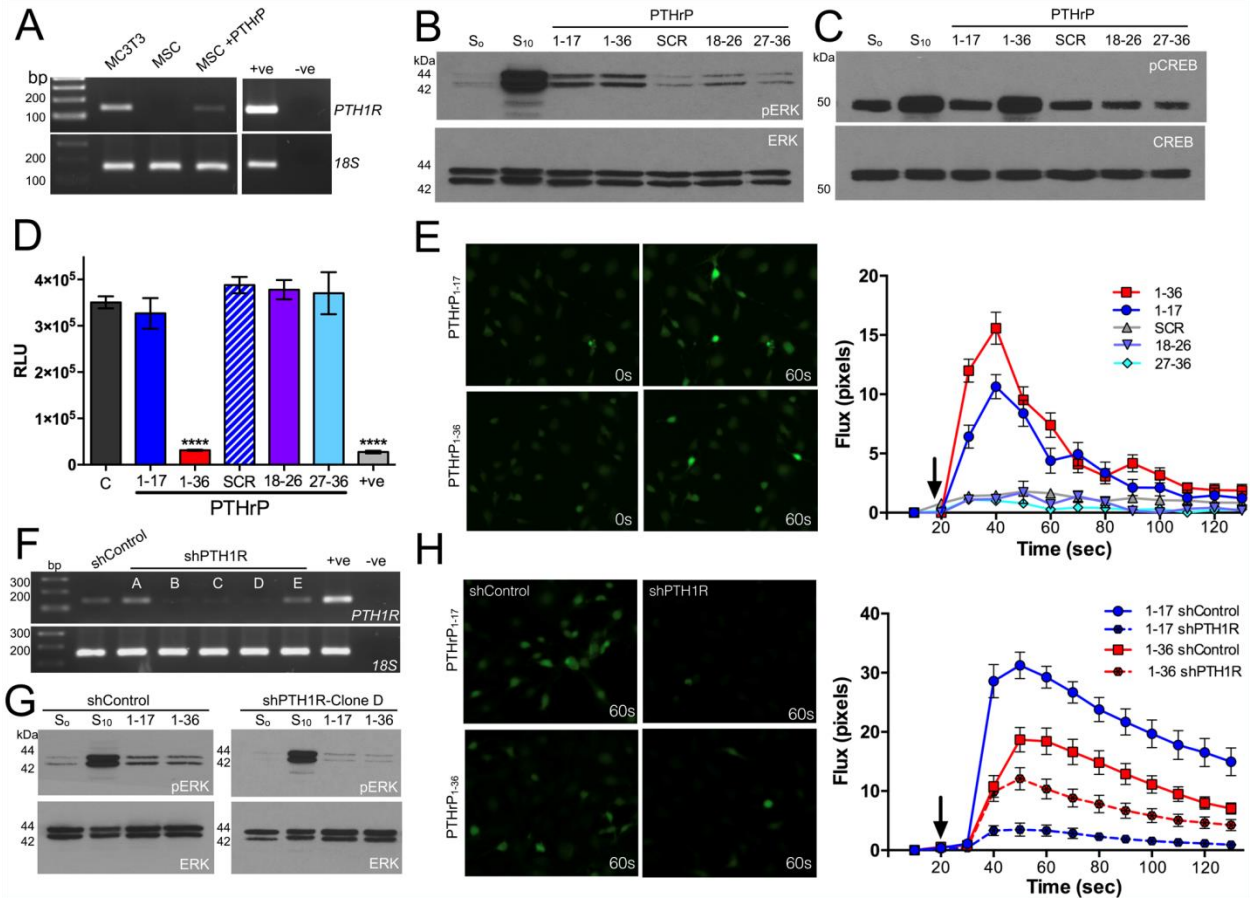

Figure 2-6. PTHrP$_{1-17}$ Has PTH1R-Dependent Signaling

*(**A**) PTH1R expression in MC3T3 osteoblasts and primary MSCs treated in the absence or presence of PTHrP$_{1-36}$ for 24 hour. +ve indicates positive control (primary mouse osteoblasts) while –ve indicates negative non-template control. Molecular weight markers are illustrated in base pairs (bps). (**B** and **C**) ERK phosphorylation (pERK) and CREB phosphorylation (pCREB) in MC3T3 osteoblasts following treatment with PTHrP peptides (10nM for 5min in serum free media). S_0 and S_{10} represent the addition of serum free and 10% serum, respectively. SCR is scrambled peptide control. (**D**) cAMP production in MC3T3 osteoblasts treated with PTHrP peptides (10 nM for 15 minutes). Asterisks denote statistical significance (*, p<0.05; ***, p<0.001). Forskolin (10 μM for 15 minutes) was used as a positive control (+ve). (**E**) Calcium flux analysis in MC3T3 osteoblasts after treatment with PTHrP peptides (10 nM). Left, representative images illustrate fluorescence activity prior to (0 seconds) and following treatment with PTHrP peptides (60 seconds). Graphs show increase in fluorescence measured in individual cells (n=20/group) over time. Arrow on graph indicates the time point at which the PTHrP peptides were added. (**F**) Generation of PTH1R knockdown (shPTH1R) MC3T3 clones (**A** thru **E**) via shRNA transduction. Scrambled control clones (shControl) were also selected for analysis. +ve indicates positive control (primary mouse osteoblasts) while –ve indicates negative non-template control. (**G**) ERK phosphorylation in shControl and shPTH1R cells (MC3T3 clone D) in response to PTHrP peptides (10 nM for 5 minutes). (**H**) Calcium flux assays were performed in shControl and shPTH1R clones after treatment with PTHrP$_{1-36}$ and PTHrP$_{1-17}$ (10 nM). Left, representative images illustrate fluorescence activity following addition of PTHrP peptides (60 seconds). Graphs show increase in fluorescence (RFU) measured in individual cells (n=20/group) over time.*

the peptides might antagonize cAMP induction in these HEK cells. The addition of the $PTHrP_{1-17}$, $PTHrP_{18-26}$, $PTHrP_{27-36}$, or all three together with $PTHrP_{1-36}$ did not affect the induction of cAMP (Figure 2-7 D). To determine if $PTHrP_{1-17}$ effects were mediated via PTH1R, we generated multiple MC3T3 osteoblast shControl and shPTH1R clones (Figure 2-6 F). The ability of $PTHrP_{1-17}$ and $PTHrP_{1-36}$ to induce ERK phosphorylation was abrogated in PTH1R knockdown cells vs. control shRNA (Figure 2-6 G). Further, calcium flux in response to $PTHrP_{1-17}$ and $PTHrP_{1-36}$ was significantly reduced in PTH1R knockdown cells (Figure 2-6 H). These effects on ERK phosphorylation and calcium flux were validated with a separate shPTH1R clone (Figure 2-8). Thus, our data indicates that $PTHrP_{1-17}$ has biological activity and activates select arms of PTH1R-directed signaling circuits.

2.3.3 **$PTHrP_{1-17}$ Promotes MSC/Osteoblast Cell Migration**

The biological effects of the MMP generated PTHrP fragments and $PTHrP_{1-36}$ were assessed in primary MSCs, MC3T3 osteoblasts, an osteoclast precursor cell line (RAW 264.7), and multiple cancer cell lines (PAIII, C4-2B, PC3-2M, SAOS-2). There were no overt effects of these four PTHrP peptides on cell growth (Figure 2-9 A-G), and treatment of osteoblasts with $PTHrP_{1-17}$ or $PTHrP_{1-36}$ did not prevent tumor necrosis factor-α (TNF-α)-induced cell death (Figure 2-9 H) [231].

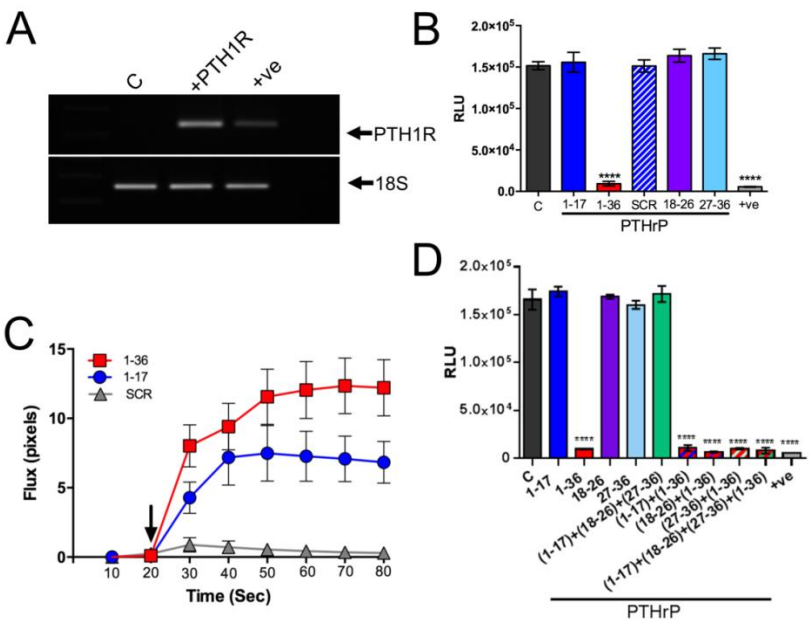

Figure 2-7. $PTHrP_{1-17}$ Induces Calcium Flux but not cAMP in HEK Expressing PTH1R

(***A***) *HEK293 cells were transfected with PTH1R expression construct. +ve indicates positive control (primary mouse osteoblasts) while –ve indicates negative non-template control. Molecular weight markers are illustrated in base pairs (bp).* (***B***) *cAMP levels in HEK-PTH1R expressing cells treated with PTHrP peptides (10 nM for 15 minutes). Asterisks denote statistical significance (*, p<0.05; ***, p<0.001). Forskolin (10 μM for 15 minutes) was used as a positive control (+ve).* (***C***) *Calcium flux analysis in MC3T3 osteoblasts after treatment with PTHrP or scrambled control peptides (10 nM). Graphs show increase in fluorescence measured in individual cells (n≥20/group) over time. Arrow on graph indicates the time point (20 seconds) at which the PTHrP peptides were added.* (***D***) *cAMP levels in HEK-PTH1R expressing cells treated with indicated combinations of PTHrP peptides (10 nM for 15 minutes).*

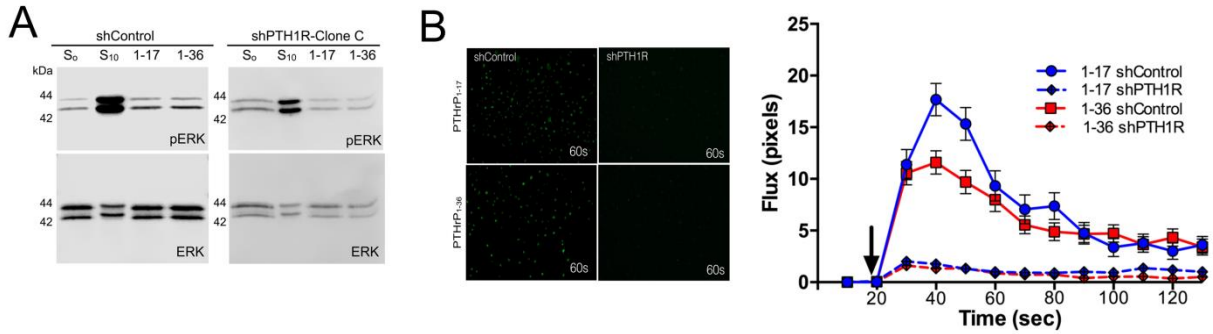

Figure 2-8. $PTHrP_{1-17}$ Stimulates ERK Phosphorylation and Calcium Flux in MC3T3 Osteoblasts via PTH1R

(***A***) *ERK phosphorylation in shControl and shPTH1R cells (MC3T3 clone C) in response to PTHrP peptides (10 nM for 5 minutes).* (***B***) *Calcium flux assays were performed in shControl and shPTH1R clones after treatment with $PTHrP_{1-36}$ and $PTHrP_{1-17}$ (10 nM). Left, representative images illustrate fluorescence activity following addition of PTHrP peptides (60 seconds). Graphs show increase in fluorescence (RFU) measured in individual cells (n≥20/group) over time. Arrow on graph indicates the time point (20 seconds) at which the PTHrP peptides were added.*

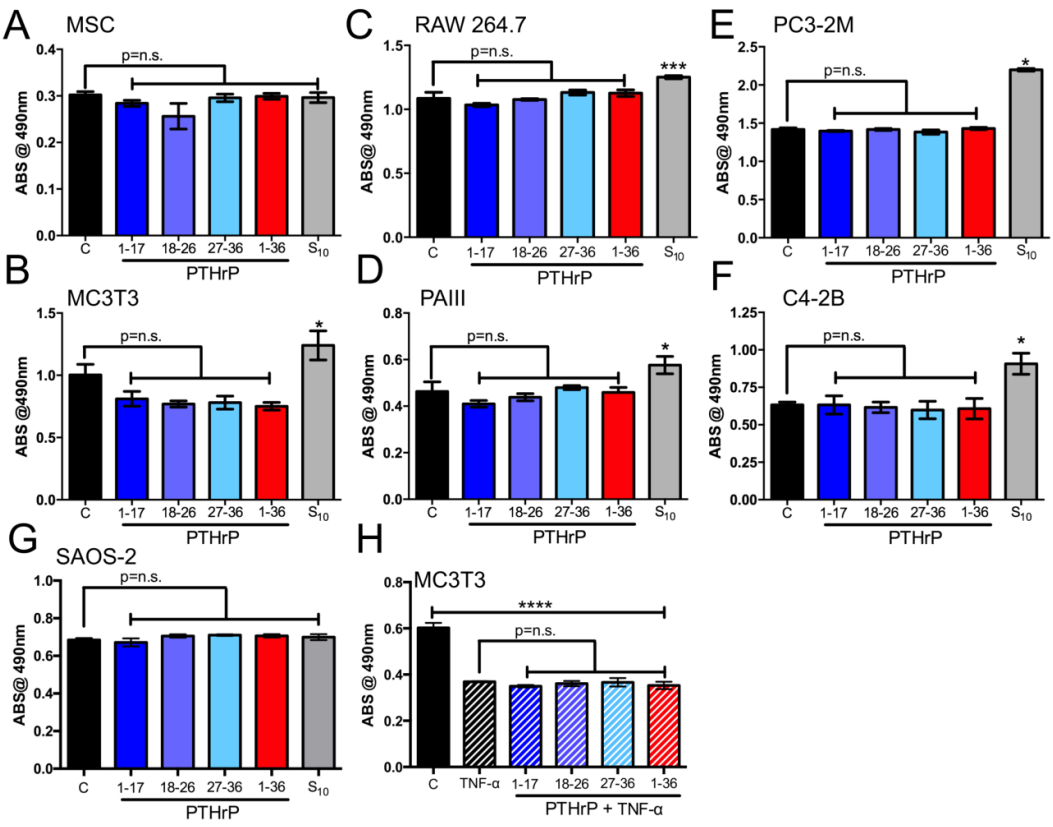

Figure 2-9. MMP-3 Generated PTHrP Peptides Do Not Affect Cell Growth or Survival

*(**A**-**G**) MSC, MC3T3 osteoblasts, RAW 264.7 monocytes, prostate cancer cells lines, PAIII, PC3-2M and C4-2B and the osteosarcoma cell line SAOS-2 were treated with PTHrP fragments (10 nM for 24 hours) conditions. MTT assay was used as a readout for cell number. Normal growth media (10% Serum: S_{10}) was used as a positive control. (**H**) MC3T3 osteoblasts were treated with TNFα (5 ng/ml for 48 hours) in the presence or absence of 10nM $PTHrP_{1-17}$ and $PTHrP_{1-36}$. Asterisks denote significance ($p<0.05$) while n.s. indicates non-significant differences.*

However, in assessing the effects of the PTHrP peptides on MSC and osteoblast proliferation, treated cells acquired a migratory phenotype, characterized by a more elongated shape (Figure 2-10 A). PTHrP has been shown to contribute to the recruitment of osteoblasts *in vivo* [26]. In keeping with this observation, both $PTHrP_{1-36}$ and $PTHrP_{1-17}$ significantly increased migration of MSCs and MC3T3 cells (Figure 2-10 B). These effects of $PTHrP_{1-17}$ are PTH1R dependent, as knockdown of PTH1R abolished $PTHrP_{1-17}$-induced osteoblast migration (Figure 2-10 C).

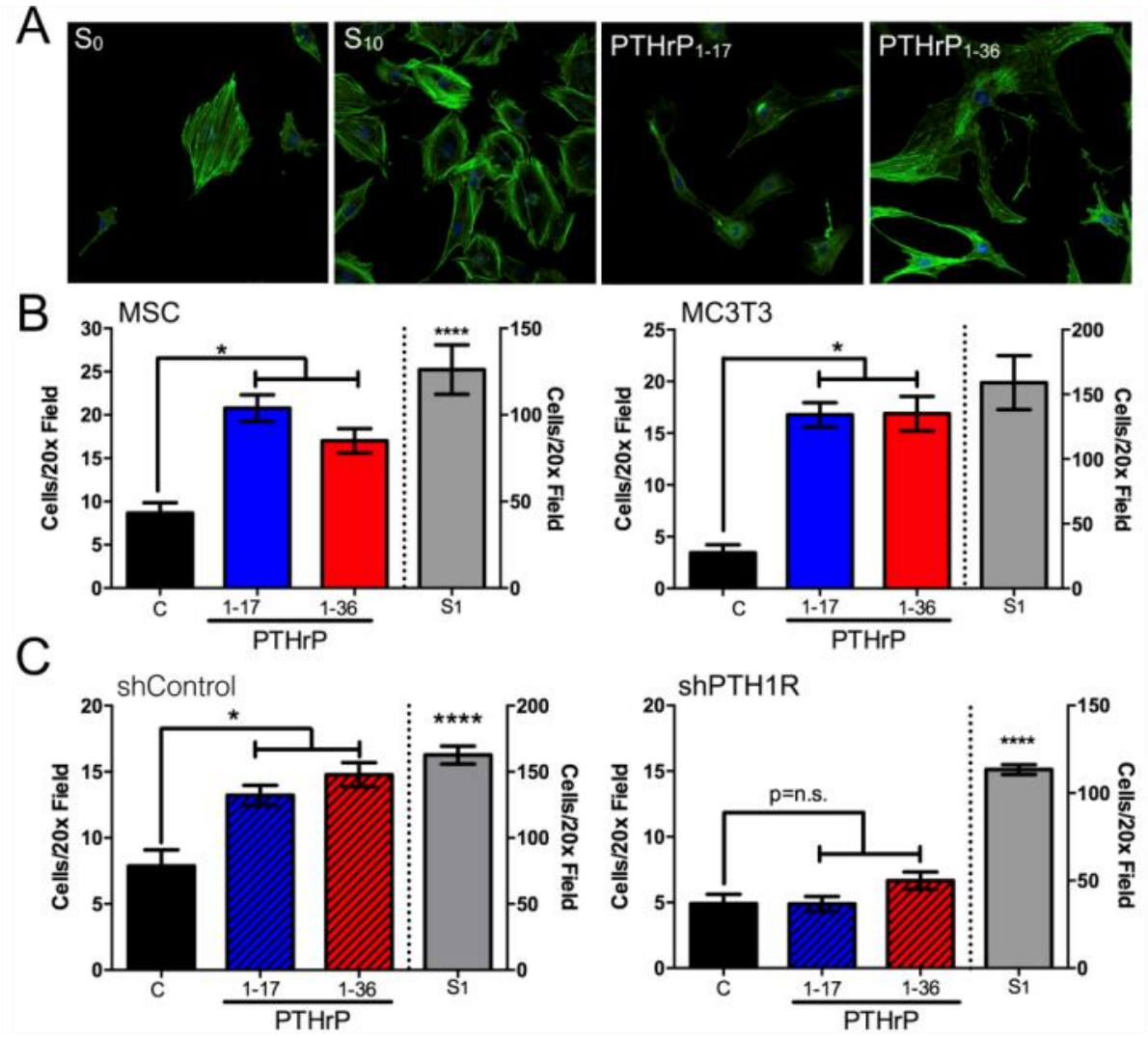

Figure 2-10. $PTHrP_{1-17}$ Promotes MSC and Osteoblast Migration via PTH1R

*(**A**) Morphology of osteoblasts (MC3T3 cells) following treatment of $PTHrP_{1-17}$ or $PTHrP_{1-36}$ (10 nM for 1 hour) was determined by staining with anti-actin antibody and confocal fluorescence microscopy. (**B**) Migration of primary MSCs (left) and osteoblasts (MC3T3, right) treated with $PTHrP_{1-17}$ versus $PTHrP_{1-36}$ (10 nM for 6 hours). (**C**) The migration of shControl (left) and PTH1R knockdown (right, shPTH1R) MC3T3 osteoblasts following treatment with $PTHrP_{1-17}$ versus $PTHrP_{1-36}$ (10 nM for 5 hours). Cell number per 20x field in 5 micrographs per condition were counted. Positive control for (**B**) and (**C**) was media containing 1% serum (S_1). Asterisk denotes statistical significance ($p<0.05$); n.s., non-significant differences.*

2.3.4 $PTHrP_{1-17}$ Promotes MSC/Osteoblast Differentiation

$PTHrP_{1-36}$ is a potent regulator of osteoclastogenesis and bone resorption, but intermittent treatment of osteoblasts can promote osteoblast differentiation and bone

formation [232]. To assess effects of $PTHrP_{1-17}$ on osteoblast differentiation and mineralization, primary MSCs derived from FVB mice were treated for 16 days with $PTHrP_{1-17}$ or $PTHrP_{1-36}$ in the presence or absence of osteogenic media. Surprisingly, treatment with $PTHrP_{1-17}$ alone was sufficient to promote osteoblast differentiation of MSCs and significantly enhanced the effects of the osteogenic media as determined by Alizarin red staining and colorimetric analysis (Figure 2-11 A-B). Consistent with the ability of $PTHrP_{1-17}$ to promote mineralization, we also observed that $PTHrP_{1-17}$ could induce the expression of *Type I Collagen*, a major component of the bone extracellular matrix (Figure 2-11 C). The induction of an osteogenic gene profile in MSCs by $PTHrP_{1-17}$ was studied further using a RT^2 Profiler PCR Array. Here, changes in *Gli1* and *MMP-8* gene expression, among others, were noted. Additionally, some genes appear to be differentially regulated between $PTHrP_{1-17}$ and $PTHrP_{1-36}$, suggesting that MMP cleavage might produce PTHrP fragments, such as $PTHrP_{1-17}$, that possess unique bioactivities (Table 2-4). To test if these effects of $PTHrP_{1-17}$ were manifest *in vivo*, we used a murine model of ectopic bone formation [228]. Primary MSCs were loaded onto Gelfoam scaffolds and implanted subcutaneously. Mice were treated daily with vehicle control, $PTHrP_{1-17}$, or $PTHrP_{1-36}$ (40 μg/kg/day; intermittent treatment regimen for 21 days [233]). High-resolution μCT scans of isolated ossicles revealed bone formation in the $PTHrP_{1-17}$ and $PTHrP_{1-36}$ treated animals (Figure 2-11 D). Analysis of trichrome stained ossicle sections, which allows for the detection of collagen and bone (blue/green color), supported μCT scans and demonstrated a significant amount of osteoid in both $PTHrP_{1-17}$ and $PTHrP_{1-36}$ treated cohorts (Figure 2-11 E). Underscoring this observation, trabecular bone volume measurements of hind limbs revealed

significantly more bone in the $PTHrP_{1-17}$ and $PTHrP_{1-36}$ treated mice compared to control (Figure 2-12 A and B).

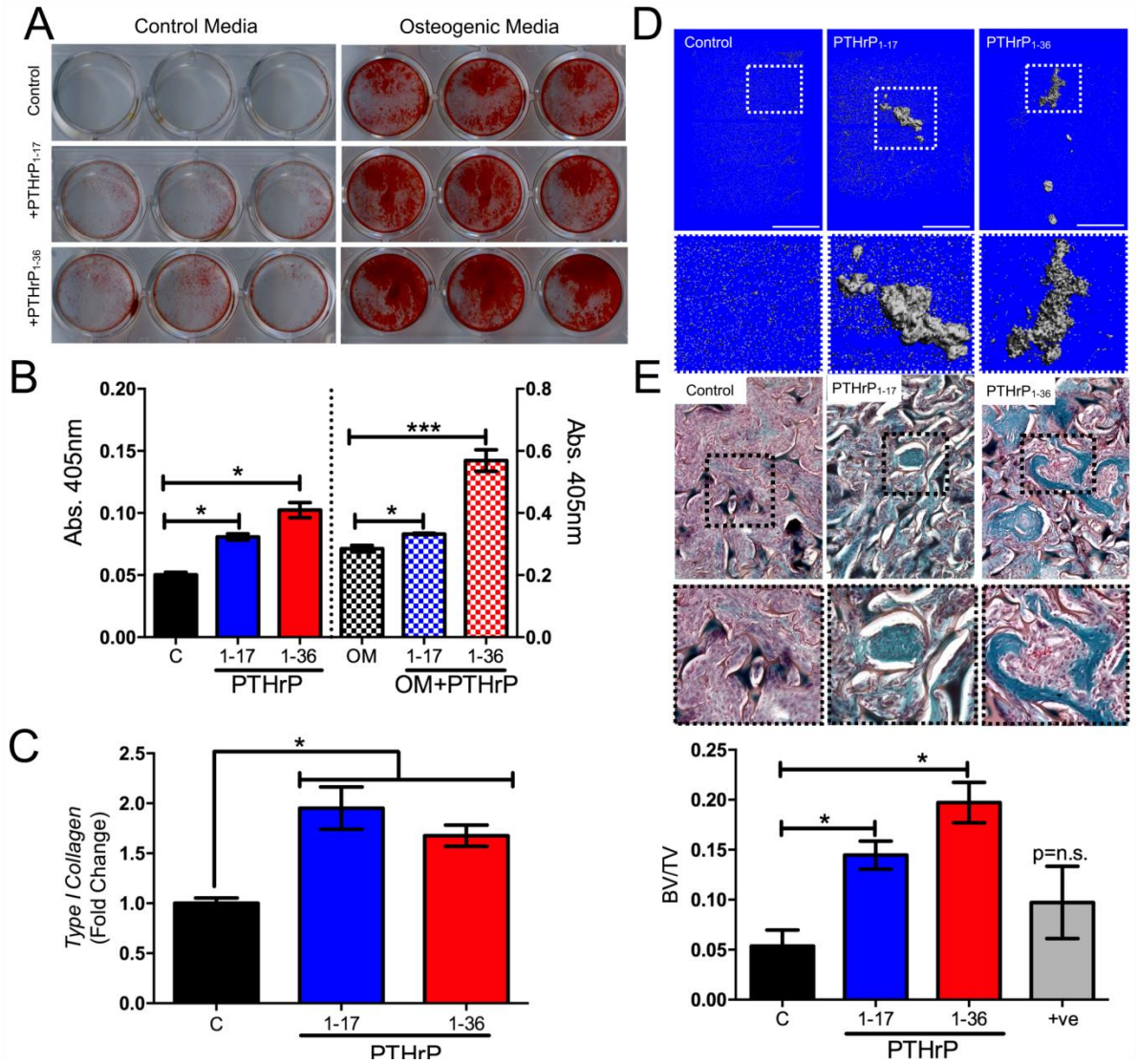

Figure 2-11. $PTHrP_{1-17}$ Promotes MSC and Osteoblast Differentiation

*(**A**) Alizarin red staining of primary MSCs (n = 3) treated with $PTHrP_{1-17}$ versus $PTHrP_{1-36}$ (10 nM every other day for 16 days) in either normal media or in osteogenic media. (**B**) Quantitation of alizarin red intensity in control and osteogenic media (OM) treated cells treated with the indicated PTHrP peptides. (**C**) Analysis of Type I Collagen expression in MC3T3 osteoblasts treated with $PTHrP_{1-17}$ or $PTHrP_{1-36}$ (10 nM for 48 hours). RT qPCR was used to quantitate the relative fold change in expression. (**D**) Representative μCT scans of ectopic ossicles in control, $PTHrP_{1-17}$ or $PTHrP_{1-36}$ treated mice (n=3/group, 4 implants/mouse). Scale bars are 1 mm. Dashed box represents area of magnification. (**E**) Trichrome stained sections derived from control, $PTHrP_{1-17}$ or $PTHrP_{1-36}$ treated mice were quantitated for the amount of bone matrix (blue-green color). Dashed box represents area of magnification. Asterisks denote significance (*p<0.05; *** p<0.001); n.s., non-significance.*

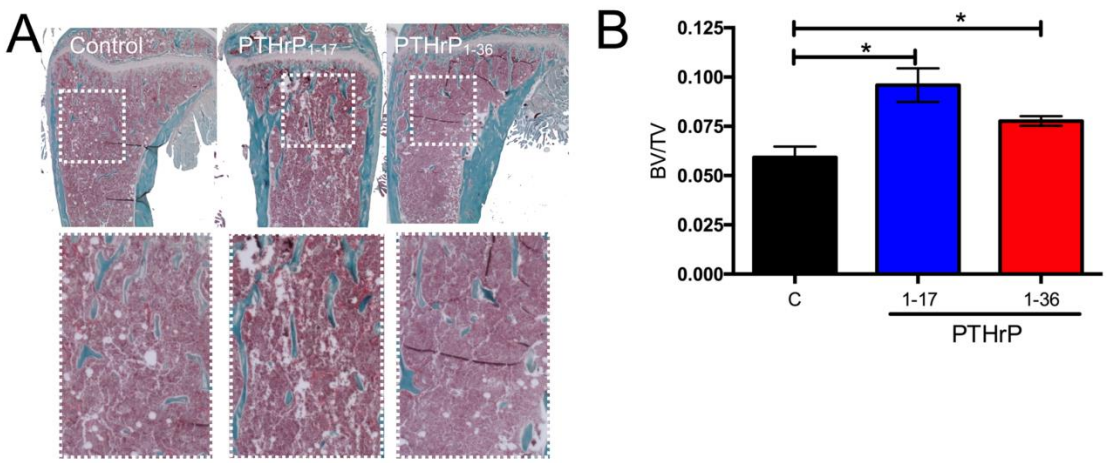

Figure 2-12. PTHrP$_{1-17}$ Promotes Bone Formation

*(**A**, **B**). BV/TV analysis of trabecular bone formation in tibias derived from ectopic ossicle bearing mice (n=3/group) treated with saline (Control), PTHrP$_{1-17}$ or PTHrP$_{1-36}$. Dashed box (**A**) represents area of magnification. Graph (**B**) indicates bone volume to tissue volume measurements (BV/TV).*

2.3.5 PTHrP$_{1-17}$ Does Not Affect Osteoclastogenesis and Bone Resorption

PTHrP$_{1-36}$ promotes bone resorption by inducing the expression of factors such as RANKL [229, 234]. Treatment of whole bone marrow co-cultures with PTHrP$_{1-36}$ revealed increased *RANKL* expression as expected, but this response was not observed following treatment with PTHrP$_{1-17}$ (Figure 2-13 A). We also noted that PTHrP$_{1-36}$ appeared to suppress the expression of *osteoprotegerin* (*OPG*), which inhibits osteoclastogenesis (Figure 2-13 A). Real time PCR analyses confirmed these observations and demonstrated PTHrP$_{1-36}$ significantly enhanced *RANKL* expression while suppressing *OPG* (Figure 2-13 B-C). PTHrP$_{1-17}$ had no effect on the expression of either of these genes. Taken together, the ratio of average *RANKL:OPG* transcripts was lower in PTHrP$_{1-17}$ versus PTHrP$_{1-36}$ treated cells (1.61 vs. 15.03, respectively). These findings suggest that PTHrP$_{1-17}$ does not contribute to osteoclastogenesis. To

test this, we performed *in vitro* osteoclast formation assays using whole bone marrow co-cultures. As expected, $PTHrP_{1-36}$ induced robust osteoclast formation, but

Table 2-4. Changes in Osteogenic Gene Expression in $PTHrP_{1-17}$ Treated MSCs

Gene	$PTHrP_{1-17}$	$PTHrP_{1-36}$
	Fold Regulation	**Fold Regulation**
Gli1	**3.29**	**2.02**
Col2a1	**2.2**	1.68
Egf	1.74	1.39
Tnf	1.66	-1.05
Dlx5	1.61	1.62
Gusb	1.44	1.54
Csf2	1.41	-1.25
Tgfb3	1.4	1.31
Col1a1	1.38	1.33
Bmp4	1.34	1.35
Flt1	1.34	-1.03
Tgfb2	1.33	1.12
Anxa5	1.27	1.38
Runx2	1.25	1
Itga3	1.2	1.31
Tnfsf11	1.2	1.87
Ctsk	1.19	1.31
Cd36	1.14	1.2
Fgfr2	1.14	1.04
Tgfbr2	1.14	-1.18
Col3a1	1.13	-1.15
Igf1r	1.12	-1.11
Alpl	1.1	-1.11
Col1a2	1.1	1.21
Bmpr1a	1.07	1.03
Bglap	1.06	1.19
Icam1	1.06	1.83
Smad1	1.06	-1.07
Col5a1	1.04	-1.07
Fgf2	1.04	-1.1
Pdgfa	1.04	1.29
Bmp1	1.03	-1.13
Smad4	1.02	-1.07
Tgfb1	1.02	1.09
Tgfbr3	1.01	-1.31
Twist1	1.01	1.02
Gapdh	1.01	-1.05
Nfkb1	-1	-1.06
B2m	-1.01	1.05
Acvr1	**-1.02**	**-1.24**
Smad2	-1.02	1.04
Sox9	-1.02	1.26
Vegfb	-1.02	-1.09
Actb	-1.02	-1.11
Itga2b	-1.03	1.19
Tgfbr1	-1.03	-1.13
Col4a1	-1.04	-1.07
Itgb1	-1.04	-1.06

Table 2-4. (continued)

Gene	$PTHrP_{1-17}$	$PTHrP_{1-36}$
	Fold Regulation	**Fold Regulation**
Sost	-1.04	-1.55
Itgav	-1.05	-1.05
Hsp90ab1	-1.06	-1.1
Bgn	-1.08	-1.12
Bmpr2	-1.08	-1.48
Smad5	-1.08	1.02
Serpinh1	-1.09	-1.08
Chrd	-1.11	-1.39
Vdr	-1.11	-1.2
Bmp2	-1.12	-1.44
Cdh11	-1.12	-1.32
Col10a1	-1.12	-1.12
Igf1	-1.13	-1.39
Mmp2	-1.14	-1.17
Fn1	-1.16	-1.47
Csf1	-1.18	-1.18
Vegfa	-1.22	-1.09
Fgfr1	-1.24	-1.23
Ihh	-1.25	1.16
Nog	-1.26	1.13
Mmp9	-1.28	1.01
Fgf1	-1.29	-1.84
Bmp3	-1.32	1.77
Bmp7	-1.32	1.16
Gdf10	-1.32	1.16
Spp1	-1.32	-1.16
Comp	-1.38	**-2.61**
Vcam1	-1.43	-1.26
Bmpr1b	-1.5	-1.78
Smad3	-1.51	-1.51
Bmp6	-1.68	-1.7
Phex	-1.8	-1.53
Mmp10	-1.96	1.04
Ahsg	**-2**	1.12
Itga2	**-2.04**	-1.31
Mmp8	**-2.14**	**-2.64**
Sp7	**-2.21**	1.52
Itgam	**-2.29**	**2.1**
Csf3	**-2.45**	**-1.95**
Col14a1	**-3.05**	**-2.04**
Bmp5	**-3.41**	1.13

$PTHrP_{1-17}$ had no effect on osteoclastogenesis (Figure 2-13 D-E). To determine if this differential effect of $PTHrP_{1-17}$ was also manifest *in vivo*, a calvarial injection assay was performed. In this model, repeated injections of $PTHrP_{1-36}$ (every 6 hours; continuous treatment regimen) over the calvaria promotes extensive osteolysis [225]. Mice

continuously treated with $PTHrP_{1-36}$ displayed areas of extensive bone resorption while those injected with $PTHrP_{1-17}$ did not (Figure 2-13 F). TRAcP staining confirmed that there were significant increases in bone-lining osteoclasts in the $PTHrP_{1-36}$ treated mice compared to $PTHrP_{1-17}$ and control groups (Figure 2-13 G). Finally, the differential effects of $PTHrP_{1-17}$ and $PTHrP_{1-36}$ on osteoclast activity were further supported by neonatal calvaria *ex vivo* assays. We found that calvaria treated with $PTHrP_{1-36}$ displayed significant degradation of the calvaria, and that there was no evidence of bone formation (Figure 2-14 A). In contrast, $PTHrP_{1-17}$ treatment significantly increased bone formation (Figure 2-14 B). Thus, $PTHrP_{1-17}$ selectively promotes osteogenesis.

2.3.6 **$PTHrP_{1-17}$ is Generated by Cancer Cells**

To address if the $PTHrP_{1-17}$ peptide could be detected in biological samples, $PTHrP_{1-17}$-specific antibodies were generated for immunoprecipitation and downstream mass spectrometry (Figure 2-15 A). The lead antibody, clone 2D11 (CPTC-PTHrP-1), detects $PTHrP_{1-17}$ and $PTHrP_{1-36}$ at concentrations as low as 10ng but did not cross react with the $PTHrP_{27-36}$ peptide (Figure 2-15 B). Immunoprecipitation followed by mass spectrometry (IP-MS) [235, 236] allowed for the detection of, and delineation between, $PTHrP_{1-17}$ and $PTHrP_{1-36}$ in multiple PTHrP peptide mixtures (Figure 2-15 C).

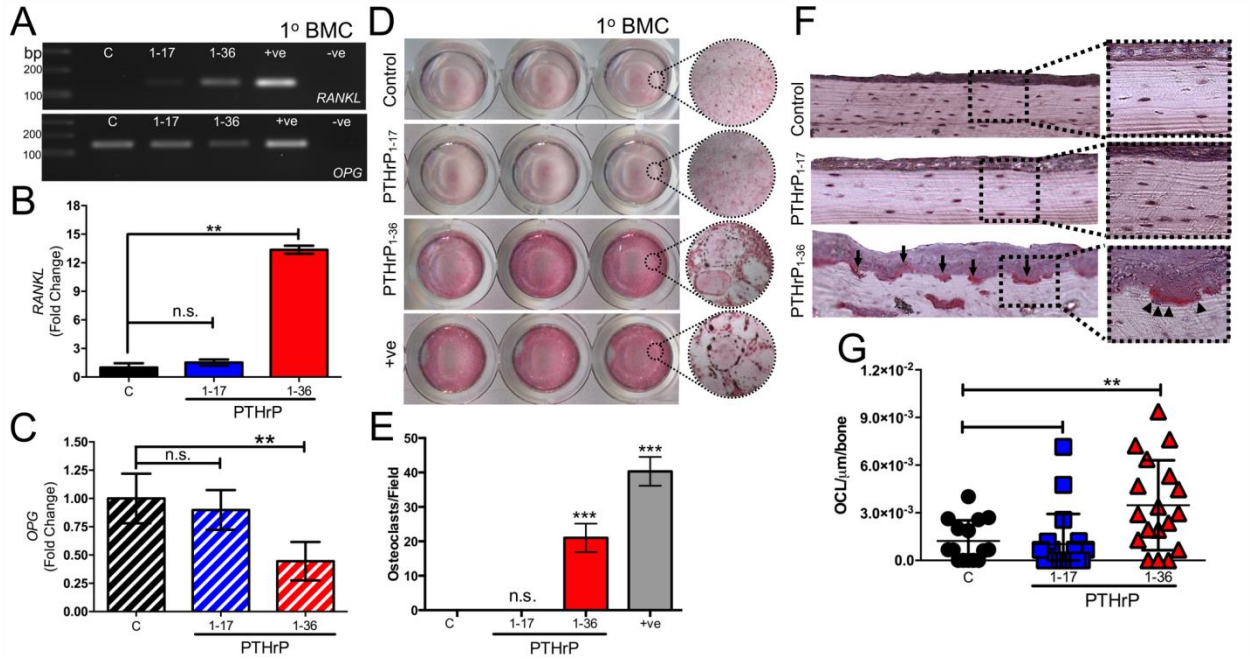

Figure 2-13. PTHrP$_{1-17}$ Does Not Stimulate Osteoclastogenesis and Bone Resorption

*(**A**) Expression of RANKL and OPG in response to PTHrP$_{1-17}$ and PTHrP$_{1-36}$ treatment (10 nM for 48 hours) in primary bone marrow cultures (1^{o}BMC). PTHrP$_{1-36}$ stimulated MC3T3 osteoblasts were used as a positive control (+ve), while non-template was used as a negative control (-ve). (**B** and **C**) RT-qPCR analyses of effects of PTHrP$_{1-17}$ or PTHrP$_{1-36}$ on RANKL (B) and OPG (C) expression in bone marrow cultures (n=3/group). (**D** and **E**) Bone marrow co-cultures were treated for 5 days with PTHrP$_{1-17}$ or PTHrP$_{1-36}$ (10 nM). Recombinant RANKL was used as a positive control (+ve). The number of TRAcP positive osteoclasts per field of view (**D**) were counted in each well (**E**). (**F** and **G**) The number of multinucleated osteoclasts/µm of bone (arrows, **F**) was determined in multiple tissue sections derived from animals in each group (n=3/group) (**G**). Asterisks denote statistical significance (*, p<0.05; **, P<0.01); n.s., non-significant values.*

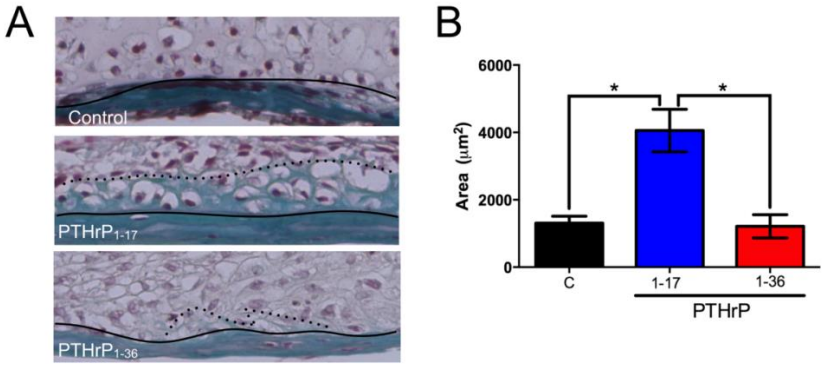

Figure 2-14. PTHrP$_{1-17}$ Increases Bone Formation in Ex Vivo Calvaria Organ Cultures

*(**A** and **B**) Neonatal ex vivo hemi-calvaria (n=3/group) were treated daily with control media, or media containing PTHrP$_{1-17}$ or PTHrP$_{1-36}$ (10 nM for 14 days). The area of new bone formation (distance between the solid and dashed line; (**A**) was measured in multiple sections for each condition (**B**). Representative images from each group are illustrated. Asterisk denotes significance (p<0.05); n.s., non-significant differences.*

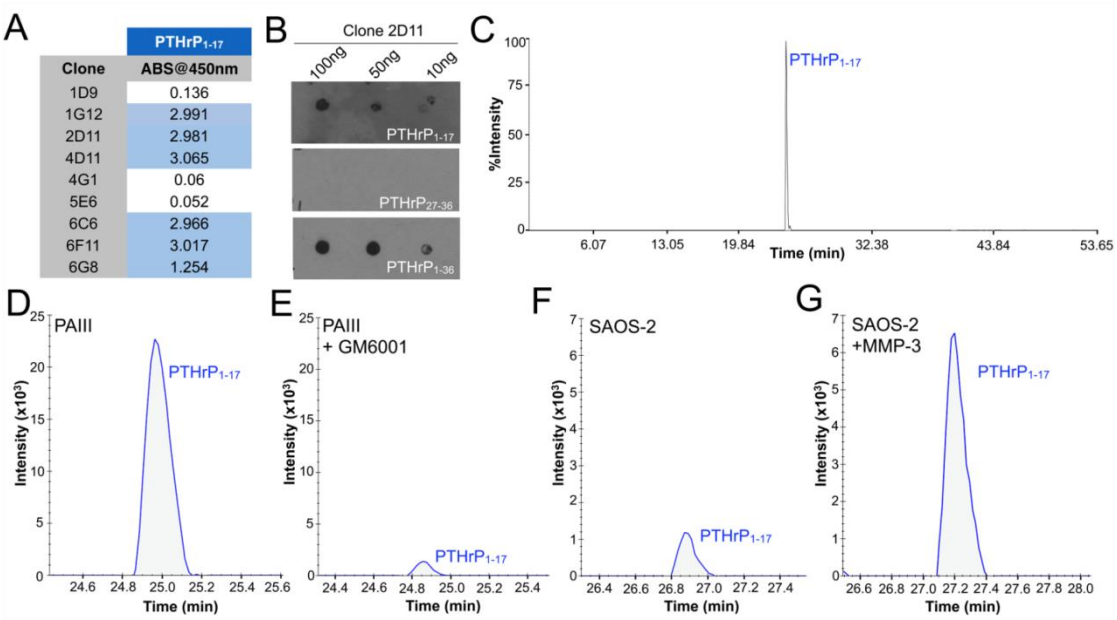

Figure 2-15. MMP Generation of PTHrP$_{1-17}$ in Cancer Cells

*(**A**) Antibodies were raised against PTHrP$_{1-17}$ and the ability of isolated clones to detect the peptide was measured by ELISA. (**B**) Dot blot titration of clone 2D11 against 100, 50 and 10 ng of PTHrP$_{1-17}$, PTHrP$_{27-36}$ and PTHrP$_{1-36}$. (**C**) IP-MS detection of PTHrP$_{1-17}$ after immunoprecipitation with 2D11 from an equimolar mixture of PTHrP$_{1-17,}$ PTHrP$_{18-26,}$ PTHrP$_{27-36}$ and PTHrP$_{1-36}$ peptides. The peak detected at 25 minute corresponds to PTHrP$_{1-17}$. (**D** and **E**) IP-MS of PTHrP$_{1-17}$ from the conditioned media of the prostate cancer cell line, PAIII treated in the absence (**D**) or presence (**E**) of the broad spectrum MMP inhibitor GM6001. (**F** and **G**). IP-MS of PTHrP$_{1-17}$ from the conditioned media of the human osteosarcoma cell line SAOS-2. SAOS-2 cells were treated in the absence (**F**) or presence of recombinant MMP-3 (**G**). The blue lines in **D**-**G** represent endogenous PTHrP$_{1-17}$ at the +3 charge state.*

PTHrP is expressed by a number of cancer cell lines, including those of a prostate and osteosarcoma origin (Figure 2-16). We collected conditioned media from PTHrP-expressing PAIII rat prostate adenocarcinoma cells incubated in the presence or absence of a broad-spectrum MMP inhibitor, GM6001. IP-MS of PAIII conditioned media clearly demonstrated the presence of PTHrP$_{1-17}$ and that MMP inhibition reduced the amount of this product (Figure 2-15 D and E).

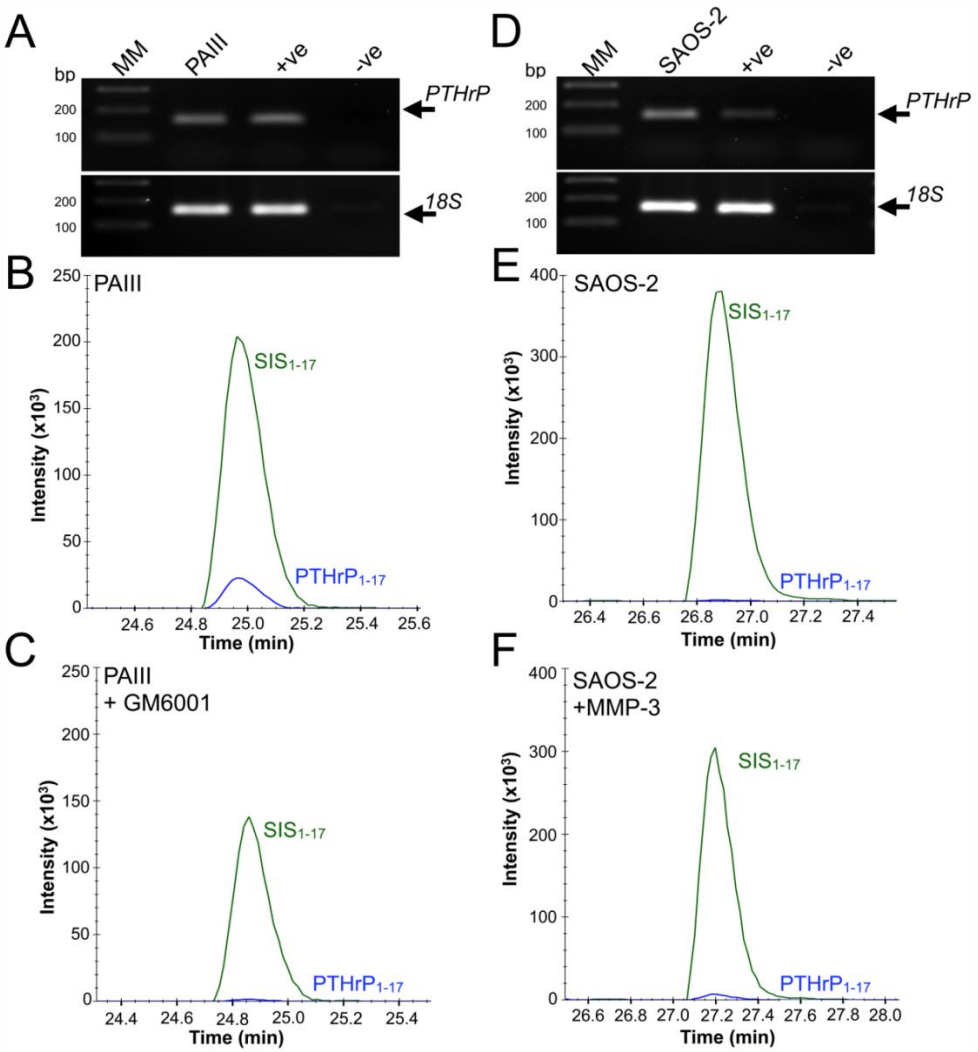

Figure 2-16. Expression and Quantitation of $PTHrP_{1-17}$ in Cancer Cells using SIS Peptides

*(**A**) Expression of PTHrP in by the prostate cancer cell line PAIII. MC3T3 osteoblasts were used as a positive control (+ve), while non-template was used as a negative control (-ve). 18S was used as a loading control. Molecular weight markers are illustrated in base pairs (bp). (**B** and **C**). IP-MS of $PTHrP_{1-17}$ from the conditioned media of PAIII cells treated in the absence (**D**) or presence (**E**) of the broad spectrum MMP inhibitor GM6001. Graphs include the SIS_{1-17} internal standards that allow for the determination of $PTHrP_{1-17}$ endogenous levels. For graphs **B**, **C**, **E** and **F**, the blue line represents endogenous $PTHrP_{1-17}$ at the +3 charge state while the green line represents the stable isotope labeled standard (SIS) $PTHrP_{1-17}$ peptide at the +3 charge state (20fmol per injection). (**D**) Expression of PTHrP in by the osteosarcoma cell line SAOS-2. A549 cells were used as a positive control (+ve), while non-template was used as a negative control (-ve). 18S was used as a loading control. Molecular weight markers are illustrated in base pairs (bp). (**E** and **F**). IP-MS of $PTHrP_{1-17}$ from the conditioned media of the prostate cancer cell line, PAIII cells were treated in the absence (**D**) or presence (**E**) of recombinant active MMP-3 (100 ng/ml overnight). Graphs include the SIS_{1-17} internal standard that allowed for the determination of $PTHrP_{1-17}$ endogenous levels.*

The incorporation of stable isotope labeled standards (SIS_{1-17}) allowed for the quantification of peak areas from IP-MS experiments and demonstrated GM6001 treatment reduced the amount of $PTHrP_{1-17}$ by 77% (PaIII = 0.13, PaIII+GM6001 = 0.03; Figure 2-16 B and C). Conversely, despite the detection of *PTHrP* transcripts in SAOS-2 osteosarcoma cells, levels of $PTHrP_{1-17}$ in SAOS-2 conditioned media were low compared to those in PAIII (Figure 2-15 F). However, overnight incubation of SAOS-2 cells with recombinant exogenous MMP-3 resulted in the enhanced detection of the $PTHrP_{1-17}$ peptide (Figure 2-15 G). Use of SIS_{1-17} demonstrated that the addition of MMP-3 increased $PTHrP_{1-17}$ levels by 400% (SAOS-2 = 0.004, SAOS-2+MMP-3 = 0.03, Figure 2-15 E and F). These data show that $PTHrP_{1-17}$ can be biologically generated by cancer cells and in turn this novel MMP generated product can selectively promote osteogenesis.

2.4 Discussion

MMPs regulate bone matrix turnover as well as the bioactivity and bioavailability of non-matrix factors such as RANKL and TGFβ that are important for bone remodeling. Here we have shown that MMPs also process $PTHrP_{1-36}$ to yield a distinct, biologically active peptide, $PTHrP_{1-17}$, which can be generated by cancer cells. Notably, $PTHrP_{1-17}$ promotes osteogenesis yet has no effect on osteoclast formation and bone resorption. This suggests that MMP-directed cleavage of $PTHrP_{1-36}$ is a new means for post-translationally regulating the potent osteolytic effects of this hormone, which has important implications for our understanding of bone remodeling and skeletal malignancies (Figure 2-17).

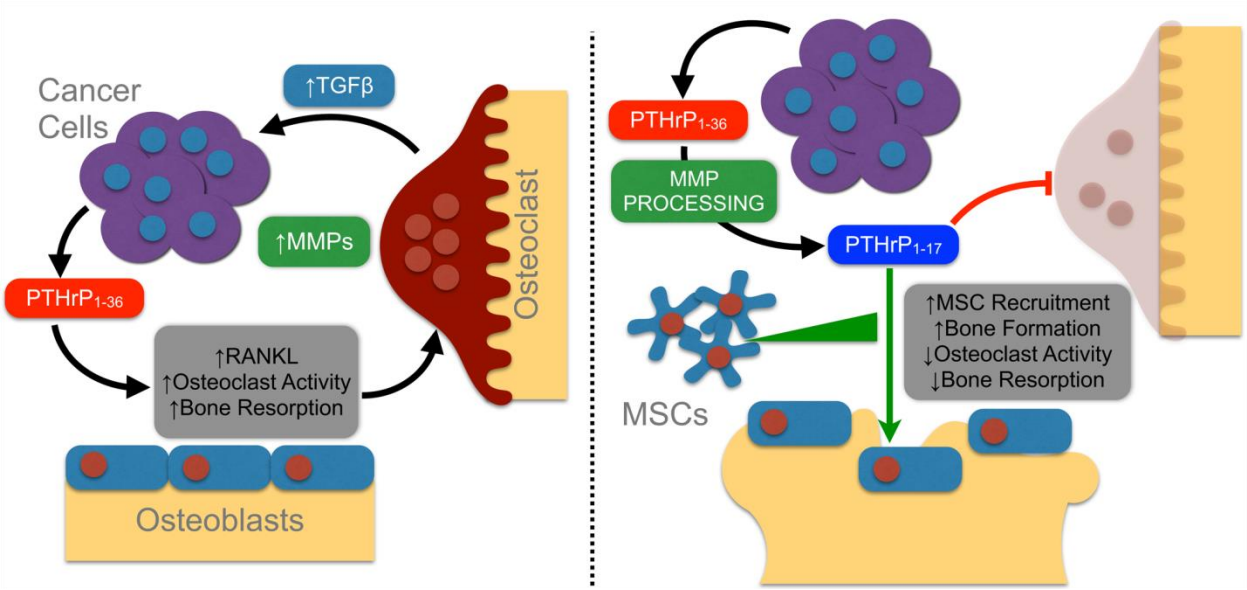

Figure 2-17. $PTHrP_{1-17}$ Working Model in Bone Metastatic Cancer

*(**A**) The initiation of the vicious cycle involves the secretion of $PTHrP_{1-36}$ from bone metastatic prostate cancer cells which leads to the induction of RANKL, osteoclastogenesis and the release of growth factors from the bone matrix such as TGFβ that enhance tumor survival. MMP expression is also heightened at the tumor bone interface. (**B**) Heightened MMP expression leads to the generation of $PTHrP_{1-17}$ that in turn can promote osteogenesis while preventing osteoclastogenesis. Further, $PTHrP_{1-17}$ can promote the recruitment of MSCs that can contribute to the osteogenic response.*

Previous studies have shown that $PTHrP_{1-36}$ is susceptible to proteolytic processing, but MMP generated $PTHrP_{1-17}$ appears to be a distinct product. PSA/kallikrein-3 and neprilysin have both been shown to generate $PTHrP_{1-23}$ [168, 169]. Our mass spectrometry data show that a 1-26 fragment can be generated by MMPs but that this species is rapidly reduced to $PTHrP_{1-17}$. Comparative kinetic analyses between enzymes capable of processing $PTHrP_{1-36}$ may reveal the dominant protease involved, but it is likely that spatial and temporal factors dictate which protease controls $PTHrP_{1-36}$ cleavage. Further, serine proteases and MMPs may reciprocally activate each other. For example, PSA can regulate MMP-2 activity while, conversely, MMPs can activate

kallikreins, suggesting that proteolytic cascades could converge to process $PTHrP_{1-36}$ [237, 238]. It is also possible that $PTHrP_{1-36}$ can induce the expression of MMPs that in turn process the hormone. For example, PTHrP is known to induce the expression of MMP-2, -3 and -9 in growth plate chondrocytes [239]; the induction of MMPs by $PTHrP_{1-36}$ may result in a feedback loop that dampens osteolytic stimuli once bone resorption has been initiated. Further, PTHrP has also been shown to induce the expression of MMP-13 [240], but interestingly, our data show MMP-13 does not yield a $PTHrP_{1-17}$ fragment, again pointing to distinct roles for specific proteases in regulating $PTHrP_{1-36}$ activity.

Adding further complexity to PTHrP regulation, a recent report has demonstrated that serum levels of $PTHrP_{12-48}$ are a prognostic marker for bone metastatic breast cancer [175], indicating that a $PTHrP_{1-11}$ fragment is also generated. Our mass spectrometry analyses show that MMPs do not reduce PTHrP further than $PTHrP_{1-17}$, implying that other proteases must be involved in generating this shorter species [128]. Whether $PTHrP_{1-11}$ retains biological activity is undetermined, but this is possible given the importance of the first two *N*-terminal amino acids in activating PTH1R [128]. Our studies indicate that $PTHrP_{1-17}$ retains biological activity and PCR array data specifically indicate that treating MSCs with $PTHrP_{1-17}$ induces changes in osteogenic gene expression similar to $PTHrP_{1-36}$. Notably, both *Gli1* and *MMP-8* expression were downregulated. Interestingly, *Gli1* is a Hedgehog (Hh) signaling transcription factor that has previously been implicated with the expression and activation of various MMPs [241-243], and the related *Gli2* transcription factor is involved in the expression of PTHrP [244, 245]. $PTHrP_{1-17}$ treatment also resulted in decreased expression of bone

morphogenetic protein 5 (*BMP5*), while BMPs 1, 2, 3, 5, 6, and 7 remained largely unchanged. It is unclear why *BMP5*, which together with other BMPs are involved in osteogenesis, would be downregulated, however there are reports implicating BMP5 in osteoclast formation [246]. Given the predominantly osteogenic activities of $PTHrP_{1-17}$, reduced BMP-5 expression may help evade osteoclastogenesis. It is also likely that some variations in osteogenic gene expression could be a result of the phasic nature of osteogenic gene expression during osteogenic differentiation [247, 248]. Importantly, our results also indicate that $PTHrP_{1-17}$ and $PTHrP_{1-36}$ induce differential gene expression. Particularly evident is the $PTHrP_{1-17}$ induced -2.29 fold decrease in *Itgam* expression whereas $PTHrP_{1-36}$ treatment resulted in a 2.10 fold increase. *Itgam* codes for CD11b which has roles in regulating osteoclastogenesis of macrophage/monocyte lineage precursors [249]. Although CD11b expression from a mesenchymal lineage is not traditionally associated with osteoclast formation, the formation of osteoclasts is dependent on activity of mesenchymal lineage cells such as osteoclasts. Decreased expression of CD11b by MSCs in response to $PTHrP_{1-17}$ might be one factor contributing to the reduced osteoclast formation seen in our studies of $PTHrP_{1-17}$; however, these cellular interactions would require further study. Additionally, it is easy to speculate that additional genes and genetic programs are differentially regulated by $PTHrP_{1-17}$ and $PTHrP_{1-36}$ as well.

$PTHrP_{1-36}$ is generated from a full-length form of PTHrP of up to 173 amino acids. We focused exclusively on peptides generated from $PTHrP_{1-36}$, however, products generated from the remaining 37-173 sequence of PTHrP can impact bone remodeling [128, 250]. For example, osteostatin is generated via cleavage of PTHrP at amino acids

107-111/139 and is a potent inhibitor of osteoclastogenesis [187, 251]. The proteases responsible for generating this fragment have not been identified, but it is tempting to speculate that MMP generation of osteogenic $PTHrP_{1-17}$ coupled with the generation of osteostatin would further promote the anabolic effects of PTHrP following the resorptive phase. It is also noteworthy that $PTHrP_{87-107}$ contains a nuclear localization sequence that supports osteoblast survival and matrix mineralization [252]. Whether this fragment is generated by MMPs remains to be explored. Understanding the precise temporal sequence of how PTHrP is cleaved is needed to define the complex roles it plays in regulating the catabolic and anabolic phases of bone remodeling.

$PTHrP_{1-36}$ activation of PTH1R leads to cAMP generation and calcium flux [155]. Our studies show that $PTHrP_{1-17}$ rapidly induces calcium flux and ERK phosphorylation in osteoblasts but unlike $PTHrP_{1-36}$, does not affect cAMP generation or CREB phosphorylation. Previous studies have shown that ERK phosphorylation is enhanced via the PKC pathway and promotes osteogenic differentiation [253]. Additionally, PTH1R-induced cAMP triggers CREB phosphorylation and the induction of RANKL [229]. In contrast to $PTHrP_{1-36}$, $PTHrP_{1-17}$ has no effect on RANKL expression in osteoblasts. Thus, we posit that $PTHrP_{1-17}$ activation of PTH1R leads to osteoblast differentiation and bone formation by promoting calcium flux and ERK phosphorylation. In accord with this notion, the *N*-terminal domain of PTHrP and PTH can stimulate calcium flux via PTH1R [254]. In contrast, other studies have shown that *N*-terminal fragments of PTHrP and PTH can stimulate PKA and cAMP activation [155, 160], yet this effect is not observed in $PTHrP_{1-17}$-treated primary bone cell cultures and osteoblast cell lines. In agreement with our findings, a recent study demonstrated that $PTHrP_{1-16}$

does not result in cAMP production but interestingly also had no effect on calcium flux using PTH1R over expressing CHO-K1 cells [155]. This may indicate that either the glutamine at amino acid position 17 in PTHrP is an important mediator of calcium flux or that PTH1R activates different signaling effectors in osteoblasts. Based on PTH1R knockdown studies it is clear that the effects of $PTHrP_{1-17}$ are dependent on PTH1R and not on another GPCR such as endothelin-A [255, 256].

Our discovery of MMP processing of PTHrP has potentially important clinical implications. For example, bone metastatic prostate cancer contains both areas of osteolysis and aberrant bone formation [257]. Osteosarcoma and prostate cancer cells are now revealed to generate both $PTHrP_{1-36}$ and $PTHrP_{1-17}$, which could explain their divergent effects on osteogenesis rather than osteolysis. This is further supported by the ability of both $PTHrP_{1-36}$ [26, 258] and $PTHrP_{1-17}$ to recruit MSCs and osteoblast precursors (Figure 2-10). $PTHrP_{1-36}$ expression is highly associated with osteolytic lesions such as bone metastatic breast cancer and multiple myeloma. While $PTHrP_{1-17}$ may also be generated in these skeletal malignancies, the overall balance of osteolytic to osteogenic factors in these scenarios favors osteolysis. Our current research centers on the detection of $PTHrP_{1-17}$ in the serum of prostate cancer patients with primary, castration resistant, and metastatic castration resistant prostate cancer to determine whether $PTHrP_{1-17}$ can be used as a potential readout for occult bone metastases or progression of bone metastatic disease. We are also using genetic approaches to eliminate MMPs in the host and cancer cell compartments to identify the key MMP responsible for the generation of $PTHrP_{1-17}$ *in vivo*. Finally, the ratio of $PTHrP_{1-36}$ to $PTHrP_{1-17}$ has implications for other diseases such as osteoporosis, and may potentially

explain the differential effects of chronic versus intermittent PTHrP administration on bone resorption versus formation.

Chapter 3. Prostate Cancer-derived Matrix Metalloproteinase-3 Promotes Tumor Growth in Bone

3.1 Introduction

The matrix metalloproteinases (MMPs) are a family of 17 secreted and 6 membrane bound zinc dependent endopeptidases traditionally associated with the ability to degrade extracellular matrix (ECM) components [259]. Since the first MMP was discovered to play a role in tadpole metamorphogenesis in 1962 [260], steady progress has been made in understanding how these enzymes are secreted and activated to influence critical biological processes such as embryogenesis and wound repair. MMPs are also associated with diseases such as cancer, where, based on their ability to degrade the extracellular matrix rich basement membrane, they were initially linked to promoting invasion and metastasis. However, it has become evident that MMPs are not simply extracellular matrix "bulldozers" and in fact collaborate with other proteases to exquisitely regulate normal physiological and cellular processes including differentiation, proliferation, and death [261].

3.1.1 Matrix Metalloproteinase Family and History

Historically, the MMP family has been classified into 6 groups: collagenases, gelatinases, stromelysins, matrilysins, and membrane type (MT). These classifications were primarily based on their original substrate specificities, sequence similarities, or domain organization patterns (Table 3-1). Structurally, a prototypical MMP consists of

an 80 amino acid pro-peptide, a 170 amino acid catalytic domain, a linker peptide (hinge region), and a 200 amino acid hemopexin domain [262]. With the exception of membrane type MMPs which remain anchored to the plasma membrane, the majority of MMPs are secreted as inactive zymogens referred to as proMMPs [259, 263]. Latency is maintained by the "cysteine switch" mechanism [264], where intramolecular interactions between a zinc molecule in the catalytic domain's active site and the conserved pro-peptide domain cysteine switch motif "PRCGXPD" inhibit proteolytic activity. Activation is achieved by delocalization of the pro-domain from the catalytic site. This can occur either by proteolytic cleavage of the pro-domain or by allosteric activation where the pro-domain is displaced without cleavage [265, 266]. The conformational change leads to dissociation of the cysteine from the zinc molecule and replaces it with water [264]. Proteases such as plasmin have been implicated in the activation of numerous proMMPs, including proMMP-1, proMMP-3, proMMP-7, proMMP-9, proMMP-10, and pro-MMP-13 [267]. Active MMPs can also to contribute to the processing and activation of additional proMMPs [268].

Figure 3-1. MMP Structural Domains

The majority of MMPs, including MMP-3, are comprised of a Signal Peptide (SP), Pro-Peptide, Catalytic Domain, Hinge Region, and Hemopexin Domain. Interactions between the catalytic and pro-peptide domains maintain proMMPs in their latent zymogen state.

The catalytic domain has traditionally been regarded as the functional portion of the enzyme since it is the domain responsible for substrate cleavage. Additionally, the catalytic domain contributes to substrate specificity via its active site cleft depth and sub site pockets, along with secondary substrate binding exosites [269]. When a substrate is bound in the catalytic domain, a water molecule is displaced from the catalytic zinc ion, leading to protonation of a glutamate residue at the active site and nucleophilic attack of the carbonyl group of the peptide bond and cleavage of the substrate [262]. A linker region connects the catalytic domain with the hemopexin domain. The hemopexin domain is important for the proteolytic activities of MMPs and is required for collagenases to cleave the collagen triple helix [270]. It can also contribute to substrate specificity [271]. Furthermore, several novel non-catalytic functions have also recently been ascribed to the hemopexin domains of MMP-3, MMP-7, and MMP-9 [272-274].

MMP activity is regulated by the endogenous expression of specific metalloproteinase inhibitors called tissue inhibitors of metalloproteinases (TIMPs) [268, 275]. TIMPs bind and insert into the MMP catalytic domain of at a 1:1 stoichiometry [270]. Four TIMPs (TIMP-1, TIMP-2, TIMP-3, and TIMP-4) have been identified, and there is some evidence suggesting that modulating their expression could be used to therapeutically target MMPs, however obtaining selectivity would likely prove difficult due to broad spectrum activity [268]. Additionally, TIMPs possess their own complicated biological activities independent of MMP inhibition. For example, TIMP-1 and TIMP-2 have both been associated with mitogenic activities of certain cell types, whereas TIMP-3 has been shown to be pro-apoptotic in certain tumor cells [276]. Therefore, the therapeutic use of TIMPs would need to be approached cautiously.

Table 3-1. The Matrix Metalloproteinase Family and Groups

Group	MMP	Enzyme Name	MW kDa (latent)	MW kDA (active)
Collagenases	MMP-1	Collagenase-1/Interstitial collagenase	55	45
	MMP-8	Collagenase-2/Neutrophil collagenase	75	58
	MMP-13	Collagenase-3	65	55
Stromelysins	MMP-3	Stromelysin-1	57	45
	MMP-10	Stromelysin-2	57	44
	MMP-11	Stromelysin-3	51	44
Gelatinases	MMP-2	Gelatinase-A	72	66
	MMP-9	Gelatinase-B	92	86
Matrilysins	MMP-7	Matrilysin-1/Pump-1	28	19
	MMP-26	Matrilysin-2	28	18
Membrane Type	MMP-14	MT1-MMP	63	n/a
	MMP-15	MT2-MMP	72	n/a
	MMP-16	MT3-MMP	64	n/a
	MMP-17	MT4-MMP	70	n/a
	MMP-24	MT5-MMP	60	n/a
	MMP-25	MT6-MMP/Leukolysin	62	n/a
Others	MMP-12	Macrophage elastase	54	45, 22
	MMP-19	n/a	57	45
	MMP-20	Enamelysin	54	22
	MMP-23	CA-MMP	Unknown (44?)	Unknown (34?)
	MMP-28	Epilysin	60	50

3.1.2 **MMP Inhibitors and Clinical Trials**

Because of their association with diseases like rheumatoid arthritis and cancer, where high expression often correlates with poor patient prognosis, MMPs were identified as candidates for pharmacological inhibition [261]. This led to the development of multiple broad spectrum MMP inhibitors. The first generation of MMP inhibitors were peptidomimetic, designed by mimicking the protein structure of collagen at the active site, and incorporated hydroxamate zinc binding groups [123]. However, alternative zinc binding groups such as carboxylates, hydrocarboxylates, and sulfhydryls, which coordinated rather than chelated the zinc, were eventually substituted for hydroxamate to provide greater flexibility and reversibility of the inhibitors. Despite efficacious anti-cancer activities in several pre-clinical *in vivo* models, the majority of these inhibitors failed to meet their endpoints in clinical trials [277, 278]. Reasons for the unsuccessful outcome are multifold, ranging from an inability to obtain an accurate readout for activity and efficacy to the actual clinical trial design and patient selection criteria [123, 277]. These difficulties were further complicated by an incomplete understanding of MMP biology as well as the design of the predominantly broad spectrum nature of the inhibitors themselves [277]. Following the unsuccessful clinical trials, a new approach was taken to study MMPs individually in order to improve targeting strategies. This new approach led to the generation of non-peptidomimetic inhibitors that took advantage of *a priori* knowledge of specific MMP active site 3D conformations and improved specificity [123]. Subsequent progress has been made applying a mechanism based targeting approach, leading to modern inhibitors like SC-3BT, which has been shown to reduce liver metastasis and improve survival in

preclinical mouse studies of T-cell lymphoma via selective inhibition of MMP-2 and MMP-9 [279]. Additional strategies including tetracycline derivatives and natural products have led to the development of inhibitors like Periostat® (FDA approved for prevention of periodontitis) and Neovastat (dual MMP/VEGF inhibitor). Together, the recent progress in developing selective inhibitors by taking advantage of improved knowledge of MMP biology and advances in chemistry provides rationale for continued efforts toward MMP inhibition in cancer [123].

3.1.3 **Rationale to Study Specific MMPs Individually**

An important conclusion from the early MMP inhibitor studies and clinical trials was that MMP biology is not as distinct as initially thought. Many of the unexpected side effects observed with the first generation of MMP inhibitors could be attributed to their broad spectrum nature. For example, batimastat (BB-94) inhibited MMP-1, -2, -3, -7, and -9 [280]. It is now recognized that many MMPs possess protective activities in addition to their causal roles during cancer progression [281]. Furthermore, despite their originally described role in extracellular matrix degradation, MMP substrates are much more diverse than initially known and include many non-matrix substrates such as growth factors, cytokines, and hormones [261]. Today, the non-matrix MMP substrate repertoire now significantly out numbers the matrix protein substrate repertoire [282].

There are currently more than 600 identified MMP substrates, and cleavage of these substrates is often essential for normal physiology [283]. Although the mechanisms are not fully understood, it is clear that numerous factors including their catalytic activities, non-catalytic functions, and temporal/spatial expression can contribute to the mixed roles observed for MMPs during tumorigenesis [284].

Consequently, MMPs need to be studied individually and with respect to specific tissues and/or cancers to develop selective inhibitors that will successfully treat disease. Researchers have looked at the roles of individual MMPs in various cancers such as breast and skin tumors where both pro- and anti-tumorigenic roles have been observed. As an example, MMP-7 has been shown to contribute to mammary tumorigenesis [57]. In contrast, ablation of MMP-8 resulted increased incidence of skin tumors in mice, suggesting that it offers protective roles [285]. Though studies of MMP-3 in cancer have been limited, the current knowledge of MMP-3 serves as a textbook example of the evolving field of MMP biology.

3.1.4 **Matrix Metalloproteinase-3**

3.1.4.1 ***Discovery, Structure, and Mutants***

MMP-3 was first identified in 1985 as a 51,000 kDa proteinase purified from rabbit synovial fibroblasts treated with tumor promoting agents such as 12-O-Tetradecanoylphorbol-13-acetate (TPA), cytochalasin B, and poly-HEMA [286]. In parallel, another group detected a highly expressed cDNA from transformed rat fibroblasts that went on to also be confirmed as MMP-3 [287]. Additional supporting evidence linking MMP-3 with cancer was demonstrated using the classic two stage initiation-promotion model of carcinogenesis, where a single dose of 7,12-DMBA followed up with repeated applications of TPA leads to the development of squamous cell carcinomas. Under these conditions, expression of MMP-3 was detected using *in situ* hybridization in 5 out of 6 tumors but not in benign papillomas [288]. Subsequent to these initial findings, many other studies have shown the correlation between MMP-3 and tumor progression [289, 290].

The utilization of animal models has greatly improved our understanding of MMPs in pathological situations as well as normal physiology. Understanding roles for MMPs in normal biology can help to identify those most suitable for inhibition and potentially avoid MMPs that might cause undesirable off target effects and toxicities if inhibited. Many animal models of systemic MMP ablation develop normally, a phenomenon believed to be a consequence of enzymatic overlap and functional redundancy in the MMP family [291]. This is true for MMP-3 knockout mice which display no overt phenotype, however developmental studies have revealed a few anomalies including altered neuromuscular junction structures [292] and a lack of secondary branching during mammary gland development [293]. Interestingly, despite cleaving numerous substrates involved with vascular development, including VEGF [294], there are no known developmental vascular phenotypes [295]. Also interesting is the lack of any skeletal abnormalities observed in other MMP null models, including MMP-9, MMP-13, and MMP-14 [296].

However, as with other MMP knockout animal models, phenotypes in MMP-3 knockout mice can manifest subsequent to challenges such as wound healing and acute injury. Several studies have reported on the importance for MMP-3 during wound healing. In particular, excisional wound healing, a necessary step for wound contraction and closure, is compromised in MMP-3 knockout mice due to deficient actin purse string formation [297]. Further studies using additional experimental wound models including dental pulp injury, contact hypersensitivity reaction, and rabbit corneal epithelial wound also support roles for MMP-3 in wound healing [298-301].

3.1.4.2 *Matrix Metalloproteinase-3 Substrates: Matrix vs. Non-Matrix*

MMP-3 cleaves a host of extracellular matrix proteins, including types II, III, IV, IX, X, and XI collagens, fibronectin, proteoglycans, and laminin [302-304]. Cleavage of these substrates contributes to the degradation of the basement membrane which facilitates the long-standing association of MMPs with cancer invasion and metastasis [296]. Degradation of the extracellular matrix has also been reported to release growth factors. Processing of many of these growth factors by MMP-3 can lead to their activation, inactivation, and occasionally result in novel functions of the cleavage products (Table 3-2). For example, insulin growth factor binding protein 3 (IGFBP3), which binds to insulin growth factor (IGF) 1 and 2 to extend its half-life and limit its activity in circulation was shown to be processed by MMP-3. The result of this processing is the release of active IGF-1 or IGF-2. The release of IGFs from IGFBP3 could be blocked by the addition of TIMP-1, implying that the mechanism of activation is MMP specific [305]. Similar to IGFs, TGF-β activity is regulated by interactions with other proteins. TGF-β is a well-known mediator of cellular activities and is secreted in a biologically inactive, latent form consisting of a TGF-β1 homodimer, latency associated protein (LAP), and latent TGF-β binding protein-1 (LTBP1). Multiple methods of TGF-β activation have been elucidated, including by proteolysis of the LAP. Such a mechanism was demonstrated for MMP-3, where rhMMP-3 was capable of cleaving the LAP to generate active TGF-β1 *in vitro,* an activity that could be blocked by both an anti-MMP-3 antibody and MMP inhibitors [306]. Similarly, heparin-binding EGF-like growth factor (HB-EGF) is cleaved in the juxtamembrane region by MMP-3, releasing soluble and bioactive HB-EGF *in vitro*. However, the regulation of basic fibroblast growth

Table 3-2. List of MMP-3 Substrates

MMP-3 Substrate	Biological Result	Reference
α1-Antichymotripsin	Inactivation	[307]
α1-Protease inhibitor	Inactivation	[307]
α2-Antiplasmin	Inactivation	[308]
α2-Macroglobulin	Hydrolysis	[309]
Aggrecan	Degradation	[310, 311]
Antithrombin-III	Inactivation	[307]
Collagens II, III, IV, IX, X, XI	Matrix degradation, growth factor release	[303, 304]
Decorin	Degradation releases TGF-β1	[312]
E-cadherin	Generates soluble ectodomain fragments that promote EMT and invasion	[313, 314]
Fibrinogen	Degradation	[315, 316]
Fibronectin	Matrix degradation, inflammation/arthritis	[317]
Heparin-binding EGF growth factor (HB-EGF)	Release of soluble, bioactive EGF	[318]
IGFBP-3	Degradation releases active IGF	[305, 319]
IL-1β	Activation	[320]
Latent TGF-β	Activation	[306]
MCP-1, -2, -3, and -4	Reduction of MCP agonism	[321]
Nidogen	Degradation	[322]
Osteopontin	Enhanced activity (cell migration)	[323]
Ovostatin	Hydrolysis	[309]
Perlecan	Degradation of perlecan releases bFGF	[324]
Plasminogen	Generation of angiostatin-like fragment	[325]
Plasminogen activator inhibitor-1 (PAI-1)	Inactivation	[326]
Pro-MMP-1, -3, -8, -9, and -13	Activation of the inactive zymogens	[327-330]
Pro-TNFα	Generates active TNFα	[331]
RANKL	Generates soluble RANKL	[211]
SDF-1	Inactivation	[332]
Serum amyloid A	Degradation	[333]
Substance P	Hydrolysis	[334]
Urokinase plasminogen activator (uPA)	Removes receptor binding domain	[335]

factor (bFGF) by MMP-3 occurs via a mechanism dependent on its ability to degrade the extracellular matrix component perlecan to which bFGF is bound. In this scenario, binding of bFGF with the five domain protein core of perlecan can actually facilitate presentation of the growth factor to cell surface receptors and receptor activation [336, 337]. MMP-3 has been reported to degrade the protein core of perlecan into multiple fragments, releasing bFGF, and potentially modulating bFGF bioactivity [324].

An important regulatory ability of MMPs is centered on cleavage and release of membrane bound molecules such as tumor necrosis factor alpha (TNFα) and FasL. The TNFα precursor is normally found anchored in the cell membrane and is solubilized by proteolytic cleavage [338]. It was first reported in 1995 that MMP-3 could cleave a recombinant pro-TNFα fusion protein to generate the mature TNFα, an observation that was reversed by adding MMP inhibitors [331]. Fas ligand (FasL) is also a member of the TNF family, and it is also processed by MMP-3. FasL exists in both membrane bound and soluble forms, with the soluble form reported to induce both pro- and anti-apoptotic activities [339, 340]. Interestingly, MMP-3 was shown to cleave membrane bound FasL at unique sites that generate novel, pro-apoptotic forms of soluble FasL [341]. The authors of the study speculate that the distinct MMP cleavage sites may offer an explanation to the inconsistent activities of soluble FasL. A follow-up study found that inducing MMP-3 expression in MC3T3 osteoblasts leads to enhanced solubilization of FasL and subsequent osteoclast apoptosis in a co-culture system [342]. The effect was abolished by specifically targeting MMP-3 using siRNA or inhibitors. Another TNF family member, RANKL, has been demonstrated to be an MMP-3 substrate as well. Like TNF-α, RANKL is anchored to the cell surface. It signals

through its receptor, RANK, in a juxtacrine manner to drive osteoclastogenesis, however MMP-3, as well as MMP-7, have been shown to cleave full-length RANKL [211]. N-terminal amino acid sequencing of the major cleavage product determined that RANKL was cleaved within the stalk region, suggesting that active, soluble RANKL is released by MMP-3 and MMP-7.

MMP-3 processing can also modify the activities of its substrates, as is observed with the cleavage of E-cadherin and osteopontin. It was first observed that expressing auto activating MMP-3 under control of a tetracycline-regulated promoter in normal mouse mammary epithelial cells resulted in EMT-like characteristics and increased invasiveness as determined by modified Boyden chamber assay. Interestingly, the application of the broad spectrum GM6001 MMP inhibitor abolished this transformation [313]. Follow up studies demonstrated that MMP-3 could produce soluble E-cadherin ectodomain fragments. These fragments were capable of inducing invasion and inhibiting cellular aggregation, which is in contrast to the canonical E-cadherin roles of suppressing invasion and aiding in epithelial aggregation. Osteopontin is a secreted phosphoprotein, which, like TGF-β, has putative roles in cell migration and survival as well as wound healing and inflammation [343, 344]. MMP-3 cleaves osteopontin at three distinct sites. The resulting cleavage products show enhanced activity compared to full length osteopontin, including migration and recruitment of macrophages [323].

Numerous instances have been also been reported where MMP-3 proteolysis can lead to inactivation of substrates, such as stromal cell-derived factor-1 (SDF-1) and monocyte chemoattractant protein-1 (MCP-1). SDF-1 is a chemokine normally involved in the regulation of hematopoietic stem cell (HSC) proliferation and survival, and it is

particularly important for the migration and homing of HSCs to the bone marrow [46, 345]. By cleaving the first four residues of SDF-1, MMP-3 processing abolishes the ability of SDF-1 to bind with CXCR-4 [332]. Similar to the SDF-1/CXCR4 axis, MCP-1 is a chemokine with normal roles in recruiting and activating monocytes. Interestingly, MMP-3 can cleave MCP-1 (as well as other family members MCP-2, 3, and 4), converting it from an agonist of CC chemokine receptors to an antagonist [321]. The inactivation of MCPs could play an important part in regulating inflammatory immune responses.

3.1.4.3 ***Non-Catalytic Roles for MMP-3***

Traditionally, most research has focused on the catalytic domains of MMPs, but non-catalytic roles for MMPs have recently been described with effects on both cell migration and survival, adding to the complexity of MMP biology [273, 274]. In addition to MMP-7 and MMP-9, there is evidence supporting non-catalytic activities for MMP-3 via its hemopexin domain. One study compared the impact of a full length MMP-3 construct with either a construct lacking the hemopexin domain or a construct featuring a point mutation in the catalytic domain. They found that in addition to inducing morphological changes characterized by cell scattering and reorganization of F-actin, the hemopexin domain was required for invasion and branching of mammary organoids in 3D cell culture gels [346]. The authors went on to discover that these changes were mediated through the interaction of the hemopexin domain with heat shock protein 90-β (HSP90β) but noted that additional factors including ANXA2, MARCKS, ADAM10, ADAMTS15, and Cathepsins A and L may also interact with the MMP-3 hemopexin domain [346]. In addition, separate reports identified that the MMP-3 hemopexin

domain alone could stimulate hypermorphic epithelial outgrowth similar to full length MMP-3 in a mammary fat pad transplantation model [272]. The study showed that the MMP-3 hemopexin domain interacts with the non-canonical Wnt ligand, Wnt5b, to sequester and inhibit ligand activity. However, MMP-3 can also proteolytically cleave the C-terminal domain as an additional mechanism of inhibiting non-canonical Wnt signaling. Together, this drives canonical Wnt signaling in the mammary gland as determined by measuring the levels nuclear β-catenin [272]. The importance of MMP-3 during mammary gland development has been well described, but in light of these new studies, it is possible that MMP-3 contributes to developmental processes in a non-catalytic manner [293, 313, 347, 348]. Similarly, the combined activities of the catalytic and hemopexin domains likely contribute to the roles that MMP-3 possesses in different cancers.

3.1.4.4 ***Pro- and Anti-Tumorigenic Roles for MMP-3 in Cancer***

3.1.4.4.1 Pro-Tumorigenic

MMPs were originally believed to promote cancer progression, and several examples of MMP-3 promoting tumorigenesis have been reported. A classic example of this was demonstrated in mammary tumorigenesis, where it was shown that upon expressing an auto-activating MMP-3 transgene in the SCp2 mouse mammary epithelial cell line, MMP-3 expression led a more invasive phenotype and enhanced mammary tumor formation [313]. Similar studies have indicated that inducing MMP-3 expression in normal mammary epithelial cells caused these cells to produce more invasive, mesenchymal like tumors [349]. Follow up studies placing MMP-3 under control of the whey acidic protein (WAP) gene promoter led to the spontaneous development of both

pre-malignant and malignant lesions in the mammary glands of mice [347]. In these studies, the effects could be reversed by co-expressing TIMP-1, suggesting that MMP-3 expression was the major factor regulating these changes. Additional studies utilizing the SCp2 mouse mammary epithelial cells have revealed that MMP-3 treatment induces a unique splice isoform of Rac1 called Rac1b. Expression of Rac1b led to increases in cellular reactive oxygen species (ROS) which in turn upregulated Snail and EMT [348]. This same study also showed that genomic instability was enhanced by MMP-3 and that it could be inhibited using the broad spectrum GM6001 MMP inhibitor. Later work expanded on these observations and demonstrated that expression of MMP-3 in mammary epithelial cells stimulated tumor formation and EMT in addition to the development of fibrosis [350]. More recently, it was shown that the induction of MMP-3 and SNAIL by TGF-β via eIF4E phosphorylation led to the initiation of EMT in primary mammary tumor cells. Blocking phosphorylation of eIF4E in a mouse mammary tumorigenesis model reduced lung metastases [351]. Silencing MMP-3 in 4T1 cells has also been shown to reduce tumor growth in multiple *in vivo* mammary tumorigenesis models and reduce lung metastasis in an orthotopic model [352].

MMP-3 also has contributory roles in other cancers of epithelial origin, including lung. In a study of primary lung cancer, MMP-3 was shown to induce Rac1b, leading to EMT and tumor development *in vivo* [353]. Recently, a similar trend has also been observed in glioma, where overexpression of Bmi-1, a regulator of tumor suppressor pathways found upregulated in multiple cancers, led to increased NF-κB activity and MMP-3 expression in T98G glioma cells. The authors report that these cells acquired increased metastatic potential as a result [354].

The cleavage of growth factors by MMP-3 may contribute to some of these reported pro-tumorigenic roles. For example, MMP-3 proteolysis of IGFBP3 increases the bioavailability of IGF, a growth factor associated with promoting cancer by enhancing growth and migration [355, 356]. Studies have shown that MMP-3 cleavage of IGFBP3 led to enhanced phosphorylation of IGF receptors and increased cellular proliferation which might promote tumor growth [357]. Similarly, increased availability of MMP-3 activated HB-EGF or TGF-β might stimulate oncogenesis. It has been shown that MMP-2 promotes breast tumor survival by controlling TGF-β activity, and MMP-7 can contribute to cutaneous squamous cell carcinoma and colon cancer by releasing and activating HB-EGF [58, 358, 359]. Another MMP-3 substrate, TNFα, is detected at higher levels in cancer patients and shown to promote tumor progression by activating NFkB and AP1 transcription factors (reviewed by [360]). TNFα has been shown to increase expression of CXCR4 and SDF-1 in ovarian cancer cells lines as well as patient biopsies leading to increased cell migration [361]. In this manner, MMP-3 mediated solubilization of TNF-α may contribute during tumorigenesis. It has also been shown that MMP-3 can cleave RANKL, and solubilization of RANKL by MMP-7 increases bone destruction induced by bone metastatic mammary tumors [211, 362].

Whereas many of the MMP-3 mediated proteolytic events are speculated to contribute to tumorigenesis, the cleavage of osteopontin and E-cadherin by MMP-3 have already been studied and linked to mechanisms that result in pro-tumor effects. There is a notable association between increased MMP expression and osteopontin expression during tumorigenesis [363]. In addition to increasing recruitment and migration of macrophages, MMP-3 generated osteopontin cleavage products also

enhanced tumor cell adhesion and migration [323]. E-cadherin cleavage also induced invasive behavior in mammary epithelial cells [314]. Though one could speculate that this was due to inactivation of E-cadherin, it was determined that the soluble fragments were actually inducing invasiveness via their own specific activities such as stimulation of signal transduction pathways [314].

3.1.4.4.2 Anti-Tumorigenic

Multiple instances of anti-tumorigenic roles for MMP-3 have also been reported. For example, a study in squamous cell carcinoma showed that although MMP-3 is expressed in all stages of tumor progression, stromal ablation of MMP-3 actually enhanced tumor initiation, leading to increases in the percentage of mice with surface lung metastases suggesting that stromal expression of MMP-3 may have a protective effect [364]. However, tumor-derived MMP-3 might have protective roles as well since a study in mammary tumorigenesis showed that induced expression of MMP-3 by MMTV did not yield any spontaneous mammary tumors after 2.5 years. When tumors were initiated experimentally using DMBA carcinogen, only 32% of the MMP-3 expressing mice developed tumors compared to 65% of the controls [365]. MMP-3 has also been shown to reduce invasion of MDA-MB-231 cells through a simulated basement membrane by degrading plasminogen into fragments that limit laminin degradation [366]. Interestingly, MMP-3 expression has been shown to be lost in advanced, aggressive breast cancer, suggesting that these protective roles may manifest clinically as well [367]. Although there are fewer studies reporting protective roles, they do suggest that continued studied is needed to fully understand in which cancers, at what

stages, from which tissues, and by what mechanisms MMP-3 might protects from or promotes tumorigenesis.

The cleavage of non-extracellular matrix factors by MMP-3 could again explain some of the anti-tumorigenic roles. For example, MMP-3 processing abolishes the ability of SDF-1 to bind with CXCR-4 [332]. Based on the previous studies demonstrating the importance of this mechanism in facilitating homing to the bone, this mechanism might offer protection against bone metastasis [47]. MCP-1 has a similar role to SDF-1. It normally functions to recruit monocytes, but it has been shown to be hijacked by tumor cells. Stromal MCP-1 has been shown to contribute to breast cancer and is also expressed by many prostate cancer cell lines and tissue specimens where it has been implicated in increasing proliferation, migration, and invasion [49, 368]. There is also evidence that it may be important for angiogenesis [369]. Therefore, inactivation of MCP-1 by MMP-3 proteolysis may also serve as a protective mechanism during cancer progression. Interestingly, the effects of TNFα on tumorigenesis can be varied [360]. While it is often found to correlate with increased tumorigenesis, evidence also suggests that high doses can lead to haemorrhagic necrosis [370]. High TNFα expression levels can also synergize with some forms of chemotherapy, likely by increasing the permeability of tumor vessels (reviewed by [371]). So although MMP-3 solubilization of TNFα could contribute to tumorigenesis as previously discussed, there is potential for this mechanism to generate anti-tumor effects depending on the context.

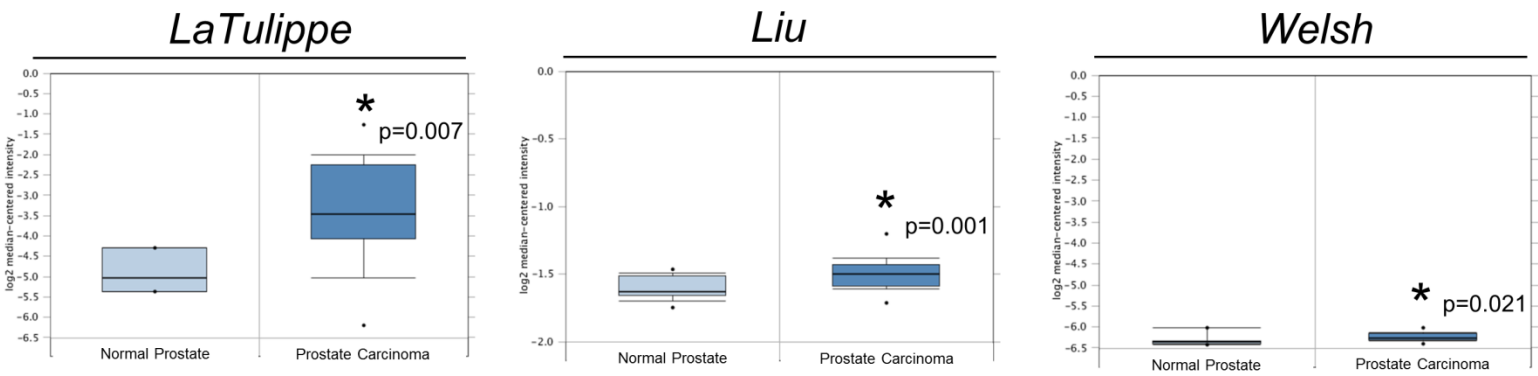

Figure 3-2. MMP-3 Expression in Normal versus Prostate Carcinoma

MMP-3 expression in normal prostate tissue versus prostate cancer was examined in three previously published datasets via Oncomine (https://www.oncomine.org). Datasets are publically available and archived as follows: LaTulippe = NCBI GEO DataSets GSE 68882, Liu = Array Express E-TABM-26, Welsh = http://public.gnf.org/cancer/prostate/). Asterisk denotes statistical significance (p<0.05).

3.1.4.5 ***MMP-3 in Prostate Cancer***

In general, MMP-3 has not been studied extensively in prostate cancer. Our own data-mining analysis of existing cancer databases via ONCOMINE (https://www.oncomine.org) shows significantly increased *MMP-3* expression in prostate carcinoma compared to normal prostate tissue in three separate datasets (LaTulippe: p=0.007, Liu: p=0.001, Welsh: p=0.021) (Figure 3-2) [372-374]. Additional analyses and wet lab studies of prostate cancer have discovered a mechanism where Eotaxin-1 drives increased MMP-3 expression to promote DU145 prostate cancer cell invasion and migration [375]. It was also shown that ERα expression in cancer associated fibroblasts (CAFs) leads to increased thrombospondin-2 (TSP-2) levels and decreased MMP-3 expression [376]. Co-implantation of 22RV1 prostate epithelial cells with these CAFs resulted in reduced levels of MMP-3 accompanied by fewer metastases and reduced angiogenesis *in vivo*. In bone, we and others have demonstrated that numerous MMPs are highly expressed in the tumor-bone microenvironment (Table 3-3), and several of these MMPs, including MMP-2, -7, and -9, have been shown to regulate factors that can affect prostate tumor growth [57-59, 211, 362]. However, no studies to date have looked at the direct impact of MMP-3 on prostate cancer growth in bone, a common organ for prostate cancer metastasis. Therefore, we sought to determine whether MMP-3 might contribute to or protect against tumor growth in bone.

Table 3-3. Elevated MMP Expression at the Tumor-Bone Interface

Laser capture microdissection and microarray analysis were used to investigate the expression of MMPs in the tumor-bone microenvironment. Compared to normal bone, MMP expression is increased at the tumor/bone interface [211].

MMP	Increase at Tumor/Bone Interface
MMP-13	3403%
MMP-7	1311%
MMP-3	366%
MMP-9	326%
MMP-2	320%
MMP-15	179%
MMP-10	129%
MMP-19	107%
MMP-11	106%
MMP-28	97%
MMP-8	96%
MMP-12	95%
MMP-24	92%
MMP-17	88%
MMP-23	85%
MMP-14	82%

Here we present evidence demonstrating that tumor derived MMP-3 contributes to prostate cancer growth in bone. We show that shRNA silencing of MMP-3 expression in prostate cancer cells reduces *in vitro* proliferation and *in vivo* intratibial tumor growth. In analyzing the conditioned media from these cells, we observed higher levels of the insulin growth factor binding protein-3 (IGFBP3), an established substrate of MMP-3 and mediator of IGF bioavailability [305, 319]. Further, MMP-3 knockdown

cells have lower levels of phosphorylated IGF-1R, ERK, and AKT compared to controls, suggesting that reduced IGF/IGF-1R signaling potentially contributes to the decreased proliferation. Taken together, our results suggest that tumor-derived MMP-3 contributes to the growth of bone metastatic prostate cancer.

3.2 Materials and Methods

3.2.1 **Tissues, Cell Lines, and Culture**

Human prostate to bone specimens were generously provided by Dr. Colm Morrissey at University of Washington Department of Urology under an Institutional Review Board (IRB) approved warm body rapid autopsy program. PAIII cells [217], LNCaP (ATCC), C4-2B (ATCC), PC-3M-luc-C6 (Caliper Life Sciences), and PC3-2M cells (Perkin Elmer) were grown in either Roswell Park Memorial Institute (RPMI) 1640 medium (LNCaP) or complete Dulbecco's Modified Eagle's Medium (DMEM) supplemented with 10% fetal bovine serum. All cell lines were periodically tested for mycoplasma (#CUL001B, R&D Systems) and short tandem repeat (STR) verified at the Moffitt Clinical Translational Research Core. For MMP-3 shRNA knockdown (Origene, pRFP-CB-shLENTI, #TR30032), PaIII cells were stably transfected and selected using standard protocols (Qiagen, Superfect, 301305).

3.2.2 **Gene Expression Analysis**

MMP-3 expression in human prostate cancer was compared to normal prostate tissue using Oncomine (https://www.oncomine.org). Three publically available prostate cancer

datasets were examined (LaTulippe, NCBI GEO Datasets GSE 688882; Liu, Array Express E-TABM-26; and Welsh, http://public.gnf.org/cancer/prostate/).

RNA was extracted with TRIzol® according to manufacturer's instructions (Invitrogen #15596). cDNA reverse transcription was performed using a High Capacity cDNA Reverse Transcription Kit (Applied Biosystems, #4368813). The concentrations of cDNA samples were determined by Nanodrop, and equal amounts (100ng per reaction) used for reactions. Primers sequences for genes of interest are: Rat *MMP-3* Forward 5'-GATGGTATTCAATCCCTCTATGG-3'; Rat *MMP-3* Reverse 5'-AACAAGACTTCTCCCCGCAG-3.' Human *MMP-3* Forward 5'-AGGCAAGACAGCAAGGCATA-3'; Human *MMP-3* Reverse 5'-GGTTCATGCTGGTGTCCTCA-3.' Rat *IGF-1R* Forward 5'-CGGTTGCTGGGTGTAGTATC-3'; Rat *IGF-1R* Reverse 5'-GCTCGGAGGAATCAGGACTA-3.' Human *IGF-1R* Forward 5'-AATGAAGTCTGGCTCCGGA-3'; Human *IGF-1R* Reverse 5'-CCCGCAGATTTCTCCACTC-3.' *18S* Forward 5'-GTAACCCGTTGAACCCCATT-3'; *18S* Reverse 5'-CCATCCAATCGGTAGTAGCG-3.' *GAPDH* Forward 5'-CCTGCACCACCAACTGCTTA-3'; *GAPDH* Reverse 5'- CCACGATGCCAAAGTTGTCA-3.'

3.2.3 **Immunoblotting and Immunostaining**

Cells were lysed with cold RIPA (150 mM NaCl, 1 mM EDTA, 1% Triton X-100, 1% sodium deoxycholate, 0.1% SDS, 20 mM Tris pH 8) containing protease and phosphatase inhibitor (Thermo Scientific, #78442) using standard procedures. Total protein concentration was determined using BCA (Pierce, #23225) and 25 µg of protein

loaded in 10% SDS-PAGE gels. Blots were blocked in 5% BSA for 1 hour followed by primary antibody for phospho-ERK (Cell Signaling Technology #9101; diluted 1:1000 in blocking solution + 0.1% Tween-20), ERK (Cell Signaling Technology #4695; diluted 1:1000 in blocking solution + 0.1% Tween-20), phospho-AKT (Cell Signaling Technology #4056, diluted 1:1000 in blocking solution + 0.1% Tween-20), AKT (Cell Signaling Technology #4691, diluted 1:1000 in blocking solution + 0.1% Tween-20), or IGF1 Receptor (phospho Y1161) (Abcam #39398, diluted 1:100 in blocking solution + 0.1% Tween-20). The blots were washed 3 x 10min in 1X TBST and incubated with HRP-conjugated anti-species secondary (Cell Signaling Technology, Rabbit #7074/Mouse #7076, diluted 1:1000 in blocking solution). Blots were developed using enhanced chemiluminescence (Pierce 32106) and exposed to light-sensitive film. Mouse cytokine arrays (Raybiotech, AAM-CYT-3) were performed using conditioned media obtained by serum starving cells for 16 hours.

For MMP-3 and phospho-Histone H3 immunofluorescence, slides were deparaffinized and rehydrated to water. Antigen retrieval was performed using Proteinase K for MMP-3 and heat-induced (pressure cooker) for phospho-Histone H3. Slides were blocked with 10% normal serum for 1 hour at room temperature. Primary antibodies (RH-MMP-3, Triple Point Biologics, 1:100; Pan-Cytokeratin, Sigma Aldrich C2562.2ML, 1:500; Phospho-Histone H3 (Ser10), Cell Signaling #9701, 1:200) were incubated overnight at 4°C. Slides were washed 3 x 10 minutes in TBST and rinsed in TBS. Secondary antibodies (Donkey Anti-Mouse Alexa Fluor 488, Thermo Scientific, 1:1000; Donkey Anti-Rabbit Alexa Fluor 568, Thermo Scientific, 1:1000) were incubated for 1 hour at room temperature. Slides were washed 3 times and mounted using

Vectashield anti-fade mounting medium with DAPI (Vector Laboratories, H-1200). Images were acquired using an upright Zeiss fluorescent microscope.

3.2.4 **Growth Assays**

Cell proliferation was measured using a Cell Titer 96® Aqueous Non-Radioactive Cell Proliferation Assay (Promega, G5421). Cells were plated in 96-well plates, 2000 cells per well, and luminescence was measured at 24, 48, and 72 hours on a Victor plate reader.

3.2.5 ***In Vivo* Tumor Studies**

All animal experiments were performed with Institutional Animal Care and Use Committee (IACUC, #IS000001283, CCL) approval from the University of South Florida. To test the effect of MMP-3 on *in vivo* tumor growth in bone, 5×10^4 PaIII cells (10 µL of ice cold PBS) were intratibially innoculated into immunocompromised male $Rag2^{-/-}$ mice (10 mice per group). A sham injection (10 µL) of PBS was injected in the contralateral limb to control for bone injury. Bioluminescent imaging (120 mg/kg luciferin in sterile PBS, Gold Biotechnology, LUCK-1G) was performed 24 hours after surgery and every 48 hours after as a correlate of tumor growth (IVIS™ Perkin Elmer). After 10 days, study animals were sacrificed and tumor and sham bearing limbs (tibia) were collected and fixed overnight in 10% neutral buffered formalin and transferred to 70% ethanol for *ex vivo* x-ray (Faxitron X-ray Corp) and µCT (Siemens). Following *ex vivo* analysis, bones were decalcified for 3 weeks in 14% EDTA (changed twice weekly) and processed for paraffin embedding. Subsequent to processing and embedding, trichrome staining was used to identify areas of trabecular bone formation (blue/green staining of type I collagen). Bone area to total area (B.Ar./T.Ar.) was determined by measuring

trabecular bone volume within a 1.0 mm long area beginning 0.5 mm distal from the growth plate using ImageJ software [219].

3.3 Results

3.3.1 MMP-3 is Expressed in Bone Metastatic Prostate Cancer Patient Specimens.

To test whether MMP-3 is expressed by human bone metastatic prostate cancers and determine the clinical relevance of its expression, we co-immunostained for cytokeratin, a marker of epithelial cell types, and MMP-3 in prostate to bone metastases derived from patients enrolled in the rapid warm body autopsy program at the University of Washington. We observed positive co-staining for MMP-3 and cytokeratin in 8 of the 9 examined patient specimens (Figure 3-3). We also noted MMP-3 positive staining in bone lining and stromal cells. Interestingly, the single specimen that did not co-stain for MMP-3 and cytokeratin did show positive staining for MMP-3 in the stroma. These results are consistent with previous reports, showing that MMP-3 is expressed by prostate cancer cells and stromal cells.

3.3.2 *MMP-3* is Expressed in Prostate Cancer Cell Lines

To select a model for subsequent *in vitro* and *in vivo* studies, we assessed whether *MMP-3* was expressed in prostate cancer cell lines (LNCaP, C4-2B, PC3-M, and PaIII) according to their ability to establish tumors in bone *in vivo*. Our data show that *MMP-3* is expressed by each of these cell lines (Figure 3-4 A). We selected PaIII for further study because of its strong expression of *MMP-3* and its ability to recapitulate mixed osteoblastic and osteolytic lesions in intratibial mouse models [377, 378]. Using

RFP tagged MMP-3 shRNA constructs we generated two stable MMP-3 knockdown PaIII clones and an shRNA control cell line (Figure 3-4 B-C).

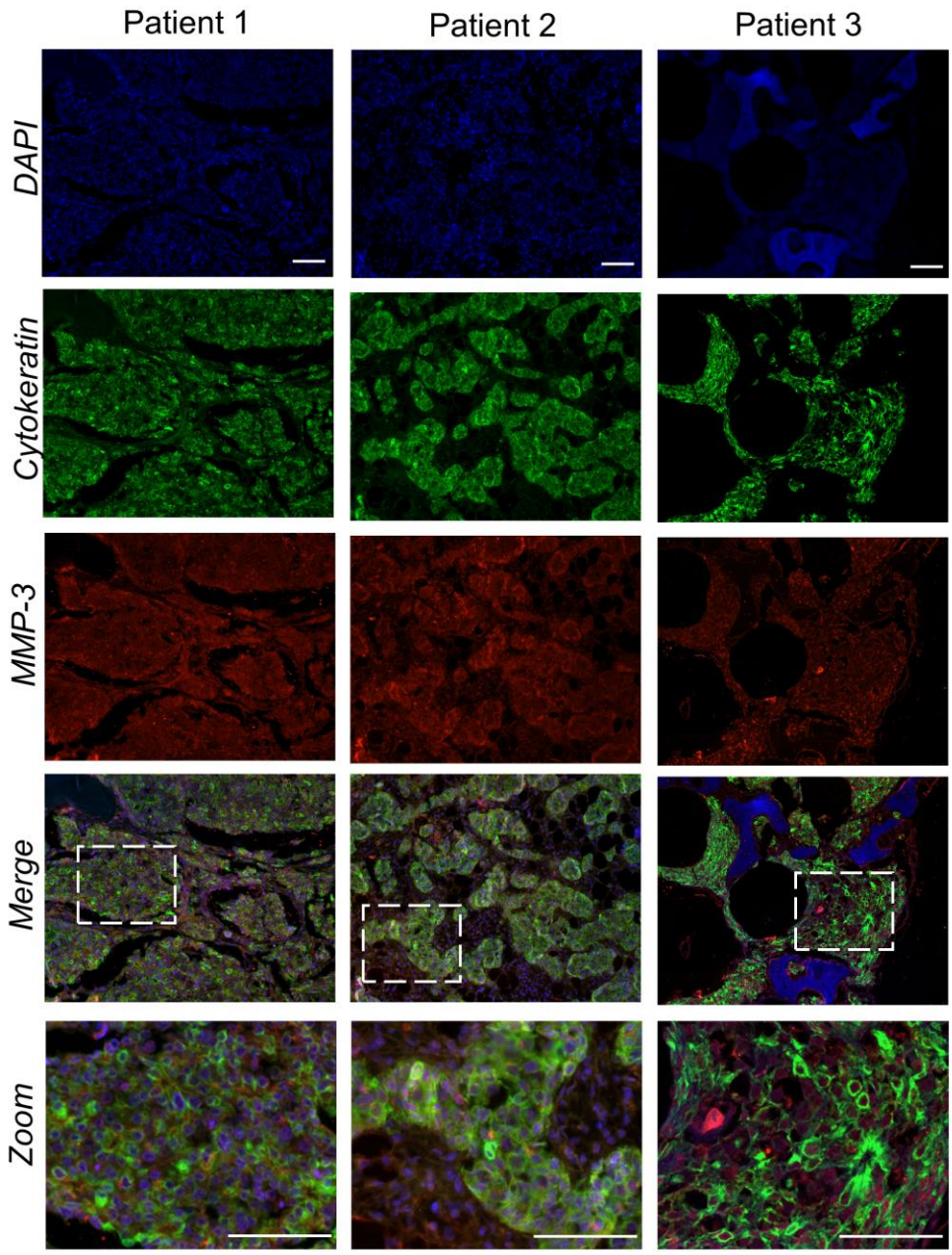

Figure 3-3. MMP-3 is Expressed by Tumor Cells in Human Prostate to Bone Metastases

Expression of MMP-3 in human prostate to bone metastasis patient sections (n=9) was determined by staining with anti-cytokeratin (green) and anti-MMP-3 (red) antibodies via fluorescent microscopy. Representative images for 3 of 9 patients are shown. Scale bars are 100 µm. Dashed box denotes area of magnification.

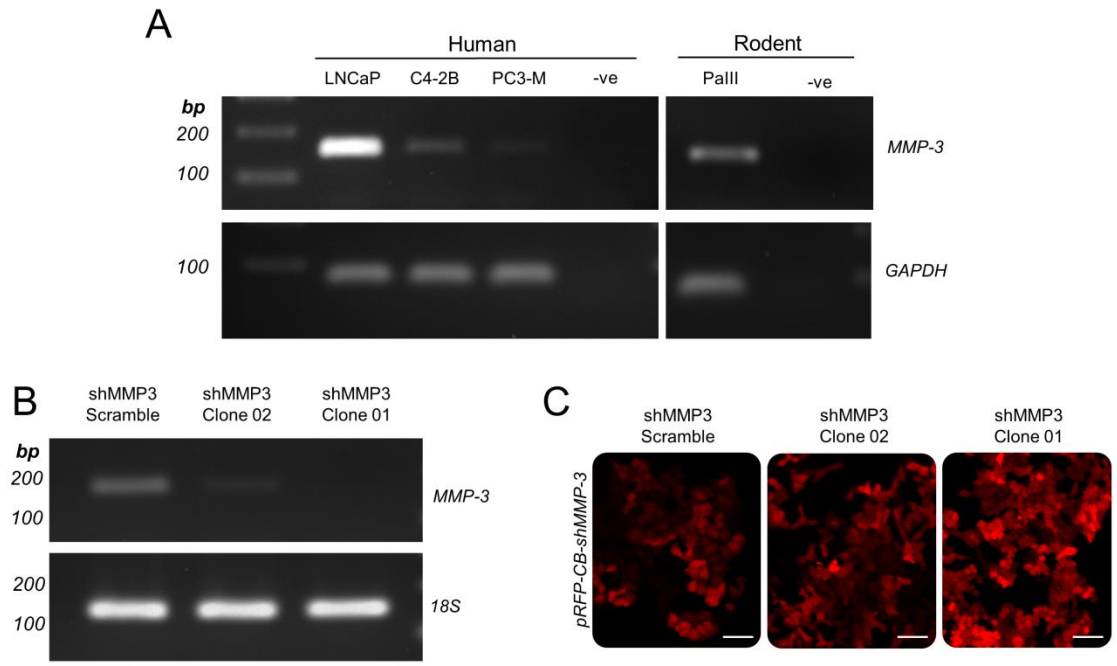

Figure 3-4. MMP-3 is Expressed in Multiple Prostate Cancer Cell Lines

*(**A**) MMP-3 expression in LNCaP, C4-2B, PC3-M, and PaIII prostate cancer cell lines. –ve indicates negative non-template control. Molecular weight markers are illustrated in base pairs (bp). (**B** and **C**) PaIII cells were stably transfected with MMP-3 and control red fluorescent protein (RFP) labeled shRNA construct to achieve MMP-3 silencing. Scale bars are 100 µm.*

3.3.3 *MMP-3* Silencing Decreases PaIII Prostate Cancer Cell Growth *In Vitro*

Previous studies have demonstrated that MMP-3 can proteolytically regulate a variety of factors involved in cell growth. Therefore, we assessed the impact of *MMP-3* silencing on *in vitro* cell growth using bioluminescence as a readout for proliferation. *MMP-3* silencing decreased proliferation of PaIII prostate cancer cells as early as 24 hours, and these effects became more pronounced at later time points (Figure 3-5). Our stable cell lines express two different levels of MMP-3 (Figure 3-4 B), and the reduction in proliferation corresponded with *MMP-3* expression levels in these cell lines.

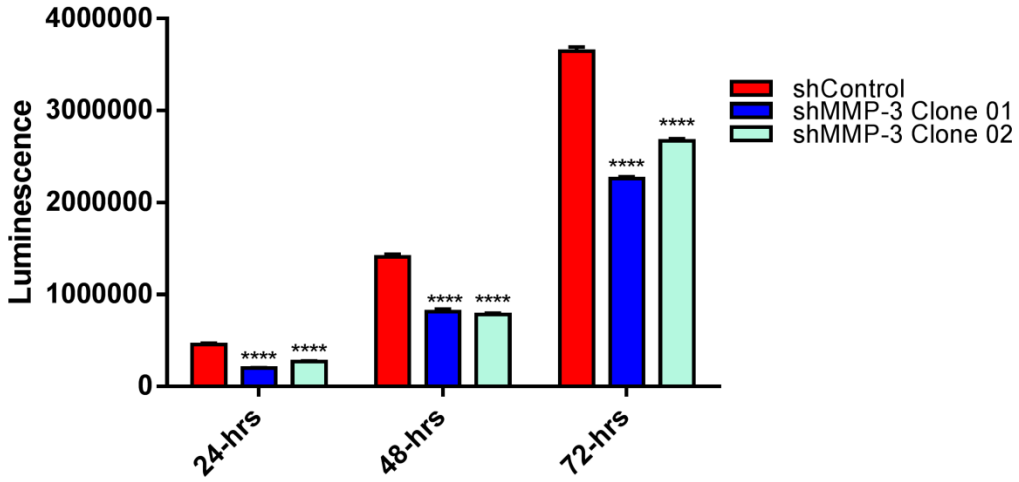

Figure 3-5. MMP-3 Promotes PaIII Proliferation

PaIII shControl, shMMP-3 polyclonal, shMMP-3 Clone 01, and shMMP-3 Clone 02 were seeded in 96 well plates (2 x 10^3 cells/well) and luminescence measured at 24, 48, and 72 hours as a surrogate for cell proliferation. Asterisk denotes statistical significance ($p<0.05$); n.s. = non-significant differences.

3.3.4 **Prostate Cancer Growth in Bone is Reduced by *MMP-3* Silencing**

To study the effect of MMP-3 expression on prostate tumor growth in bone, we injected PaIII shControl and PaIII shMMP-3 Clone 01 cells intratibially into male $Rag2^{-/-}$ C57BL/6 mice (5 x 10^4 cells, 10 mice per group) and monitored tumor growth by measuring bioluminescence over time (Figure 3-6 A). Tumors in the mice injected with PaIII shMMP-3 cells grew at a significantly slower rate compared to control tumors (Figure 3-6 B). After 10 days, mice were sacrificed and we performed *ex vivo* analyses of the tibias to study cancer associated bone disease including X-ray, µCT, and bone histomorphometry. Prostate tumor growth in bone induces extensive remodeling. To determine if there were any differences between PaIII shControl and PaIII shMMP-3 tumors on induction of osteolysis, X-ray analysis (Faxitron) was performed. Quantification of osteolytic lesion area (dark spots observed on bone surface) to total bone area showed that there was no significant difference in tumor-induced osteolysis

between PaIII shControl or PaIII shMMP-3 (Figure 3-7 A). In addition to osteolysis, bone metastatic prostate tumors can induce trabecular bone formation. We used µCT and trichrome staining/image quantification to study if there were any differences between PaIII shControl and PaIII shMMP-3 tumors on induction of osteogenesis and observed no significant change in trabecular bone volumes (Figure 3-7 B-C). Together, these data suggest that MMP-3 contributes to prostate tumor growth in bone but does not significantly alter the bone microenvironment or structure.

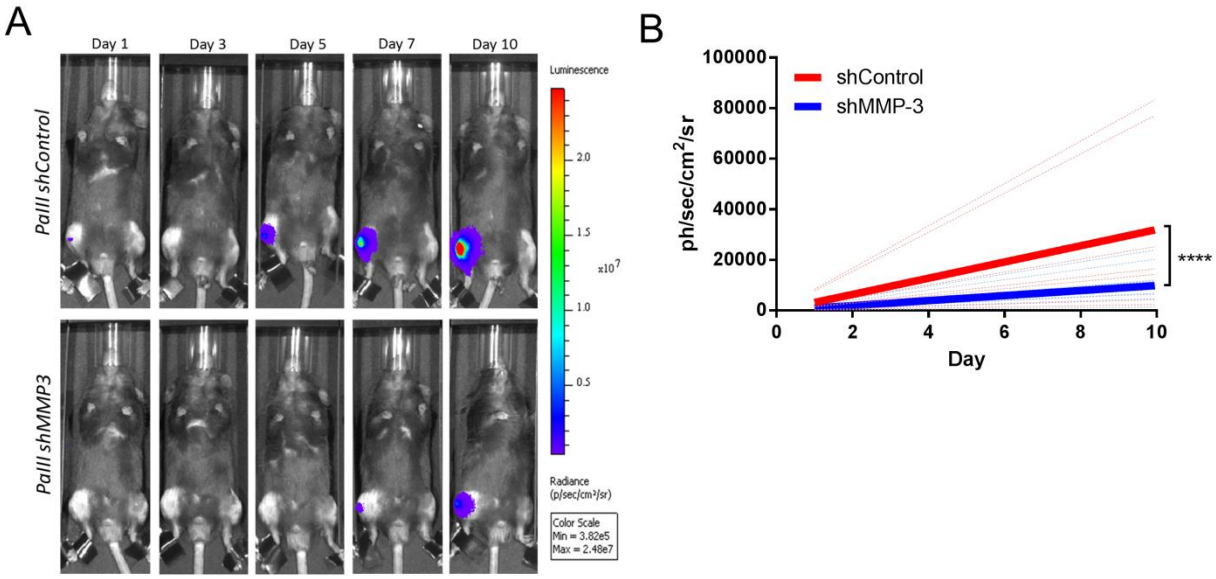

Figure 3-6. MMP-3 Silencing Reduces In Vivo Prostate Tumor Growth in Bone

*(**A**) PaIII shControl and shMMP-3 Clone 01 cells (5 x 10^4 in 10 µL) were injected intratibially in 6 week old male Rag2$^{-/-}$ mice (n=9/group). Saline was injected in the contralateral limb to control for injury. Bioluminescence was measured to monitor tumor growth for 10 days. (**B**) Linear regression analysis of tumor growth rates over 10 days (PaII shControl = red, PaIII shMMP-3 = blue).*

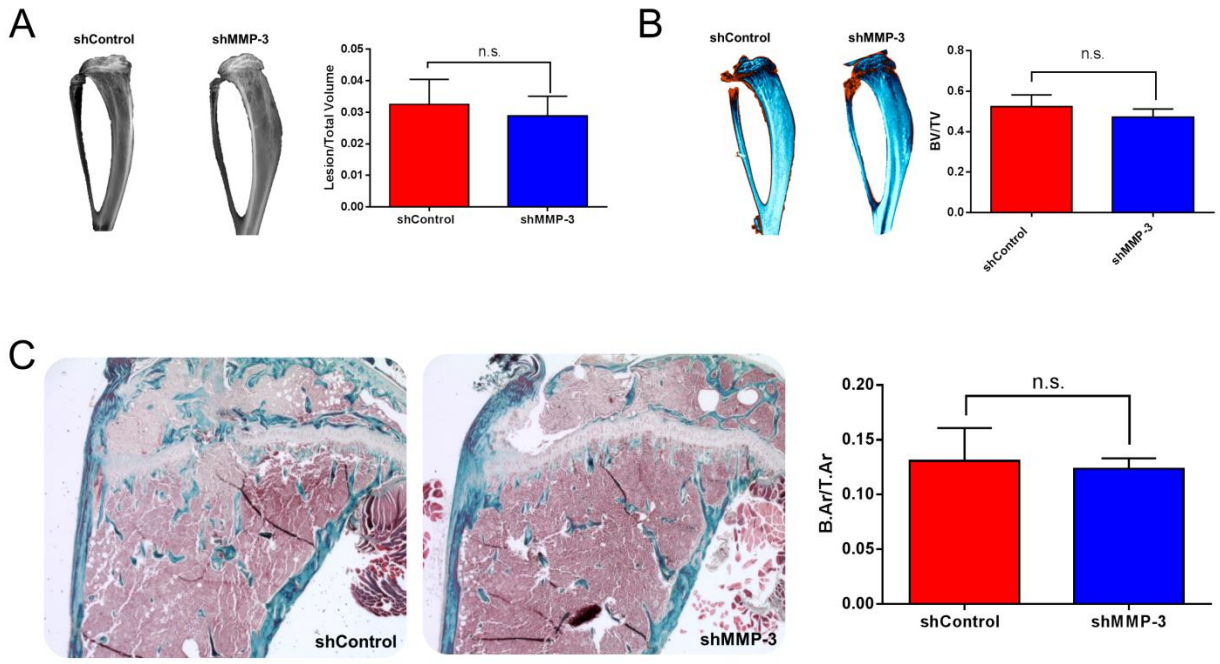

Figure 3-7. MMP-3 Silencing in PaIII Tumor Cells Does Not Alter Tumor-Induced Changes in Bone Structure

*(**A**) X-ray analysis and quantitation of tumor-induced osteolysis in tibias bearing PaIII shControl and shMMP-3 Clone 01 tumors. (**B**) µCT analysis and quantitiation of trabecular bone volume in tumor bearing tibias. (**C**) Trichrome stained sections derived from PaIII shControl and shMMP-3 Clone 01 tumor bearing tibias were quantitated for the amount of trabecular bone (blue-green color). n.s. = non-significance.*

3.3.5 **Candidate Approach to Assess MMP-3 Mechanism of Action**

To gain further insight into the mechanism by which MMP-3 contributes to *in vitro* and *in vivo* cancer cell growth, we performed cytokine array analysis of 62 cytokines to study the secreted protein content of conditioned media from PaIII shMMP-3 and PaIII shControl cell lines (Figure 3-8 A). Conditioned media was collected by serum starving cells overnight and diluting to equal total protein concentrations as determined by BCA. Densitometry analysis of the array blots revealed that several proteins in the conditioned media of PaIII shMMP-3 cells were increased over control, including insulin

growth factor binding proteins (IGFBPs) 3, 5, and 6 (Figure 3-8 B). In contrast, the internal control was actually slightly decreased as assessed by densitometry analysis (LI-COR Image Studio), suggesting that these increases in IGFBPs were even greater (not shown). Notably, IGFBP3, an established MMP-3 substrate, was among the most elevated (1.59-fold over control). The PaIII conditioned media was collected after only 16 hours of incubation, so we would expect more remarkable increases with longer incubation periods. These data show that *MMP-3* silencing in PaIII cells results in increased levels of IGFBPs, including IGFBP3, indicating that the MMP-3 processing of IGFBP3 may be important for the observed growth effect in MMP-3 knockout PaIII cells.

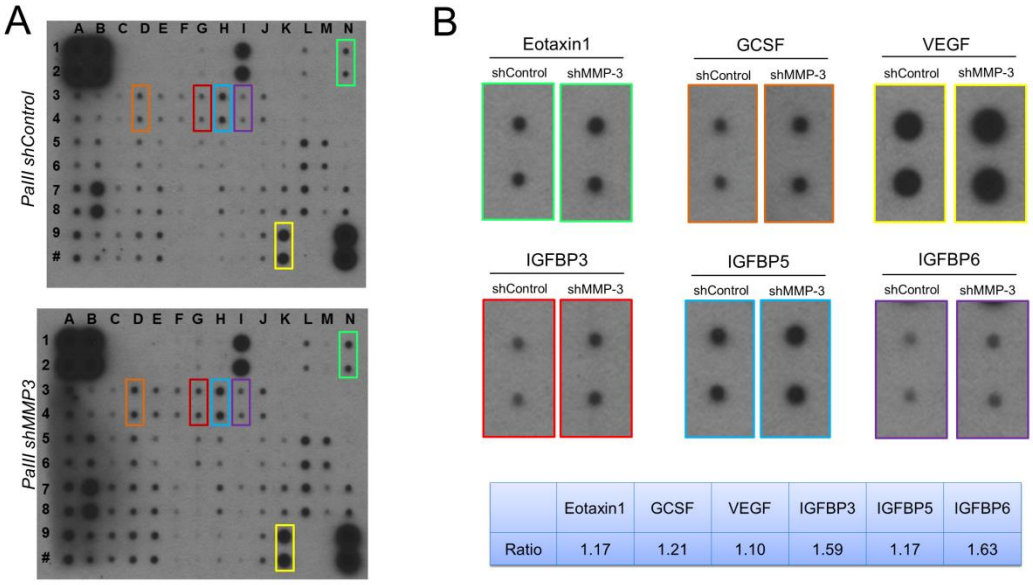

	Eotaxin1	GCSF	VEGF	IGFBP3	IGFBP5	IGFBP6
Ratio	1.17	1.21	1.10	1.59	1.17	1.63

Figure 3-8. IGFBPs are Elevated in MMP-3 Silenced PaIII Cancer Cell Conditioned Media

*(**A**) Cytokine array blots from PaIII shControl and PaIII shMMP-3 cell line conditioned media. (**B**) Densitometry analysis of cytokine array blots (Licor Image Studio).*

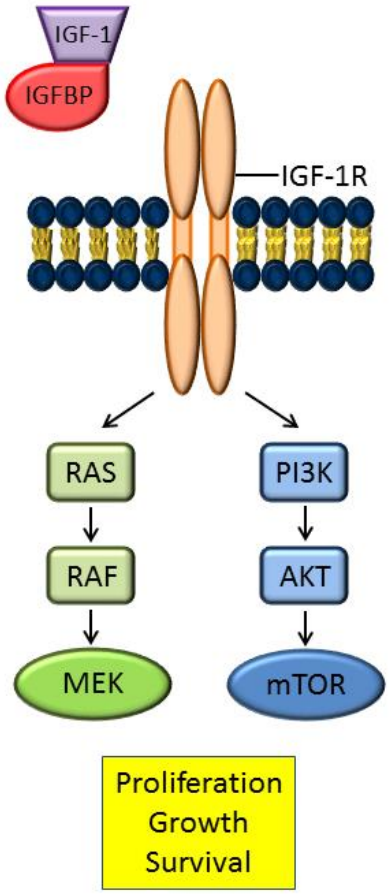

Figure 3-9. Insulin Growth Factor Receptor (IGF-1R) Signaling Pathways

IGF-1R is a cell membrane receptor tyrosine kinase (RTK) responsible for mediating insulin-like growth factor (IGF-1) activity in wide range of tissues and organs. Activation of either the MAPK or PI3K mediates biological processes like cell proliferation, growth, and survival. The bioavailability of IGF-1 in circulation is tightly modulated by six IGFBPs such as IGFBP-3.

3.3.6 **Reduced IGF-1R Activity in PaIII shMMP-3 Cells**

IGFBP3 binds and sequesters IGF proteins (IGF-1 and IGF-2) with high affinity to modulate their activity, predominantly resulting in anti-proliferative and anti-growth effects by preventing activation of the insulin growth factor receptor (IGF-1R) (Figure 3-9). To test if MMP-3 effects on proliferation were associated with reduced IGF-1/IGF-1R signaling, we first assessed the expression of *IGF-1R* in the PaIII cell lines by PCR.

Both the PaIII shControl and PaIII shMMP-3 cell lines showed robust *IGF-1R* expression (Figure 3-10 A). We next looked at the phosphorylation of IGF-1R and its downstream kinases ERK and AKT in PaIII shControl and PaIII shMMP-3 cell lines grown under standard culture conditions (no stimulation) by Western blot. These studies indicated a reduction of IGF-1R phosphorylation in PaIII shMMP-3 cell lines compared to PaIII shControl when normalized to Actin as a loading control. Reduced IGF-1R phosphorylation was accompanied by decreases in both ERK and AKT phosphorylation, both of which are potent inducers of proliferation, when normalized to total ERK or total AKT loading controls, (Figure 3-10 B-C). The contribution of MMP-3 expression to tumor growth was also observed in tissue sections derived from *in vivo* intratibial tumor growth studies by calculating the mitotic index (MI). Using phospho-Histone H3 immunofluorescence staining, an indicator of cells undergoing mitosis, and Definiens histology analysis software, we calculated the number of cells undergoing mitosis versus the number of cells not undergoing mitosis and noted a significant decrease in the MI for PaIII shMMP-3 tumors (PaIII shControl = 20.37% vs. PaIII shMMP-3 = 4.33%) (Figure 3-10 D). Taken together, these data show that reduced proliferation caused by MMP-3 knockdown in PaIII prostate cancer cells is potentially a result of decreased IGF-1R signaling.

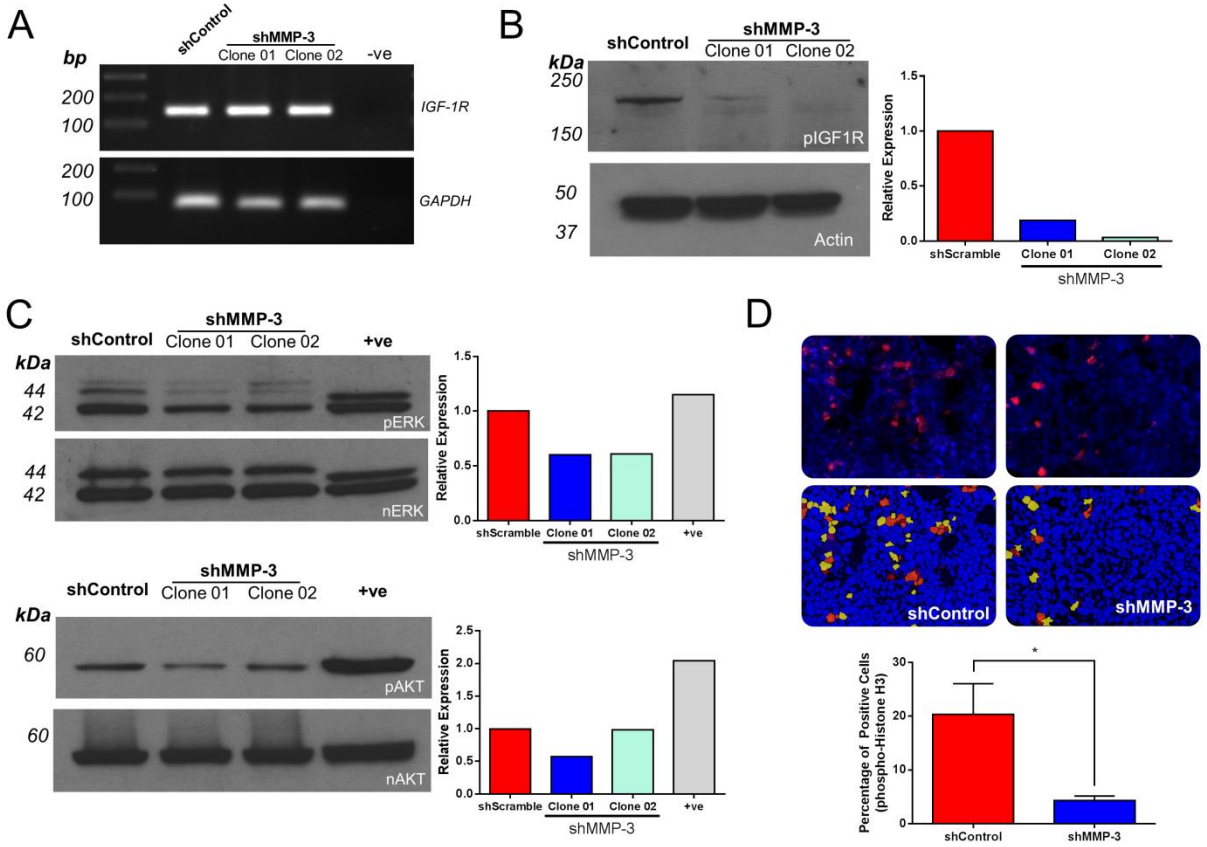

Figure 3-10. MMP-3 Silencing Reduces IGF-1R Signaling

*(**A**) IGF-1R expression in PaIII shControl and PaIII shMMP-3 cells. –ve indicates negative, non-template control. Molecular weight markers are illustrated in base pairs (bp). (**B**) IGF-1R phosphorylation in PaIII shControl, shMMP-3 Clone 01, and shMMP-3 Clone 02 cells. (**C**) Phosphorylated ERK(pERK), total ERK (nERK), phosphorylated AKT (pAKT), and total AKT (nAKT) in in PaIII shControl, shMMP-3 Clone 01, and shMMP-3 Clone 02 cells. +ve indicates positive control (mouse mesenchymal stem cells stimulated with epidermal growth factor (EGF)). (**D**) Phospho-Histone H3 immunofluorescence staining and quantitation in tissue sections derived from PaIII shControl and shMMP-3 Clone 01 tumor bearing tibias. Percentages of total cells (blue) stained positive for phospho Histone-H3 (red=high, orange=medium, yellow=low) per 20x field were calculated. Asterisk denotes statistical significance ($p<0.05$).*

3.4 Discussion

MMPs have been shown to be overexpressed in many cancers, where they possess both pro- and anti-tumorigenic roles by degrading and regulating extracellular and non-extracellular matrix proteins [280]. Here, we have shown that silencing MMP-3

in prostate cancer cells inhibits their growth *in vitro* and *in vivo*. Further, we found increased levels of IGFBP3, a known MMP-3 substrate [305], and decreased IGF-1R, ERK, and AKT phosphorylation in the *MMP-3* silenced cells. This suggests that increased MMP-3 expression by prostate cancer cells contributes to tumor growth by cleaving IGFBP3, thereby increasing the activity of the proliferation driving IGF-1/IGF-1R signaling pathway. This has important clinical implications for the future treatment of metastatic prostate cancer as the development of both MMP and IGF-1R inhibitors progresses.

Previous studies of MMP-3 in cancer have shown pro- and anti-tumorigenic roles. For example, in breast cancer there are conflicting reports where MMP-3 can contribute or protect during cancer progression [347, 349, 365, 366]. It is possible that the net effect of MMP-3 could change as the disease advances, therefore MMP-3 needs to be studied in a context dependent manner. In prostate cancer, MMP-3 is detected at higher expression levels compared to normal prostate tissues, however there have only been a couple of MMP-3 focused studies. These studies have shown that MMP-3 expression contributes to metastasis and angiogenesis [376] and migration and invasion [375], but no studies to date have looked at the direct impact on prostate cancer growth in bone. Our studies found that tumor-derived MMP-3 expression contributes to prostate cancer cell growth *in vitro* as well as tumor growth in bone using *in vivo* intratibial models. Additionally, we noted that in addition to expression by tumor cells in our human prostate to bone metastasis samples, MMP-3 is expressed in stromal cell types. There is evidence that the roles of MMPs can depend on tissue expression,

therefore it would be interesting to study the specific impact of stromal MMP-3 in bone metastatic prostate cancer in future studies.

Prostate cancer to bone metastasis induces extensive remodeling of the bone and is hallmarked by a combination of osteogenesis and osteolysis. Despite its effects on tumor growth in bone, our studies did not reveal any significant differences in tumor-induced osteolysis or osteogenesis by MMP-3 expression. MMP-3 can cleave many important factors involved with bone remodeling, including PTHrP, RANKL, and TGF-β, in addition to its extracellular matrix remodeling capacities, so it is surprising that no differences were observed. However, previous studies of MMP-3 knockout mice have revealed no skeletal phenotypes, unlike others such as MMP-2, -9, and -13 which demonstrate significant skeletal impairments.

Numerous MMP-3 substrates have been previously identified, and these substrates are often responsible for determining pro- and anti-tumorigenic effects. Like other MMP studies, we must also consider the spatial and temporal expression of the proteases. Our cytokine array identified several proteins expressed by the PaIII prostate cancer cells, so it is plausible that these might co-localize with MMP-3. IGFBP3 is a known target of MMP-3 while IGFBP5 and IGFBP6 can be processed by MMP-2, -7, -9, or -12 [379-381]. However, IGFBP5 and 6 bind with greater affinity to IGF-2 whereas IGBP3 binds preferentially to IGF-1 [382]. In addition to IGFBP3, 5, and 6, we observed increased VEGF in the conditioned media of PaIII shMMP-3 cells. Previous studies have shown that matrix bound VEGF-A can be released and processed into soluble fragments by multiple MMPs, including MMP-3, which possessed altered neovascular activities compared to an MMP-resistant form of VEGF

[294]. Further studies have shown that MT1-MMP can increase *VEGF-A* transcription by interacting with vascular endothelial growth factor receptor 2 (VEGFR-2) [383], but it is unclear whether this effect can be induced by other MMPs. We also noted increased levels of additional proteins such as Eotaxin1 and G-CSF. To our knowledge, these have not been previously shown to be regulated by MMPs, but might be interesting to investigate if and how MMP-3 modulates their expression. It is worth noting that Eotaxin1 was shown to increase MMP-3 expression in DU145 cells which led increased invasiveness and migration [375], suggesting a possible reciprocal interaction. Similarly, there are reports where G-CSF stimulates MMP-2 expression and migration in mesenchymal stem cells [384]. Although our results implicate reduced IGF/IGF-1R signaling, it is both plausible and likely that other signaling pathways are affected by *MMP-3* silencing and may contribute to the differences noted in proliferation and tumor growth.

Given the numerous pro- and anti-tumorigenic roles described for MMP-3 in other cancers, MMP-3 may not be the best suited for the development of selective inhibitors. However, uncovering the pro- and anti-tumorigenic roles for MMP-3 and elucidating its substrates provides alternative therapeutic targets. IGF-1 is expressed by bone osteoblasts, osteoclasts, and osteocytes where its downstream signaling events are vital for development and metabolism [385]. The roles of the IGF signaling axis have also been well documented in many cancers where it is predominantly associated with pro-growth and pro-survival effects on tumor cells [355]. Studies have also shown that the IGF axis is involved in development and progression of prostate cancer [356]. IGF-1 and IGF-2 have both been implicated in the proliferation and

invasion of prostate cancer cells and progression to androgen independence, however there is some controversy as studies of transgenic mice have demonstrated that deletion of IGF-1R in combination with inactivation of p53 in prostate cells could lead to more aggressive cancer [386]. Both tumor- and bone-derived IGF-1 is also a factor in the “vicious cycle” [387, 388], suggesting that IGF-1/IGF-1R signal transduction may be particularly potent in prostate to bone metastases. Consistent with most epidemiological findings, our results suggest that reduced IGF-1R signaling in the PaIII shMMP-3 cells decreases proliferation *in vitro* and *in vivo*. Based on the predominantly oncogenic effects of the IGF-1R pathway, there are numerous ongoing efforts to target the IGF signaling axis in prostate cancer. Preclinical studies of both monoclonal neutralizing antibodies and tyrosine kinase inhibitors have consistently shown therapeutic efficacy, but their performance in clinical trials have generally been disappointing or complicated by a wide array of side effects [382]. This is likely a product of the ubiquitous tissue expression of IGF-1R and its important physiological functions. One current approach to improve the efficacy of IGF-1R inhibitors in prostate cancer is to give them in combination with other therapies, including androgen deprivation and chemotherapy [389]. According to these and previous findings from our group, we would speculate that developing a dual inhibitor consisting of an IGF-1R inhibitor and a bone seeking bisphosphonate might improve these therapies. The use of this strategy has greatly improved the efficacy of MMP inhibitors in bone metastatic disease by permitting tissue selective (i.e. bone) targeting [123, 124]. We hypothesize that this strategy would reduce the local activities of IGFs while preserving IGF-1R signaling in normal, non-cancerous tissues. In conclusion, we have shown that MMP-3

contributes to prostate cancer growth in bone by increasing tumor cell proliferation, and that the cleavage of IGFBP3 by MMP-3, which regulates IGF-1 activity, potentially contributes to the increased proliferation.

Chapter 4. Summary, Clinical Implications, and Future Work

Metastasis is a chief component of cancer mortality, being responsible for up to 90% of cancer deaths [390]. Cancer can metastasize to multiple organs including the lungs, brain, lymph nodes, liver, and bone. For reasons that are only beginning to be understood, certain cancers metastasize more prevalently to specific organs, with the predilection of prostate cancer cells to colonize bone being a case in point. Today, men diagnosed with primary, localized prostate cancer have a favorable prognosis with a 5-year survival rate of nearly 100% [4]. As evidenced by these statistics, early detection is the best scenario, but the clinical reality is that a significant number of men will initially present with advanced prostate cancer and have bone metastases already established. Given the associated decline in quality of life and high mortality rates for metastatic cancer, discovering the underlying mechanisms of bone metastasis and developing clinically translatable therapies is of the utmost importance. Equally important is the development of improved strategies to screen men for prostate cancer and carefully identify and monitor patients with early stage disease who are at risk for developing metastases.

The original vicious cycle of bone metastasis describes the interactions between tumor cells, osteoblasts, and osteoclasts, but new components and mechanisms are continually being integrated [56]. By improving our understanding of the disease, these additions will provide potentially novel therapeutic targets. Although MMPs have been implicated in invasion and metastasis for nearly 3 decades, work from our lab and

others has expanded these roles, demonstrating that many MMPs are involved in regulating vicious cycle cytokines and growth factors such as RANKL, IGF, TGF-β, VEGF, and now PTHrP [53]. PTHrP has long been acknowledged for its potent bone resorbing capacities in skeletal malignancies like breast cancer and multiple myeloma, but it can also promote osteogenesis via its actions on the osteoblast compartment when dosed intermittently [26, 167]. Our data show that MMP cleavage of mature $PTHrP_{1-36}$ generates a 17 amino acid N-terminal peptide ($PTHrP_{1-17}$) that does not induce osteoclastogenesis while retaining the ability to induce osteoblast differentiation and stimulate bone formation. This mechanism could potentially explain why some cancers, such as prostate, generate predominantly osteogenic lesions. Interestingly, in our mass spectrometry analysis of cancer cell conditioned media, $PTHrP_{1-17}$ was detected in prostate cancer and osteosarcoma cell conditioned media, both of which are characterized by osteogenesis and bone forming lesions, but not in breast cancer which is traditionally hallmarked by the presence osteolytic lesions. A more extensive characterization of cell lines and *in vivo* specimens would be necessary to draw further conclusions, but it would be fascinating to investigate whether $PTHrP_{1-17}$ is found most often in cancers that produce osteogenic metastases and to better understand the interplay of factors related to the osteolytic/osteogenic balance.

We have also shown that there is selectivity of MMPs toward PTHrP. As an example, MMP-13 does not generate $PTHrP_{1-17}$. Our laser capture microdissection and microarray analysis of MMP expression was performed on prostate to bone metastases, showing significantly increased expression of MMP-2, -3, -7, -9, and -13. Although these MMPs are known to be increased in many cancers, it would be interesting to

perform a similar experiment on bone metastases from other cancers, such as breast, to study the differential expression of MMPs. Importantly, the increased commercial availability of reliable fluorometric MMP activity assays will allow us to explore the actual activity of MMPs in bone metastatic cancers of different origins. This information might help us to better understand the MMP mediated generation of $PTHrP_{1-17}$ and possibly yield clues to explain the osteolytic versus osteogenic pathologies observed in bone metastases.

Currently, prostate specific antigen (PSA) is the standard test for screening men for prostate cancer. PSA is a serine protease produced by prostate cells that can be measured in blood. Usually, men with prostate cancer have elevated PSA levels (>4.0 ng/mL), but benign conditions or infections can also cause PSA levels to rise [391]. Because of this, there is controversy surrounding the use of this test, including who should and should not be tested and what levels constitute cause for concern [391]. A primary problem with PSA screening is that the tests have been known to report both false-negatives and false-positives. One study reported that only about 25% of men with elevated PSA who underwent a prostate biopsy actually had prostate cancer [392]. Although PSA is likely to remain the standard screening method for the foreseeable future, and efforts are being made to improve its accuracy, there is also pressure to find new prognostic biomarkers. Recently, it was reported that a $PTHrP_{12-48}$ fragment could serve as plasma-derived biomarker associated with bone metastasis in breast cancer patients [175]. Given the osteogenic nature of both prostate to bone metastases and MMP generated $PTHrP_{1-17}$, perhaps $PTHrP_{1-17}$, or PTHrP fragments that we have yet to study, might correlate with bone metastasis in prostate cancer. Using the $PTHrP_{1-17}$

antibody and mass spectrometry will allow us to study serum, plasma, and urine from prostate cancer patients with or without bone metastases and determine any correlation. In addition to prognostic uses, the levels of $PTHrP_{1-17}$ might also correlate with the effectiveness of experimental therapies such as MMP inhibitors.

Besides their functional roles, MMPs may hold potential as prognostic or diagnostic cancer biomarkers as well. Multiple MMPs from readily available sources like urine, serum, and plasma have been evaluated in cancers such as colorectal, pancreatic, breast, ovarian, bladder, prostate, and lung [393]. In some instances, the expression of certain MMPs has been found to correlate with the presence, stage, and/or grade of disease. For example, the study of MMP-9 in breast cancer has revealed that plasma levels actually decrease following primary tumor resection. In patients who relapse, increases in plasma levels of MMP-9 are detected. Notably, the rise in MMP-9 expression is detected prior to the actual clinical diagnosis of recurrence [394]. Although MMP-3 is not currently used as a biomarker, existing data where its expression correlates with poor prognosis in colorectal cancer, and serum levels of MMP-3 in oral squamous provide rationale for its consideration and further study [289, 290].

Within the bone field, there is a need for agents capable of stimulating bone formation to treat diseases like osteoporosis. The use of PTH and PTHrP has been studied for these purposes after it was first shown in the 1930s that intermittent/daily injections of PTH could lead to increases in bone formation [128, 395]. However, the anabolic effects are only manifest when PTH is administered intermittently. Sustained exposure favors osteoclast formation by driving the production of RANKL from

osteoblasts. Following its discovery, it was determined that PTHrP had anabolic activities similar to PTH, but $PTHrP_{1-36}$ was initially thought to be free of PTH's potent resorptive effects [148, 149]. In a 3-month trial comparing PTHrP and PTH in three groups of 35 post-menopausal women, $PTHrP_{1-36}$ increased bone mineral density, and although there was a slight delay compared to PTH_{1-34} (2-mo vs. 3-mo), $PTHrP_{1-36}$ treatment eventually led to increased CTX bone resorption markers [396]. Differences in potency were also noted, with the lower potency of $PTHrP_{1-36}$ being attributed to its restriction to the cell surface whereas PTH_{1-34} was more readily internalized and able to persistently signal through PTH1R. Additionally, it is believed that the susceptibility of $PTHrP_{1-36}$ to proteolytic cleavage might limit its bioavailability and usefulness as a systemic treatment [128].

Although the native, full-length PTH and PTHrP proteins may not be best suited as anabolic treatments, there has been strong interest in using the PTH or PTHrP structure as a starting point to develop peptide analogs that promote bone formation. Currently, one PTH analog called teriparatide (FORTEO®) is FDA approved for the treatment of osteoporosis. Although effective, practitioners have noted that some patients experience severe hypercalcemia which can actually lead to bone loss [397, 398]. Recently an analog based on PTHrP called abaloparatide was developed as an alternative to teriparatide and is currently being investigated in phase III clinical trials. Abaloparatide modifies 5 of the 13 residues between amino acids 22 and 34 of PTHrP, however the rationale for these changes has not yet been published or explained. Results of earlier clinical trials show that abaloparatide increases bone mineral density and reduce fractures in post-menopausal women, however any risk or potential for bone

resorption has not been mentioned [151]. In our studies, MMP generated $PTHrP_{1-17}$ retains the anabolic activities of $PTHrP_{1-36}$ but does not stimulate bone resorption. During ectopic ossicle formation assays, mice were systemically administered daily (intermittent) $PTHrP_{1-17}$, and post-mortem histomorphometry of long bones revealed increases in trabecular bone volume. Importantly, using *in vivo* calvarial injection assays, a protocol specifically designed to stimulate bone resorption via continuous exposure to PTHrP, we found that $PTHrP_{1-17}$ neither increased osteoclast numbers nor enhanced bone resorption, both of which were observed with $PTHrP_{1-36}$. Furthermore, our *in vitro* analyses suggest that $PTHrP_{1-17}$ may not be further degraded proteolytically as it was still detected after an hour of incubation with MMPs as well as in cell culture conditioned media collected over 24 hours. Therefore our bioactivity studies of $PTHrP_{1-17}$ suggest that the N-terminal residues are capable of eliciting anabolic effects and may hold potential for further development as an anabolic agent for treating bone disease.

Our mass spectrometry studies indicate that multiple MMPs can generate $PTHrP_{1-17}$, including MMP-2, -3, -7, and -9 but not MMP-13, suggesting that there is specificity for certain MMPs toward the PTHrP sequence or structure. Although we have explored the activity of MMP-3 toward PTHrP at multiple timepoints and focused on MMPs highly expressed in the tumor-bone microenvironment, it would be interesting to see which other MMPs are capable of cleaving PTHrP and to further study the kinetics of these enzymes. Since numerous proteases, including several MMPs, are found in the tumor microenvironment, it will be important to understand these dynamics. We know that enzymes like PSA and neprilysin can cleave PTHrP [168, 169], but it

remains to be determined if and how they might compete with MMPs and other proteases *in vivo.*

In future studies, we would like to explore whether $PTHrP_{1-17}$ is produced by normal tissues where it might possess roles during routine skeletal metabolism. Osteoblasts are known to produce PTHrP [147], therefore we would evaluate $PTHrP_{1-17}$ in a panel of osteoblast, osteoblast-like, and osteocyte cell lines. Our lab and others have developed and maintain colonies of MMP-null mice, including MMP-2, MMP-3, MMP-7, and MMP-9, that would allow us to study if there is a predominant MMP involved in PTHrP processing and compare this to WT mice. Initially, we could establish primary mesenchymal stem cell and osteoblast cultures from these mice and examine the secretion of $PTHrP_{1-17}$ in the conditioned media. We could also collect plasma and bone marrow flushes from these mice as a more relevant *in vivo* source for immunoprecipitation and mass spectrometry analysis. To further our understanding of PTHrP processing by MMPs in a prostate cancer setting, we could use CRISPR or traditional RNA interference methods to silence select MMPs *in vitro.* This could be done in PaIII cancer cells as we know they secrete detectable levels of $PTHrP_{1-17}$ and can be used for *in vivo* intratibial models. The development of the $PTHrP_{1-17}$ specific antibody and refined mass spectrometry protocols for its detection will be a valuable tool as we continued to study PTHrP processing in more detail in the future.

In this work, we have primarily focused on $PTHrP_{1-17}$ as it appears to retain partial similarity to the mature, full length form of PTHrP. However, our studies found that several MMPs could generate $PTHrP_{18-26}$ and $PTHrP_{27-36}$ as well as fragments from $PTHrP_{1-36}$. Although they did not possess activity in our signaling assays, nor did they

antagonize the activities of $PTHrP_{1-17}$ or $PTHrP_{1-36}$, there could be as of yet to be determined roles for these fragments. We also have not studied the effects of MMPs on the C-terminal (amino acids 37-141) portion of the protein. Many fragments and protein products have been detected from this region, including osteostatin, which has multiple previously identified anti-resorptive activities [181]. Surprisingly, very little is known about the proteases involved in cleaving this portion of PTHrP. Therefore, in future work, we would like to investigate if MMPs are involved in the generation of osteostatin or other novel fragments from the C-terminus.

The interaction between $PTHrP_{1-17}$ and PTH1R leaves unanswered questions as well. Normally, PTHrP interacts with PTH1R by the "two site model," however the $PTHrP_{1-17}$ fragment lacks the C-terminal portion of PTHrP that has been shown to interact with the receptor's N-terminal domain. Using available resources at Moffitt, we could use protein crystallization to develop a model of $PTHrP_{1-17}$/PTH1R interaction and visualize the precise orientation of receptor ligation. It may also be possible that $PTHrP_{1-17}$ and/or other fragments could elicit cellular activities by alternative receptors. Researchers in the field have speculated that the Endothelin receptor could be involved with signaling of other PTHrP fragments like $PTHrP_{1-16}$, however further study of this idea is needed [256]. We have explored this idea briefly using affinity precipitation mass spectrometry where we treat osteoblasts with biotinylated $PTHrP_{1-17}$ and immunoprecipitate to observe protein binding partners. We would like to expand these studies in future work as it could offer valuable directions in determining additional activities for $PTHrP_{1-17}$. In addition to studying $PTHrP_{1-17}$ in osteoblasts, we would

include prostate cancer cell lines as well. Identifying binding partners or receptors involved in prostate cancer cells could reveal possible reciprocal effects of $PTHrP_{1-17}$.

Persistent research has gradually elucidated cancer specific roles for individual MMPs, and we are beginning to have a clear picture of which MMPs contribute versus protect during tumorigenesis. For example, MMP-3 has been implicated in contributing to mammary tumorigenesis but protecting in squamous cell carcinoma [313, 364]. Our tumor growth studies have focused on MMP-3 produced by the cancer cells. Although most MMPs are secreted, they can act locally and unique roles for MMPs derived from specific cell types have been reported [58, 362]. Therefore, it is possible that host/stromal MMP-3 may have different roles in prostate tumor growth in bone that tumor-derived MMP-3. Using MMP-3 null mice, we would like to study the impact of stromal MMP-3 on prostate tumor growth in bone. We could also combine study the combined effect of total (tumor and stroma) MMP-3 ablation. The addition of these experiments will enable us to fully understand MMP-3's activities and utility as a therapeutic target in prostate to bone metastases.

The biochemical understanding of MMPs has improved and we can now better target individual MMPs based on their active sites, sub site pockets, secondary substrate binding exosites, and even some non-catalytic activities [269, 272]. Applying mechanism based targeting approaches has led to the development of modern highly selective MMP inhibitors. The ability to selectively target MMPs is being further developed to incorporate strategies that allow tissue specific inhibition. Bisphosphonates specifically target bone due to their affinity for hydroxyapatite and have been used clinically to treat skeletal malignancy for several years [90, 399]. Work

from our lab and colleagues at the University of Bari to chemically modify bisphosphonates by attaching an MMP inhibiting moiety to create “dual inhibitors” has shown promising preclinical results in *in vivo* 4T1 and PyMT-R221A bone metastatic breast cancer models [123, 124]. Despite the fact that MMP-3 may not be the best MMP for inhibition, these strategies will be important for the MMP field in allowing the selective inhibition of predominantly pro-tumorigenic MMPs like MMP-2.

Table 4-1. Experimental Therapies for Metastatic Prostate Cancer

Drug Name	Target	Action	Trial Results	Reference
Orteronel	CYP17A1 (17,20 lyase activity)	Reduces circulating testosterone levels	Decreased number of CTCs, improved radiographic PFS	[400, 401]
Ipilimumab	CTLA-4	T-cell activation	Ongoing	[402, 403]
Nivolumab	PD-1	T-cell activation	Ongoing	[404]
Prostvac-VF	Delivery of PSA transgene	T-cell activation	Improved median survival	[85, 405]
Cabozantinib	c-MET, VEGF-R2	Inhibits tyrosine kinase activity	Partial resolution of bone lesions, decreased number of CTCs, decreased pain	[406]
Tasquinomod	Thrombospondin S100A9	Anti-angiogenic, reduces MDSC recruitment	Improved median PFS, stable bone alkaline phosphatase levels	[407]
Custirsen	Clusterin	Improves docetaxel response	Extended median survival, extended PFS, improved PSA declines	[408]

Only within the last decade have therapies that extend overall survival for men with metastatic prostate cancer become FDA approved. Many of these approved therapies as well as therapies under current investigation (Table 4-1) have shifted focus

away from traditional approaches such as chemotherapy and androgen inhibitors which solely target the cancer cells and instead consider the tumor microenvironment. The most recent agent to receive FDA approval for mCRPC is radium-223 [97]. The bone seeking properties of radium-223 as well as other radiopharmaceuticals make them particularly useful in the treatment of bone metastases. In a study of men with mCRPC previously treated with radiotherapy, radium-223 showed improved overall survival, time to PSA progression, and reduced alkaline phosphatase levels (measure of bone remodeling). In addition, radium-223 also delayed the time to first SRE [99]. Previous radiopharmaceuticals used to treat mCRPC were only effective at reducing pain, therefore, radium-223 represents an important leap forward for the field [97]. Understanding the roles for MMPs and their interaction with other factors in the vicious cycle as well as the development of selective MMP inhibitors will continue to generate novel methods to control metastasis.

References Cited

1. www.cancer.org. *Key Statistics for Prostate Cancer*. 2017 [cited 2017 1-21-2017].
2. UK, P.C., *Rare Prostate Cancers.*
3. www.cancer.org, *Survival rates for prostate cancer.* American Cancer Society, 2014.
4. www.cancer.org, *Survival Rates for Prostate Cancer.* 2017.
5. Huggins, C., Hodges C.V., *Studies on Prostatic Cancer. I. The Effect of Castration, of Estrogen and of Androgen Injection on Serum Phosphatases in Metastatic Carcinoma of the Prostate.* Cancer Research, 1941. **1**: p. 293-297.
6. Seruga, B., A. Ocana, and I.F. Tannock, *Drug resistance in metastatic castration-resistant prostate cancer.* Nat Rev Clin Oncol, 2011. **8**(1): p. 12-23.
7. Cookson MS, R.B., Dahm P, Engstrom C, Freedland SJ, Hussain M, Lin DW, Lowrance WT, Murad MH, Oh WK, Penson DF, Kibel AS, *Castration-Resistant Prostate Cancer: AUA Guideline.* American Urological Association, 2014.
8. Cancer Genome Atlas Research, N., *The Molecular Taxonomy of Primary Prostate Cancer.* Cell, 2015. **163**(4): p. 1011-25.
9. Keller, E.T. and J. Brown, *Prostate cancer bone metastases promote both osteolytic and osteoblastic activity.* J Cell Biochem, 2004. **91**(4): p. 718-29.
10. Bubendorf, L., et al., *Metastatic patterns of prostate cancer: an autopsy study of 1,589 patients.* Human Pathology, 2000. **31**(5): p. 578-583.
11. Crawford, E.D. and D. Petrylak, *Castration-resistant prostate cancer: descriptive yet pejorative?* J Clin Oncol, 2010. **28**(23): p. e408.
12. Huang, X., C.H. Chau, and W.D. Figg, *Challenges to improved therapeutics for metastatic castrate resistant prostate cancer: from recent successes and failures.* J Hematol Oncol, 2012. **5**: p. 35.
13. Benjamin, R., *Neurologic complications of prostate cancer.* Am Fam Physician, 2002. **65**(9): p. 1834-40.
14. Fidler, I.J., *The pathogenesis of cancer metastasis: the 'seed and soil' hypothesis revisited.* Nat Rev Cancer, 2003. **3**(6): p. 453-8.
15. Fidler, I.J., *Selection of successive tumour lines for metastasis.* Nat New Biol, 1973. **242**(118): p. 148-9.
16. Franken, B., et al., *Circulating tumor cells, disease recurrence and survival in newly diagnosed breast cancer.* Breast Cancer Res, 2012. **14**(5): p. R133.
17. Gilbert, S.F., *Developmental Biology*. 6th ed. 2000, Sunderland, MA: Sinauer Associates.
18. in *Bone Health and Osteoporosis: A Report of the Surgeon General*. 2004: Rockville (MD).
19. Frost, H., *Bone Biodynamics*. 1964, Boston, MA: Little, Brown, and Company. 687.
20. Ash, P., J.F. Loutit, and K.M. Townsend, *Osteoclasts derived from haematopoietic stem cells.* Nature, 1980. **283**(5748): p. 669-70.
21. Crockett, J.C., et al., *Bone remodelling at a glance.* J Cell Sci, 2011. **124**(Pt 7): p. 991-8.
22. Manolagas, S.C., *Birth and death of bone cells: basic regulatory mechanisms and implications for the pathogenesis and treatment of osteoporosis.* Endocr Rev, 2000. **21**(2): p. 115-37.
23. Sims, N.A. and T.J. Martin, *Coupling the activities of bone formation and resorption: a multitude of signals within the basic multicellular unit.* Bonekey Rep, 2014. **3**: p. 481.

24. Komori, T., *Regulation of osteoblast differentiation by transcription factors.* J Cell Biochem, 2006. **99**(5): p. 1233-9.
25. Favus, M.J., *Primer on the Metabolic Bone Diseases and Disorders of Mineral Metabolism.* 2006.
26. Miao, D., et al., *Osteoblast-derived PTHrP is a potent endogenous bone anabolic agent that modifies the therapeutic efficacy of administered PTH 1-34.* J Clin Invest, 2005. **115**(9): p. 2402-11.
27. Huang, W., et al., *Signaling and transcriptional regulation in osteoblast commitment and differentiation.* Front Biosci, 2007. **12**: p. 3068-92.
28. Miller, S.C., et al., *Bone lining cells: structure and function.* Scanning Microsc, 1989. **3**(3): p. 953-60; discussion 960-1.
29. Bonewald, L.F., *The amazing osteocyte.* J Bone Miner Res, 2011. **26**(2): p. 229-38.
30. Paget, G., *Remarks on a Case of Alternate Partial Anaesthesia.* Br Med J, 1889. **1**(1462): p. 1-3.
31. Ewing, J., *Neoplastic Diseases*. 6 ed. 1928, Philadelphia: W.B. Saunders.
32. Poste, G. and I.J. Fidler, *The pathogenesis of cancer metastasis.* Nature, 1980. **283**(5743): p. 139-46.
33. Roudier, M.P., et al., *Bone histology at autopsy and matched bone scintigraphy findings in patients with hormone refractory prostate cancer: the effect of bisphosphonate therapy on bone scintigraphy results.* Clin Exp Metastasis, 2003. **20**(2): p. 171-80.
34. Koeneman, K.S., F. Yeung, and L.W. Chung, *Osteomimetic properties of prostate cancer cells: a hypothesis supporting the predilection of prostate cancer metastasis and growth in the bone environment.* Prostate, 1999. **39**(4): p. 246-61.
35. Thomas, R., et al., *Differential expression of osteonectin/SPARC during human prostate cancer progression.* Clin Cancer Res, 2000. **6**(3): p. 1140-9.
36. Lin, D.L., et al., *Bone metastatic LNCaP-derivative C4-2B prostate cancer cell line mineralizes in vitro.* Prostate, 2001. **47**(3): p. 212-21.
37. Chu, G.C. and L.W. Chung, *RANK-mediated signaling network and cancer metastasis.* Cancer Metastasis Rev, 2014. **33**(2-3): p. 497-509.
38. Kaplan, R.N., et al., *VEGFR1-positive haematopoietic bone marrow progenitors initiate the pre-metastatic niche.* Nature, 2005. **438**(7069): p. 820-7.
39. Webber, J., et al., *Cancer exosomes trigger fibroblast to myofibroblast differentiation.* Cancer Res, 2010. **70**(23): p. 9621-30.
40. Thery, C., L. Zitvogel, and S. Amigorena, *Exosomes: composition, biogenesis and function.* Nat Rev Immunol, 2002. **2**(8): p. 569-79.
41. Peinado, H., et al., *Melanoma exosomes educate bone marrow progenitor cells toward a pro-metastatic phenotype through MET.* Nat Med, 2012. **18**(6): p. 883-91.
42. Di Vizio, D., et al., *Oncosome formation in prostate cancer: association with a region of frequent chromosomal deletion in metastatic disease.* Cancer Res, 2009. **69**(13): p. 5601-9.
43. Sanchez, C.A., et al., *Exosomes from bulk and stem cells from human prostate cancer have a differential microRNA content that contributes cooperatively over local and pre-metastatic niche.* Oncotarget, 2016. **7**(4): p. 3993-4008.
44. Di Vizio, D., et al., *Large oncosomes in human prostate cancer tissues and in the circulation of mice with metastatic disease.* Am J Pathol, 2012. **181**(5): p. 1573-84.
45. Taichman, R.S., *Blood and bone: two tissues whose fates are intertwined to create the hematopoietic stem-cell niche.* Blood, 2005. **105**(7): p. 2631-9.
46. Lapidot, T. and O. Kollet, *The essential roles of the chemokine SDF-1 and its receptor CXCR4 in human stem cell homing and repopulation of transplanted immune-deficient NOD/SCID and NOD/SCID/B2m(null) mice.* Leukemia, 2002. **16**(10): p. 1992-2003.

47. Wang, J., R. Loberg, and R.S. Taichman, *The pivotal role of CXCL12 (SDF-1)/CXCR4 axis in bone metastasis.* Cancer Metastasis Rev, 2006. **25**(4): p. 573-87.
48. Singh, R.K. and B.L. Lokeshwar, *The IL-8-regulated chemokine receptor CXCR7 stimulates EGFR signaling to promote prostate cancer growth.* Cancer Res, 2011. **71**(9): p. 3268-77.
49. Lu, Y., et al., *Monocyte chemotactic protein-1 (MCP-1) acts as a paracrine and autocrine factor for prostate cancer growth and invasion.* Prostate, 2006. **66**(12): p. 1311-8.
50. Lu, Y., et al., *CXCL16 functions as a novel chemotactic factor for prostate cancer cells in vitro.* Mol Cancer Res, 2008. **6**(4): p. 546-54.
51. Roudier, M.P., et al., *Histopathological assessment of prostate cancer bone osteoblastic metastases.* J Urol, 2008. **180**(3): p. 1154-60.
52. Mundy, G.R., *Metastasis to bone: causes, consequences and therapeutic opportunities.* Nat Rev Cancer, 2002. **2**(8): p. 584-93.
53. Lynch, C.C., *Matrix metalloproteinases as master regulators of the vicious cycle of bone metastasis.* Bone, 2011. **48**(1): p. 44-53.
54. Faccio, R., *Immune regulation of the tumor/bone vicious cycle.* Ann N Y Acad Sci, 2011. **1237**: p. 71-8.
55. Casimiro, S., T.A. Guise, and J. Chirgwin, *The critical role of the bone microenvironment in cancer metastases.* Mol Cell Endocrinol, 2009. **310**(1-2): p. 71-81.
56. Cook, L.M., et al., *Integrating new discoveries into the "vicious cycle" paradigm of prostate to bone metastases.* Cancer Metastasis Rev, 2014. **33**(2-3): p. 511-25.
57. Lynch, C.C., et al., *Matrix metalloproteinase 7 mediates mammary epithelial cell tumorigenesis through the ErbB4 receptor.* Cancer Res, 2007. **67**(14): p. 6760-7.
58. Thiolloy, S., et al., *An osteoblast-derived proteinase controls tumor cell survival via TGF-beta activation in the bone microenvironment.* PLoS One, 2012. **7**(1): p. e29862.
59. Bruni-Cardoso, A., et al., *Osteoclast-Derived Matrix Metalloproteinase-9 Directly Affects Angiogenesis in the Prostate Tumor-Bone Microenvironment.* Mol Cancer Res, 2010.
60. Yang, L., et al., *Expansion of myeloid immune suppressor Gr+CD11b+ cells in tumor-bearing host directly promotes tumor angiogenesis.* Cancer Cell, 2004. **6**(4): p. 409-21.
61. Pang, Y., et al., *TGF-beta Signaling in Myeloid Cells Is Required for Tumor Metastasis.* Cancer Discov, 2013. **3**(8): p. 936-51.
62. Sawant, A., et al., *Myeloid-derived suppressor cells function as novel osteoclast progenitors enhancing bone loss in breast cancer.* Cancer Res, 2013. **73**(2): p. 672-82.
63. Danilin, S., et al., *Myeloid-derived suppressor cells expand during breast cancer progression and promote tumor-induced bone destruction.* Oncoimmunology, 2012. **1**(9): p. 1484-1494.
64. Biswas, S.K., A. Sica, and C.E. Lewis, *Plasticity of macrophage function during tumor progression: regulation by distinct molecular mechanisms.* J Immunol, 2008. **180**(4): p. 2011-7.
65. Dirkx, A.E., et al., *Monocyte/macrophage infiltration in tumors: modulators of angiogenesis.* J Leukoc Biol, 2006. **80**(6): p. 1183-96.
66. Petrylak, D.P., et al., *Docetaxel and estramustine compared with mitoxantrone and prednisone for advanced refractory prostate cancer.* N Engl J Med, 2004. **351**(15): p. 1513-20.
67. Tannock, I.F., et al., *Docetaxel plus prednisone or mitoxantrone plus prednisone for advanced prostate cancer.* N Engl J Med, 2004. **351**(15): p. 1502-12.
68. Agarwal, N., et al., *New agents for prostate cancer.* Ann Oncol, 2014.
69. Egan, A., et al., *Castration-resistant prostate cancer: adaptive responses in the androgen axis.* Cancer Treat Rev, 2014. **40**(3): p. 426-33.
70. Chang, K.H., et al., *Dihydrotestosterone synthesis bypasses testosterone to drive castration-resistant prostate cancer.* Proc Natl Acad Sci U S A, 2011. **108**(33): p. 13728-33.

71. Ishizaki, F., et al., *Androgen deprivation promotes intratumoral synthesis of dihydrotestosterone from androgen metabolites in prostate cancer.* Sci Rep, 2013. **3**: p. 1528.
72. Chang, K.H., et al., *A gain-of-function mutation in DHT synthesis in castration-resistant prostate cancer.* Cell, 2013. **154**(5): p. 1074-84.
73. de Bono, J.S., et al., *Abiraterone and increased survival in metastatic prostate cancer.* N Engl J Med, 2011. **364**(21): p. 1995-2005.
74. Ryan, C.J., et al., *Abiraterone in metastatic prostate cancer without previous chemotherapy.* N Engl J Med, 2013. **368**(2): p. 138-48.
75. Pinto, A., *Beyond abiraterone: new hormonal therapies for metastatic castration-resistant prostate cancer.* Cancer biology & therapy, 2014. **15**(2): p. 149-55.
76. www.fda.gov, *Enzalutamide (XTANDI Capsules).* U.S. Food and Drug Administration, 2012.
77. Scher, H.I., et al., *Increased survival with enzalutamide in prostate cancer after chemotherapy.* N Engl J Med, 2012. **367**(13): p. 1187-97.
78. Fizazi, K., et al., *Novel and bone-targeted agents for CRPC.* Ann Oncol, 2012. **23 Suppl 10**: p. x264-7.
79. Tran, C., et al., *Development of a second-generation antiandrogen for treatment of advanced prostate cancer.* Science, 2009. **324**(5928): p. 787-90.
80. Beer, T.M., et al., *Enzalutamide in Metastatic Prostate Cancer before Chemotherapy.* N Engl J Med, 2014.
81. Merseburger, A.S., G.P. Haas, and C.A. von Klot, *An update on enzalutamide in the treatment of prostate cancer.* Ther Adv Urol, 2015. **7**(1): p. 9-21.
82. Mita, A.C., et al., *Phase I and pharmacokinetic study of XRP6258 (RPR 116258A), a novel taxane, administered as a 1-hour infusion every 3 weeks in patients with advanced solid tumors.* Clin Cancer Res, 2009. **15**(2): p. 723-30.
83. de Bono, J.S., et al., *Prednisone plus cabazitaxel or mitoxantrone for metastatic castration-resistant prostate cancer progressing after docetaxel treatment: a randomised open-label trial.* Lancet, 2010. **376**(9747): p. 1147-54.
84. www.cancer.gov, *FDA Approval for Cabazitaxel.* National Cancer Institute, 2013.
85. Kantoff, P.W., et al., *Sipuleucel-T immunotherapy for castration-resistant prostate cancer.* N Engl J Med, 2010. **363**(5): p. 411-22.
86. www.cancer.gov, *FDA Approval for Sipuleucel-T.* National Cancer Institute, 2013.
87. Schweizer, M.T. and C.G. Drake, *Immunotherapy for prostate cancer: recent developments and future challenges.* Cancer Metastasis Rev, 2014. **33**(2-3): p. 641-55.
88. Pieczonka, C.M., et al., *Sipuleucel-T for the Treatment of Patients With Metastatic Castrate-resistant Prostate Cancer: Considerations for Clinical Practice.* Rev Urol, 2015. **17**(4): p. 203-10.
89. Huber, M.L., et al., *Interdisciplinary critique of sipuleucel-T as immunotherapy in castration-resistant prostate cancer.* J Natl Cancer Inst, 2012. **104**(4): p. 273-9.
90. Rogers, M.J., D.J. Watts, and R.G. Russell, *Overview of bisphosphonates.* Cancer, 1997. **80**(8 Suppl): p. 1652-60.
91. Saad, F., et al., *Long-term efficacy of zoledronic acid for the prevention of skeletal complications in patients with metastatic hormone-refractory prostate cancer.* J Natl Cancer Inst, 2004. **96**(11): p. 879-82.
92. www.cancer.gov, *FDA Approval for Denosumab.* National Cancer Institute, 2013.
93. Fizazi, K., et al., *Denosumab versus zoledronic acid for treatment of bone metastases in men with castration-resistant prostate cancer: a randomised, double-blind study.* Lancet, 2011. **377**(9768): p. 813-22.
94. Helo, S., J.P. Manger, and T.L. Krupski, *Role of denosumab in prostate cancer.* Prostate Cancer Prostatic Dis, 2012. **15**(3): p. 231-6.

95. Armstrong, A.P., et al., *RANKL acts directly on RANK-expressing prostate tumor cells and mediates migration and expression of tumor metastasis genes.* Prostate, 2008. **68**(1): p. 92-104.
96. Miller, R.E., et al., *RANK ligand inhibition plus docetaxel improves survival and reduces tumor burden in a murine model of prostate cancer bone metastasis.* Mol Cancer Ther, 2008. **7**(7): p. 2160-9.
97. www.cancer.gov, *FDA Approval for Radium 223 Dichloride.* National Cancer Institute, 2013.
98. Cheetham, P.J. and D.P. Petrylak, *Alpha particles as radiopharmaceuticals in the treatment of bone metastases: mechanism of action of radium-223 chloride (Alpharadin) and radiation protection.* Oncology (Williston Park), 2012. **26**(4): p. 330-7, 341.
99. Parker, C., et al., *Alpha emitter radium-223 and survival in metastatic prostate cancer.* N Engl J Med, 2013. **369**(3): p. 213-23.
100. Tomblyn, M., *The role of bone-seeking radionuclides in the palliative treatment of patients with painful osteoblastic skeletal metastases.* Cancer Control, 2012. **19**(2): p. 137-44.
101. Iagaru, A., et al., *Pilot prospective evaluation of 99mTc-MDP scintigraphy, 18F NaF PET/CT, 18F FDG PET/CT and whole-body MRI for detection of skeletal metastases.* Clin Nucl Med, 2013. **38**(7): p. e290-6.
102. O'Sullivan, G.J., F.L. Carty, and C.G. Cronin, *Imaging of bone metastasis: An update.* World J Radiol, 2015. **7**(8): p. 202-11.
103. Shiozawa, Y., et al., *The bone marrow niche: habitat to hematopoietic and mesenchymal stem cells, and unwitting host to molecular parasites.* Leukemia, 2008. **22**(5): p. 941-50.
104. Vessella, R.L., K. Pantel, and S. Mohla, *Tumor cell dormancy: an NCI workshop report.* Cancer biology & therapy, 2007. **6**(9): p. 1496-504.
105. Lam, H.M., R.L. Vessella, and C. Morrissey, *The role of the microenvironment-dormant prostate disseminated tumor cells in the bone marrow.* Drug Discov Today Technol, 2014. **11**: p. 41-7.
106. Shiozawa, Y., et al., *Annexin II/annexin II receptor axis regulates adhesion, migration, homing, and growth of prostate cancer.* J Cell Biochem, 2008. **105**(2): p. 370-80.
107. Shiozawa, Y., et al., *GAS6/AXL axis regulates prostate cancer invasion, proliferation, and survival in the bone marrow niche.* Neoplasia, 2010. **12**(2): p. 116-27.
108. Taichman, R.S., et al., *GAS6 receptor status is associated with dormancy and bone metastatic tumor formation.* PLoS One, 2013. **8**(4): p. e61873.
109. Dormady, S.P., X.M. Zhang, and R.S. Basch, *Hematopoietic progenitor cells grow on 3T3 fibroblast monolayers that overexpress growth arrest-specific gene-6 (GAS6).* Proc Natl Acad Sci U S A, 2000. **97**(22): p. 12260-5.
110. Kim, J.K., et al., *TBK1 regulates prostate cancer dormancy through mTOR inhibition.* Neoplasia, 2013. **15**(9): p. 1064-74.
111. Bragado, P., et al., *Microenvironments dictating tumor cell dormancy.* Recent Results Cancer Res, 2012. **195**: p. 25-39.
112. Bragado, P., et al., *TGF-beta2 dictates disseminated tumour cell fate in target organs through TGF-beta-RIII and p38alpha/beta signalling.* Nat Cell Biol, 2013. **15**(11): p. 1351-61.
113. Kobayashi, A., et al., *Bone morphogenetic protein 7 in dormancy and metastasis of prostate cancer stem-like cells in bone.* The Journal of experimental medicine, 2011. **208**(13): p. 2641-55.
114. Ghajar, C.M., et al., *The perivascular niche regulates breast tumour dormancy.* Nat Cell Biol, 2013. **15**(7): p. 807-17.
115. Shiozawa, Y., et al., *Human prostate cancer metastases target the hematopoietic stem cell niche to establish footholds in mouse bone marrow.* J Clin Invest, 2011. **121**(4): p. 1298-312.
116. Gerlinger, M., et al., *Intratumor heterogeneity and branched evolution revealed by multiregion sequencing.* The New England journal of medicine, 2012. **366**(10): p. 883-92.

117. Gerlinger, M., et al., *Intratumour Heterogeneity in Urologic Cancers: From Molecular Evidence to Clinical Implications.* Eur Urol, 2014.
118. Drake, J.M., et al., *Metastatic castration-resistant prostate cancer reveals intrapatient similarity and interpatient heterogeneity of therapeutic kinase targets.* Proceedings of the National Academy of Sciences of the United States of America, 2013. **110**(49): p. E4762-9.
119. Sweeney, C., et al., *Impact on overall survival (OS) with chemohormonal therapy versus hormonal therapy for hormone-sensitive newly metastatic prostate cancer (mPrCa): An ECOG-led phase III randomized trial.* JOurnal of Clinical Oncology, 2014. **32**(5s, Abstr LBA2).
120. Hidalgo, M., et al., *Patient-derived xenograft models: an emerging platform for translational cancer research.* Cancer Discov, 2014. **4**(9): p. 998-1013.
121. Nguyen, H.M., et al., *LuCaP Prostate Cancer Patient-Derived Xenografts Reflect the Molecular Heterogeneity of Advanced Disease an--d Serve as Models for Evaluating Cancer Therapeutics.* Prostate, 2017.
122. Cook, L.M., et al., *Predictive computational modeling to define effective treatment strategies for bone metastatic prostate cancer.* Sci Rep, 2016. **6**: p. 29384.
123. Tauro, M., J. McGuire, and C.C. Lynch, *New approaches to selectively target cancer associated matrix metalloproteinase activity.* Cancer and Metastasis Reviews, 2014. **In Press**.
124. Tauro, M., et al., *Bone seeking matrix metalloproteinase-2 inhibitors prevent bone metastatic breast cancer growth.* Mol Cancer Ther, 2017.
125. Esposito, M. and Y. Kang, *Targeting tumor-stromal interactions in bone metastasis.* Pharmacol Ther, 2014. **141**(2): p. 222-33.
126. Rosol, T.J. and C.C. Capen, *Mechanisms of cancer-induced hypercalcemia.* Lab Invest, 1992. **67**(6): p. 680-702.
127. Albright, F., *Case records of the Massachusetts General Hospital-case 27461.* New England Journal of Medicine, 1941. **225**: p. 789-791.
128. Martin, T.J., *Parathyroid Hormone-Related Protein, Its Regulation of Cartilage and Bone Development, and Role in Treating Bone Diseases.* Physiol Rev, 2016. **96**(3): p. 831-71.
129. Burtis, W.J., *Parathyroid hormone-related protein: structure, function, and measurement.* Clin Chem, 1992. **38**(11): p. 2171-83.
130. Suva, L.J., et al., *A parathyroid hormone-related protein implicated in malignant hypercalcemia: cloning and expression.* Science, 1987. **237**(4817): p. 893-6.
131. Strewler, G.J., et al., *Parathyroid hormonelike protein from human renal carcinoma cells. Structural and functional homology with parathyroid hormone.* J Clin Invest, 1987. **80**(6): p. 1803-7.
132. Moseley, J.M., et al., *Parathyroid hormone-related protein purified from a human lung cancer cell line.* Proc Natl Acad Sci U S A, 1987. **84**(14): p. 5048-52.
133. McCauley, L.K. and T.J. Martin, *Twenty-five years of PTHrP progress: from cancer hormone to multifunctional cytokine.* J Bone Miner Res, 2012. **27**(6): p. 1231-9.
134. Southby, J., et al., *Immunohistochemical localization of parathyroid hormone-related protein in human breast cancer.* Cancer Res, 1990. **50**(23): p. 7710-6.
135. Powell, G.J., et al., *Localization of parathyroid hormone-related protein in breast cancer metastases: increased incidence in bone compared with other sites.* Cancer Res, 1991. **51**(11): p. 3059-61.
136. Guise, T.A., et al., *Evidence for a causal role of parathyroid hormone-related protein in the pathogenesis of human breast cancer-mediated osteolysis.* J Clin Invest, 1996. **98**(7): p. 1544-9.
137. Kremer, R., et al., *ras Activation of human prostate epithelial cells induces overexpression of parathyroid hormone-related peptide.* Clin Cancer Res, 1997. **3**(6): p. 855-9.

138. Liao, J., et al., *Tumor expressed PTHrP facilitates prostate cancer-induced osteoblastic lesions.* Int J Cancer, 2008. **123**(10): p. 2267-78.
139. Francini, G., et al., *Production of parathyroid hormone and parathyroid-hormone-related protein by breast cancer cells in culture.* J Cancer Res Clin Oncol, 1993. **119**(7): p. 421-5.
140. Ikeda, K., et al., *Expression of messenger ribonucleic acids encoding a parathyroid hormone-like peptide in normal human and animal tissues with abnormal expression in human parathyroid adenomas.* Mol Endocrinol, 1988. **2**(12): p. 1230-6.
141. Karaplis, A.C., et al., *Lethal skeletal dysplasia from targeted disruption of the parathyroid hormone-related peptide gene.* Genes Dev, 1994. **8**(3): p. 277-89.
142. Wysolmerski, J.J., et al., *Rescue of the parathyroid hormone-related protein knockout mouse demonstrates that parathyroid hormone-related protein is essential for mammary gland development.* Development, 1998. **125**(7): p. 1285-94.
143. Philbrick, W.M., et al., *Parathyroid hormone-related protein is required for tooth eruption.* Proc Natl Acad Sci U S A, 1998. **95**(20): p. 11846-51.
144. Wysolmerski, J.J., et al., *Overexpression of parathyroid hormone-related protein or parathyroid hormone in transgenic mice impairs branching morphogenesis during mammary gland development.* Development, 1995. **121**(11): p. 3539-47.
145. Foley, J., et al., *PTHrP regulates epidermal differentiation in adult mice.* J Invest Dermatol, 1998. **111**(6): p. 1122-8.
146. Lanske, B., et al., *Ablation of the PTHrP gene or the PTH/PTHrP receptor gene leads to distinct abnormalities in bone development.* J Clin Invest, 1999. **104**(4): p. 399-407.
147. Martin, T.J., *Osteoblast-derived PTHrP is a physiological regulator of bone formation.* J Clin Invest, 2005. **115**(9): p. 2322-4.
148. Horwitz, M.J., et al., *Parathyroid hormone-related protein for the treatment of postmenopausal osteoporosis: defining the maximal tolerable dose.* J Clin Endocrinol Metab, 2010. **95**(3): p. 1279-87.
149. Horwitz, M.J., et al., *Short-term, high-dose parathyroid hormone-related protein as a skeletal anabolic agent for the treatment of postmenopausal osteoporosis.* J Clin Endocrinol Metab, 2003. **88**(2): p. 569-75.
150. Stewart, A.F., et al., *Six-month daily administration of parathyroid hormone and parathyroid hormone-related protein peptides to adult ovariectomized rats markedly enhances bone mass and biomechanical properties: a comparison of human parathyroid hormone 1-34, parathyroid hormone-related protein 1-36, and SDZ-parathyroid hormone 893.* J Bone Miner Res, 2000. **15**(8): p. 1517-25.
151. Miller, P.D., et al., *Effect of Abaloparatide vs Placebo on New Vertebral Fractures in Postmenopausal Women With Osteoporosis: A Randomized Clinical Trial.* JAMA, 2016. **316**(7): p. 722-33.
152. Leder, B.Z., et al., *Effects of abaloparatide, a human parathyroid hormone-related peptide analog, on bone mineral density in postmenopausal women with osteoporosis.* J Clin Endocrinol Metab, 2015. **100**(2): p. 697-706.
153. Sheikh, S.P., et al., *Similar structures and shared switch mechanisms of the beta2-adrenoceptor and the parathyroid hormone receptor. Zn(II) bridges between helices III and VI block activation.* J Biol Chem, 1999. **274**(24): p. 17033-41.
154. Abou-Samra, A.B., et al., *Expression cloning of a common receptor for parathyroid hormone and parathyroid hormone-related peptide from rat osteoblast-like cells: a single receptor stimulates intracellular accumulation of both cAMP and inositol trisphosphates and increases intracellular free calcium.* Proc Natl Acad Sci U S A, 1992. **89**(7): p. 2732-6.

155. Cupp, M.E., et al., *Parathyroid hormone (PTH) and PTH-related peptide domains contributing to activation of different PTH receptor-mediated signaling pathways.* J Pharmacol Exp Ther, 2013. **345**(3): p. 404-18.
156. Datta, N.S., et al., *Role of PTH1R internalization in osteoblasts and bone mass using a phosphorylation-deficient knock-in mouse model.* J Endocrinol, 2010. **207**(3): p. 355-65.
157. Ferrandon, S., et al., *Sustained cyclic AMP production by parathyroid hormone receptor endocytosis.* Nat Chem Biol, 2009. **5**(10): p. 734-42.
158. Pioszak, A.A., et al., *Structural basis for parathyroid hormone-related protein binding to the parathyroid hormone receptor and design of conformation-selective peptides.* J Biol Chem, 2009. **284**(41): p. 28382-91.
159. Gardella, T.J. and H. Juppner, *Molecular properties of the PTH/PTHrP receptor.* Trends Endocrinol Metab, 2001. **12**(5): p. 210-7.
160. Luck, M.D., P.H. Carter, and T.J. Gardella, *The (1-14) fragment of parathyroid hormone (PTH) activates intact and amino-terminally truncated PTH-1 receptors.* Mol Endocrinol, 1999. **13**(5): p. 670-80.
161. Cole, J.A., et al., *Structure-activity relationships of parathyroid hormone analogs in the opossum kidney cell line.* J Bone Miner Res, 1989. **4**(5): p. 723-30.
162. Takasu, H., et al., *Amino-terminal modifications of human parathyroid hormone (PTH) selectively alter phospholipase C signaling via the type 1 PTH receptor: implications for design of signal-specific PTH ligands.* Biochemistry, 1999. **38**(41): p. 13453-60.
163. Jouishomme, H., et al., *Further definition of the protein kinase C activation domain of the parathyroid hormone.* J Bone Miner Res, 1994. **9**(6): p. 943-9.
164. Liu, B., D. Goltzman, and S.A. Rabbani, *Processing of pro-PTHRP by the prohormone convertase, furin: effect on biological activity.* Am J Physiol, 1995. **268**(5 Pt 1): p. E832-8.
165. Orloff, J.J., et al., *Parathyroid hormone-related protein as a prohormone: posttranslational processing and receptor interactions.* Endocr Rev, 1994. **15**(1): p. 40-60.
166. Miao, D., et al., *Parathyroid hormone-related peptide is required for increased trabecular bone volume in parathyroid hormone-null mice.* Endocrinology, 2004. **145**(8): p. 3554-62.
167. Stewart, A.F., *PTHrP(1-36) as a skeletal anabolic agent for the treatment of osteoporosis.* Bone, 1996. **19**(4): p. 303-6.
168. Cramer, S.D., Z. Chen, and D.M. Peehl, *Prostate specific antigen cleaves parathyroid hormone-related protein in the PTH-like domain: inactivation of PTHrP-stimulated cAMP accumulation in mouse osteoblasts.* J Urol, 1996. **156**(2 Pt 1): p. 526-31.
169. Ruchon, A.F., et al., *Cellular localization of neprilysin in mouse bone tissue and putative role in hydrolysis of osteogenic peptides.* J Bone Miner Res, 2000. **15**(7): p. 1266-74.
170. Philbrick, W.M., et al., *Defining the roles of parathyroid hormone-related protein in normal physiology.* Physiol Rev, 1996. **76**(1): p. 127-73.
171. Soifer, N.E., et al., *Parathyroid hormone-related protein. Evidence for secretion of a novel mid-region fragment by three different cell types.* J Biol Chem, 1992. **267**(25): p. 18236-43.
172. Hook, V.Y., et al., *Proteolysis of ProPTHrP(1-141) by "prohormone thiol protease" at multibasic residues generates PTHrP-related peptides: implications for PTHrP peptide production in lung cancer cells.* Biochem Biophys Res Commun, 2001. **285**(4): p. 932-8.
173. Hendy, G.N., et al., *Proparathyroid hormone is preferentially cleaved to parathyroid hormone by the prohormone convertase furin. A mass spectrometric study.* J Biol Chem, 1995. **270**(16): p. 9517-25.
174. Zhang, K., et al., *Effects of parathyroid hormone-related protein on osteogenic and adipogenic differentiation of human mesenchymal stem cells.* Eur Rev Med Pharmacol Sci, 2014. **18**(11): p. 1610-7.

175. Washam, C.L., et al., *Identification of PTHrP(12-48) as a plasma biomarker associated with breast cancer bone metastasis.* Cancer Epidemiol Biomarkers Prev, 2013. **22**(5): p. 972-83.
176. Hastings, R.H., et al., *Parathyroid hormone-related protein-(38-64) regulates lung cell proliferation after silica injury.* Am J Physiol Lung Cell Mol Physiol, 2002. **283**(1): p. L12-21.
177. Luparello, C., et al., *Midregion parathyroid hormone-related protein inhibits growth and invasion in vitro and tumorigenesis in vivo of human breast cancer cells.* J Bone Miner Res, 2001. **16**(12): p. 2173-81.
178. Luparello, C., R. Sirchia, and B. Lo Sasso, *Midregion PTHrP regulates Rip1 and caspase expression in MDA-MB231 breast cancer cells.* Breast Cancer Res Treat, 2008. **111**(3): p. 461-74.
179. Philbrick, W., *Parathyroid hormone-related protein: Gene structure, biosynthesis, metabolism, and regulation. In: The parathyroids.* 2001.
180. Luparello, C., R. Sirchia, and D. Pupello, *PTHrP [67-86] regulates the expression of stress proteins in breast cancer cells inducing modifications in urokinase-plasminogen activator and MMP-1 expression 5.* Journal of Cell Science, 2003. **116**(Pt 12): p. 2421-2430.
181. Rihani-Basharat, S. and D. Lewinson, *PTHrP(107-111) inhibits in vivo resorption that was stimulated by PTHrP(1-34) when applied intermittently to neonatal mice.* Calcif Tissue Int, 1997. **61**(5): p. 426-8.
182. Fenton, A.J., T.J. Martin, and G.C. Nicholson, *Long-term culture of disaggregated rat osteoclasts: inhibition of bone resorption and reduction of osteoclast-like cell number by calcitonin and PTHrP[107-139].* J Cell Physiol, 1993. **155**(1): p. 1-7.
183. Chen, H.L., et al., *Parathyroid hormone and parathyroid hormone-related protein exert both pro- and anti-apoptotic effects in mesenchymal cells.* J Biol Chem, 2002. **277**(22): p. 19374-81.
184. Kaji, H., et al., *Carboxyl-terminal peptides from parathyroid hormone-related protein stimulate osteoclast-like cell formation.* Endocrinology, 1995. **136**(3): p. 842-8.
185. Boileau, G., et al., *Characterization of PHEX endopeptidase catalytic activity: identification of parathyroid-hormone-related peptide107-139 as a substrate and osteocalcin, PPi and phosphate as inhibitors.* Biochem J, 2001. **355**(Pt 3): p. 707-13.
186. Errecart, M.T., et al., *Methodology.* J Sch Health, 1995. **65**(8): p. 295-301.
187. Valin, A., et al., *Antiproliferative effect of the C-terminal fragments of parathyroid hormone-related protein, PTHrP-(107-111) and (107-139), on osteoblastic osteosarcoma cells.* J Cell Physiol, 1997. **170**(2): p. 209-15.
188. Whitfield, J.F., et al., *C-terminal fragments of parathyroid hormone-related protein, PTHrP-(107-111) and (107-139), and the N-terminal PTHrP-(1-40) fragment stimulate membrane-associated protein kinase C activity in rat spleen lymphocytes.* J Cell Physiol, 1994. **158**(3): p. 518-22.
189. Esbrit, P., et al., *C-terminal parathyroid hormone-related protein increases vascular endothelial growth factor in human osteoblastic cells.* J Am Soc Nephrol, 2000. **11**(6): p. 1085-92.
190. Lopez-Otin, C. and J.S. Bond, *Proteases: multifunctional enzymes in life and disease.* J Biol Chem, 2008. **283**(45): p. 30433-7.
191. Fingleton, B. and C.C. Lynch, *A new dress code for MMPs: cleavage optional.* Dev Cell, 2010. **18**(1): p. 3-4.
192. Turk, B., *Targeting proteases: successes, failures and future prospects.* Nat Rev Drug Discov, 2006. **5**(9): p. 785-99.
193. Perez-Silva, J.G., et al., *The Degradome database: expanding roles of mammalian proteases in life and disease.* Nucleic Acids Res, 2016. **44**(D1): p. D351-5.
194. Artenstein, A.W. and S.M. Opal, *Proprotein convertases in health and disease.* N Engl J Med, 2011. **365**(26): p. 2507-18.

195. Hara, M., et al., *[Some physico-chemical characteristics of " -seminoprotein", an antigenic component specific for human seminal plasma. Forensic immunological study of body fluids and secretion. VII].* Nihon Hoigaku Zasshi, 1971. **25**(4): p. 322-4.
196. Balk, S.P., Y.J. Ko, and G.J. Bubley, *Biology of prostate-specific antigen.* J Clin Oncol, 2003. **21**(2): p. 383-91.
197. Mattsson, J.M., et al., *Proteolytic activity of prostate-specific antigen (PSA) towards protein substrates and effect of peptides stimulating PSA activity.* PLoS One, 2014. **9**(9): p. e107819.
198. Hong, S.K., *Kallikreins as biomarkers for prostate cancer.* Biomed Res Int, 2014. **2014**: p. 526341.
199. Webber, M.M., A. Waghray, and D. Bello, *Prostate-specific antigen, a serine protease, facilitates human prostate cancer cell invasion.* Clin Cancer Res, 1995. **1**(10): p. 1089-94.
200. Saraswati, S., et al., *Galectin-3 is a substrate for prostate specific antigen (PSA) in human seminal plasma.* Prostate, 2011. **71**(2): p. 197-208.
201. Cohen, P., et al., *Prostate-specific antigen (PSA) is an insulin-like growth factor binding protein-3 protease found in seminal plasma.* J Clin Endocrinol Metab, 1992. **75**(4): p. 1046-53.
202. Kanety, H., et al., *Serum insulin-like growth factor-binding protein-2 (IGFBP-2) is increased and IGFBP-3 is decreased in patients with prostate cancer: correlation with serum prostate-specific antigen.* J Clin Endocrinol Metab, 1993. **77**(1): p. 229-33.
203. Williams, S.A., et al., *Does PSA play a role as a promoting agent during the initiation and/or progression of prostate cancer?* Prostate, 2007. **67**(3): p. 312-29.
204. Dallas, S.L., et al., *Preferential production of latent transforming growth factor beta-2 by primary prostatic epithelial cells and its activation by prostate-specific antigen.* J Cell Physiol, 2005. **202**(2): p. 361-70.
205. Iwamura, M., et al., *Alteration of the hormonal bioactivity of parathyroid hormone-related protein (PTHrP) as a result of limited proteolysis by prostate-specific antigen.* Urology, 1996. **48**(2): p. 317-25.
206. Deftos, L.J., et al., *Comparative tissue distribution of the processing enzymes "prohormone thiol protease," and prohormone convertases 1 and 2, in human PTHrP-producing cell lines and mammalian neuroendocrine tissues.* Endocrine, 2001. **15**(2): p. 217-24.
207. Lopez-Otin, C. and L.M. Matrisian, *Emerging roles of proteases in tumour suppression.* Nat Rev Cancer, 2007. **7**(10): p. 800-8.
208. Krane, S.M. and M. Inada, *Matrix metalloproteinases and bone.* Bone, 2008. **43**(1): p. 7-18.
209. Lynch, C.C., *Matrix metalloproteinases as master regulators of the vicious cycle of bone metastasis.* Bone, 2010.
210. Lopez-Otin, C. and C.M. Overall, *Protease degradomics: a new challenge for proteomics.* Nature reviews. Molecular cell biology, 2002. **3**(7): p. 509-19.
211. Lynch, C.C., et al., *MMP-7 promotes prostate cancer-induced osteolysis via the solubilization of RANKL.* Cancer Cell, 2005. **7**(5): p. 485-96.
212. Winding, B., et al., *Synthetic matrix metalloproteinase inhibitors inhibit growth of established breast cancer osteolytic lesions and prolong survival in mice.* Clinical Cancer Research, 2002. **8**(6): p. 1932-1939.
213. Bonfil, R.D., et al., *Inhibition of human prostate cancer growth, osteolysis and angiogenesis in a bone metastasis model by a novel mechanism-based selective gelatinase inhibitor.* International Journal of Cancer, 2006. **118**(11): p. 2721-2726.
214. Croucher, P.I., M.M. McDonald, and T.J. Martin, *Bone metastasis: the importance of the neighbourhood.* Nat Rev Cancer, 2016. **16**(6): p. 373-86.
215. Guise, T.A., *Parathyroid hormone-related protein and bone metastases.* Cancer, 1997. **80**(8 Suppl): p. 1572-80.

216. Mundy, G.R., *Metastasis to bone: causes, consequences and therapeutic opportunities.* Nature Reviews Cancer, 2002. **2**(8): p. 584-593.
217. Hodde, J.P., et al., *Small intestinal submucosa does not promote PAIII tumor growth in Lobund-Wistar rats.* J Surg Res, 2004. **120**(2): p. 189-94.
218. Wu, T.T., et al., *Establishing human prostate cancer cell xenografts in bone: induction of osteoblastic reaction by prostate-specific antigen-producing tumors in athymic and SCID/bg mice using LNCaP and lineage-derived metastatic sublines.* Int J Cancer, 1998. **77**(6): p. 887-94.
219. Helfrich, M.H. and S. Ralston, *Bone research protocols*. Methods in molecular medicine. 2003, Totowa, N.J.: Humana Press. xiv, 448 p.
220. Livak, K.J. and T.D. Schmittgen, *Analysis of relative gene expression data using real-time quantitative PCR and the 2(-Delta Delta C(T)) Method.* Methods, 2001. **25**(4): p. 402-8.
221. Remily-Wood, E.R., et al., *A database of reaction monitoring mass spectrometry assays for elucidating therapeutic response in cancer.* Proteomics Clin Appl, 2011. **5**(7-8): p. 383-96.
222. Gallien, S., et al., *Targeted proteomic quantification on quadrupole-orbitrap mass spectrometer.* Mol Cell Proteomics, 2012. **11**(12): p. 1709-23.
223. MacLean, B., et al., *Skyline: an open source document editor for creating and analyzing targeted proteomics experiments.* Bioinformatics, 2010. **26**(7): p. 966-8.
224. Zhao, W., et al., *Bone resorption induced by parathyroid hormone is strikingly diminished in collagenase-resistant mutant mice.* J Clin Invest, 1999. **103**(4): p. 517-24.
225. Yates, A.J., et al., *Effects of a synthetic peptide of a parathyroid hormone-related protein on calcium homeostasis, renal tubular calcium reabsorption, and bone metabolism in vivo and in vitro in rodents.* J Clin Invest, 1988. **81**(3): p. 932-8.
226. Mohammad, K.S., J.M. Chirgwin, and T.A. Guise, *Assessing new bone formation in neonatal calvarial organ cultures.* Methods Mol Biol, 2008. **455**: p. 37-50.
227. Datta, N.S., et al., *Cyclin D1 as a target for the proliferative effects of PTH and PTHrP in early osteoblastic cells.* J Bone Miner Res, 2007. **22**(7): p. 951-64.
228. Holmbeck, K., et al., *MT1-MMP-deficient mice develop dwarfism, osteopenia, arthritis, and connective tissue disease due to inadequate collagen turnover.* Cell, 1999. **99**(1): p. 81-92.
229. Park, H.J., et al., *The cooperation of CREB and NFAT is required for PTHrP-induced RANKL expression in mouse osteoblastic cells.* J Cell Physiol, 2015. **230**(3): p. 667-79.
230. Bilezikian, J.P., et al., *The parathyroids : basic and clinical concepts*. Third edition. ed. 2015. xxv, 919 pages.
231. Jilka, R.L., et al., *Osteoblast programmed cell death (apoptosis): modulation by growth factors and cytokines.* J Bone Miner Res, 1998. **13**(5): p. 793-802.
232. Esbrit, P. and M.J. Alcaraz, *Current perspectives on parathyroid hormone (PTH) and PTH-related protein (PTHrP) as bone anabolic therapies.* Biochem Pharmacol, 2013. **85**(10): p. 1417-23.
233. Pettway, G.J., et al., *Anabolic actions of PTH (1-34): use of a novel tissue engineering model to investigate temporal effects on bone.* Bone, 2005. **36**(6): p. 959-70.
234. Fukushima, H., et al., *Parathyroid-hormone-related protein induces expression of receptor activator of NF-{kappa}B ligand in human periodontal ligament cells via a cAMP/protein kinase A-independent pathway.* J Dent Res, 2005. **84**(4): p. 329-34.
235. Anderson, N.L., et al., *Mass spectrometric quantitation of peptides and proteins using Stable Isotope Standards and Capture by Anti-Peptide Antibodies (SISCAPA).* J Proteome Res, 2004. **3**(2): p. 235-44.
236. Katafuchi, T., et al., *Detection of FGF15 in plasma by stable isotope standards and capture by anti-peptide antibodies and targeted mass spectrometry.* Cell Metab, 2015. **21**(6): p. 898-904.
237. Yoon, H., et al., *Activation profiles of human kallikrein-related peptidases by matrix metalloproteinases.* Biol Chem, 2013. **394**(1): p. 137-47.

238. Pezzato, E., et al., *Prostate carcinoma and green tea: PSA-triggered basement membrane degradation and MMP-2 activation are inhibited by (-)epigallocatechin-3-gallate.* Int J Cancer, 2004. **112**(5): p. 787-92.
239. Kawashima-Ohya, Y., et al., *Effects of parathyroid hormone (PTH) and PTH-related peptide on expressions of matrix metalloproteinase-2, -3, and -9 in growth plate chondrocyte cultures.* Endocrinology, 1998. **139**(4): p. 2120-7.
240. Ibaragi, S., et al., *Parathyroid hormone-related peptide regulates matrix metalloproteinase-13 gene expression in bone metastatic breast cancer cells.* Anticancer Res, 2010. **30**(12): p. 5029-36.
241. Lu, J.T., et al., *Hedgehog signaling pathway mediates invasion and metastasis of hepatocellular carcinoma via ERK pathway.* Acta Pharmacol Sin, 2012. **33**(5): p. 691-700.
242. Kwon, Y.J., et al., *Gli1 enhances migration and invasion via up-regulation of MMP-11 and promotes metastasis in ERalpha negative breast cancer cell lines.* Clin Exp Metastasis, 2011. **28**(5): p. 437-49.
243. Nagai, S., et al., *Gli1 contributes to the invasiveness of pancreatic cancer through matrix metalloproteinase-9 activation.* Cancer Sci, 2008. **99**(7): p. 1377-84.
244. Sterling, J.A., et al., *The hedgehog signaling molecule Gli2 induces parathyroid hormone-related peptide expression and osteolysis in metastatic human breast cancer cells.* Cancer Res, 2006. **66**(15): p. 7548-53.
245. Johnson, R.W., et al., *TGF-beta promotion of Gli2-induced expression of parathyroid hormone-related protein, an important osteolytic factor in bone metastasis, is independent of canonical Hedgehog signaling.* Cancer Res, 2011. **71**(3): p. 822-31.
246. Wutzl, A., et al., *Bone morphogenetic proteins 5 and 6 stimulate osteoclast generation.* J Biomed Mater Res A, 2006. **77**(1): p. 75-83.
247. Valenti, M.T., et al., *Gene expression analysis in osteoblastic differentiation from peripheral blood mesenchymal stem cells.* Bone, 2008. **43**(6): p. 1084-92.
248. Mizuno, M. and Y. Kuboki, *Osteoblast-related gene expression of bone marrow cells during the osteoblastic differentiation induced by type I collagen.* J Biochem, 2001. **129**(1): p. 133-8.
249. Hayashi, H., et al., *The role of Mac-1 (CD11b/CD18) in osteoclast differentiation induced by receptor activator of nuclear factor-kappaB ligand.* FEBS Lett, 2008. **582**(21-22): p. 3243-8.
250. Amizuka, N., et al., *Recent studies on the biological action of parathyroid hormone (PTH)-related peptide (PTHrP) and PTH/PTHrP receptor in cartilage and bone.* Histol Histopathol, 2000. **15**(3): p. 957-70.
251. Cuthbertson, R.M., B.E. Kemp, and J.A. Barden, *Structure study of osteostatin PTHrP[Thr107](107-139).* Biochim Biophys Acta, 1999. **1432**(1): p. 64-72.
252. Garcia-Martin, A., et al., *Functional roles of the nuclear localization signal of parathyroid hormone-related protein (PTHrP) in osteoblastic cells.* Mol Endocrinol, 2014. **28**(6): p. 925-34.
253. Lai, C.F., et al., *Erk is essential for growth, differentiation, integrin expression, and cell function in human osteoblastic cells.* J Biol Chem, 2001. **276**(17): p. 14443-50.
254. Azarani, A., D. Goltzman, and J. Orlowski, *Structurally diverse N-terminal peptides of parathyroid hormone (PTH) and PTH-related peptide (PTHRP) inhibit the Na+/H+ exchanger NHE3 isoform by binding to the PTH/PTHRP receptor type I and activating distinct signaling pathways.* J Biol Chem, 1996. **271**(25): p. 14931-6.
255. Takuwa, Y., et al., *Endothelin-1 activates phospholipase C and mobilizes Ca2+ from extra- and intracellular pools in osteoblastic cells.* Am J Physiol, 1989. **257**(6 Pt 1): p. E797-803.
256. Schluter, K.D., C. Katzer, and H.M. Piper, *A N-terminal PTHrP peptide fragment void of a PTH/PTHrP-receptor binding domain activates cardiac ET(A) receptors.* Br J Pharmacol, 2001. **132**(2): p. 427-32.

257. Frieling, J.S., D. Basanta, and C.C. Lynch, *Current and emerging therapies for bone metastatic castration-resistant prostate cancer.* Cancer Control, 2015. **22**(1): p. 109-20.
258. Mak, I.W., R.E. Turcotte, and M. Ghert, *Parathyroid hormone-related protein (PTHrP) modulates adhesion, migration and invasion in bone tumor cells.* Bone, 2013. **55**(1): p. 198-207.
259. Nagase, H. and J.F. Woessner, Jr., *Matrix metalloproteinases.* Journal Biological Chemistry, 1999. **274**(31): p. 21491-21494.
260. Gross, J. and C.M. Lapiere, *Collagenolytic activity in amphibian tissues: a tissue culture assay.* Proc Natl Acad Sci U S A, 1962. **48**: p. 1014-22.
261. Egeblad, M. and Z. Werb, *New functions for the matrix metalloproteinases in cancer progression.* Nat Rev Cancer, 2002. **2**(3): p. 161-74.
262. Nagase, H., R. Visse, and G. Murphy, *Structure and function of matrix metalloproteinases and TIMPs.* Cardiovasc Res, 2006. **69**(3): p. 562-73.
263. Harper, E., K.J. Bloch, and J. Gross, *The zymogen of tadpole collagenase.* Biochemistry, 1971. **10**(16): p. 3035-41.
264. Van Wart, H.E. and H. Birkedal-Hansen, *The cysteine switch: a principle of regulation of metalloproteinase activity with potential applicability to the entire matrix metalloproteinase gene family.* Proc Natl Acad Sci U S A, 1990. **87**(14): p. 5578-82.
265. Nagase, H., *Activation mechanisms of matrix metalloproteinases.* Biol Chem, 1997. **378**(3-4): p. 151-60.
266. Hadler-Olsen, E., et al., *Regulation of matrix metalloproteinase activity in health and disease.* FEBS J, 2011. **278**(1): p. 28-45.
267. Lijnen, H.R., *Plasmin and matrix metalloproteinases in vascular remodeling.* Thromb Haemost, 2001. **86**(1): p. 324-33.
268. Visse, R. and H. Nagase, *Matrix metalloproteinases and tissue inhibitors of metalloproteinases: structure, function, and biochemistry.* Circ Res, 2003. **92**(8): p. 827-39.
269. Overall, C.M., *Matrix metalloproteinase substrate binding domains, modules and exosites. Overview and experimental strategies.* Methods Mol Biol, 2001. **151**: p. 79-120.
270. Gomis-Ruth, F.X., et al., *The helping hand of collagenase-3 (MMP-13): 2.7 A crystal structure of its C-terminal haemopexin-like domain.* J Mol Biol, 1996. **264**(3): p. 556-66.
271. Overall, C.M., *Molecular determinants of metalloproteinase substrate specificity: matrix metalloproteinase substrate binding domains, modules, and exosites.* Mol Biotechnol, 2002. **22**(1): p. 51-86.
272. Kessenbrock, K., et al., *A role for matrix metalloproteinases in regulating mammary stem cell function via the Wnt signaling pathway.* Cell Stem Cell, 2013. **13**(3): p. 300-13.
273. Sakamoto, T. and M. Seiki, *Cytoplasmic tail of MT1-MMP regulates macrophage motility independently from its protease activity.* Genes Cells, 2009. **14**(5): p. 617-26.
274. Redondo-Munoz, J., et al., *Matrix metalloproteinase-9 promotes chronic lymphocytic leukemia b cell survival through its hemopexin domain.* Cancer Cell, 2010. **17**(2): p. 160-72.
275. Bauer, E.A., et al., *Collagenase production by human skin fibroblasts.* Biochem Biophys Res Commun, 1975. **64**(1): p. 232-40.
276. Gomez, D.E., et al., *Tissue inhibitors of metalloproteinases: structure, regulation and biological functions.* Eur J Cell Biol, 1997. **74**(2): p. 111-22.
277. Coussens, L.M., B. Fingleton, and L.M. Matrisian, *Matrix metalloproteinase inhibitors and cancer: trials and tribulations.* Science, 2002. **295**(5564): p. 2387-2392.
278. Overall, C.M. and C. Lopez-Otin, *Strategies for MMP inhibition in cancer: innovations for the post-trial era.* Nat Rev Cancer, 2002. **2**(9): p. 657-72.
279. Kruger, A., et al., *Antimetastatic activity of a novel mechanism-based gelatinase inhibitor.* Cancer Res, 2005. **65**(9): p. 3523-6.

280. Gialeli, C., A.D. Theocharis, and N.K. Karamanos, *Roles of matrix metalloproteinases in cancer progression and their pharmacological targeting.* FEBS J, 2011. **278**(1): p. 16-27.
281. Overall, C.M. and C.P. Blobel, *In search of partners: linking extracellular proteases to substrates.* Nat Rev Mol Cell Biol, 2007. **8**(3): p. 245-57.
282. Rodriguez, D., C.J. Morrison, and C.M. Overall, *Matrix metalloproteinases: what do they not do? New substrates and biological roles identified by murine models and proteomics.* Biochim Biophys Acta, 2010. **1803**(1): p. 39-54.
283. Morrison, C.J., et al., *Matrix metalloproteinase proteomics: substrates, targets, and therapy.* Curr Opin Cell Biol, 2009. **21**(5): p. 645-53.
284. Overall, C.M. and O. Kleifeld, *Tumour microenvironment - opinion: validating matrix metalloproteinases as drug targets and anti-targets for cancer therapy.* Nat Rev Cancer, 2006. **6**(3): p. 227-39.
285. Balbin, M., et al., *Loss of collagenase-2 confers increased skin tumor susceptibility to male mice.* Nat Genet, 2003. **35**(3): p. 252-7.
286. Chin, J.R., G. Murphy, and Z. Werb, *Stromelysin, a connective tissue-degrading metalloendopeptidase secreted by stimulated rabbit synovial fibroblasts in parallel with collagenase. Biosynthesis, isolation, characterization, and substrates.* J Biol Chem, 1985. **260**(22): p. 12367-76.
287. Matrisian, L.M., et al., *Epidermal growth factor and oncogenes induce transcription of the same cellular mRNA in rat fibroblasts.* EMBO J, 1985. **4**(6): p. 1435-40.
288. Matrisian, L.M., et al., *The mRNA coding for the secreted protease transin is expressed more abundantly in malignant than in benign tumors.* Proc Natl Acad Sci U S A, 1986. **83**(24): p. 9413-7.
289. Andisheh-Tadbir, A., et al., *Upregulation of serum vascular endothelial growth factor and matrix metalloproteinase-3 in patients with oral squamous cell carcinoma.* Tumour Biol, 2014. **35**(6): p. 5689-93.
290. Zucker, S. and J. Vacirca, *Role of matrix metalloproteinases (MMPs) in colorectal cancer.* Cancer Metastasis Rev, 2004. **23**(1-2): p. 101-17.
291. Johnson, L.L., R. Dyer, and D.J. Hupe, *Matrix metalloproteinases.* Curr Opin Chem Biol, 1998. **2**(4): p. 466-71.
292. VanSaun, M., A.A. Herrera, and M.J. Werle, *Structural alterations at the neuromuscular junctions of matrix metalloproteinase 3 null mutant mice.* J Neurocytol, 2003. **32**(9): p. 1129-42.
293. Wiseman, B.S., et al., *Site-specific inductive and inhibitory activities of MMP-2 and MMP-3 orchestrate mammary gland branching morphogenesis.* J Cell Biol, 2003. **162**(6): p. 1123-33.
294. Lee, S., et al., *Processing of VEGF-A by matrix metalloproteinases regulates bioavailability and vascular patterning in tumors.* J Cell Biol, 2005. **169**(4): p. 681-91.
295. Miner, J.H., *Extracellular Matrix in Development and Disease*. 1st ed. Advances in Developmental Biology, ed. P.M. Wassarman. Vol. 15. 2005, Boston: Elsevier.
296. Page-McCaw, A., A.J. Ewald, and Z. Werb, *Matrix metalloproteinases and the regulation of tissue remodelling.* Nat Rev Mol Cell Biol, 2007. **8**(3): p. 221-33.
297. Bullard, K.M., et al., *Impaired wound contraction in stromelysin-1-deficient mice.* Ann Surg, 1999. **230**(2): p. 260-5.
298. Zheng, L., et al., *Matrix metalloproteinase-3 accelerates wound healing following dental pulp injury.* Am J Pathol, 2009. **175**(5): p. 1905-14.
299. Pilcher, B.K., et al., *Role of matrix metalloproteinases and their inhibition in cutaneous wound healing and allergic contact hypersensitivity.* Ann N Y Acad Sci, 1999. **878**: p. 12-24.

300. Wang, M., et al., *Matrix metalloproteinase deficiencies affect contact hypersensitivity: stromelysin-1 deficiency prevents the response and gelatinase B deficiency prolongs the response.* Proc Natl Acad Sci U S A, 1999. **96**(12): p. 6885-9.
301. Girard, M.T., et al., *Stromal fibroblasts synthesize collagenase and stromelysin during long-term tissue remodeling.* J Cell Sci, 1993. **104 (Pt 4)**: p. 1001-11.
302. Ye, S., et al., *Progression of coronary atherosclerosis is associated with a common genetic variant of the human stromelysin-1 promoter which results in reduced gene expression.* J Biol Chem, 1996. **271**(22): p. 13055-60.
303. Wu, J.J., et al., *Sites of stromelysin cleavage in collagen types II, IX, X, and XI of cartilage.* J Biol Chem, 1991. **266**(9): p. 5625-8.
304. Nagase, H., *Matrix Metalloproteinase 3/Stromelysin 1*. 3rd ed. ed. Handbook of proteolytic enzymes, ed. G.S. Neil D. Rawlings. 2013, Boston: Academic Press.
305. Fowlkes, J.L., et al., *Matrix metalloproteinases degrade insulin-like growth factor-binding protein-3 in dermal fibroblast cultures.* Journal Biological Chemistry, 1994. **269**: p. 25742-25746.
306. Maeda, S., et al., *Activation of latent transforming growth factor beta1 by stromelysin 1 in extracts of growth plate chondrocyte-derived matrix vesicles.* Journal of Bone and Mineral Research, 2001. **16**(7): p. 1281-1290.
307. Mast, A.E., et al., *Kinetics and physiologic relevance of the inactivation of alpha 1-proteinase inhibitor, alpha 1-antichymotrypsin, and antithrombin III by matrix metalloproteinases-1 (tissue collagenase), -2 (72-kDa gelatinase/type IV collagenase), and -3 (stromelysin).* J Biol Chem, 1991. **266**(24): p. 15810-6.
308. Lijnen, H.R., B. Van Hoef, and D. Collen, *Inactivation of the serpin alpha(2)-antiplasmin by stromelysin-1.* Biochim Biophys Acta, 2001. **1547**(2): p. 206-13.
309. Enghild, J.J., et al., *Interaction of human rheumatoid synovial collagenase (matrix metalloproteinase 1) and stromelysin (matrix metalloproteinase 3) with human alpha 2-macroglobulin and chicken ovostatin. Binding kinetics and identification of matrix metalloproteinase cleavage sites.* J Biol Chem, 1989. **264**(15): p. 8779-85.
310. Flannery, C.R., M.W. Lark, and J.D. Sandy, *Identification of a stromelysin cleavage site within the interglobular domain of human aggrecan. Evidence for proteolysis at this site in vivo in human articular cartilage.* J Biol Chem, 1992. **267**(2): p. 1008-14.
311. Poe, M., R.L. Stein, and J.K. Wu, *High pressure gel-permeation assay for the proteolysis of human aggrecan by human stromelysin-1: kinetic constants for aggrecan hydrolysis.* Arch Biochem Biophys, 1992. **298**(2): p. 757-9.
312. Imai, K., et al., *Degradation of decorin by matrix metalloproteinases: identification of the cleavage sites, kinetic analyses and transforming growth factor-beta 1 release.* Biochemical Journal, 1997. **322**(Pt 3): p. 809-814.
313. Lochter, A., et al., *Matrix metalloproteinase stromelysin-1 triggers a cascade of molecular alterations that leads to stable epithelial-to-mesenchymal conversion and a premalignant phenotype in mammary epithelial cells.* J Cell Biol, 1997. **139**(7): p. 1861-72.
314. Noe, V., et al., *Release of an invasion promoter E-cadherin fragment by matrilysin and stromelysin-1.* J Cell Sci, 2001. **114**(Pt 1): p. 111-118.
315. Bini, A., et al., *Degradation of cross-linked fibrin by matrix metalloproteinase 3 (stromelysin 1): hydrolysis of the gamma Gly 404-Ala 405 peptide bond.* Biochemistry, 1996. **35**(40): p. 13056-63.
316. Bini, A., et al., *Characterization of stromelysin 1 (MMP-3), matrilysin (MMP-7), and membrane type 1 matrix metalloproteinase (MT1-MMP) derived fibrin(ogen) fragments D-dimer and D-like monomer: NH2-terminal sequences of late-stage digest fragments.* Biochemistry, 1999. **38**(42): p. 13928-36.

317. Zhang, X., et al., *A Comparative Study of Fibronectin Cleavage by MMP-1, -3, -13, and -14.* Cartilage, 2012. **3**(3): p. 267-77.
318. Suzuki, M., et al., *Matrix metalloproteinase-3 releases active heparin-binding EGF-like growth factor by cleavage at a specific juxtamembrane site.* J Biol Chem, 1997. **272**(50): p. 31730-7.
319. Fowlkes, J.L., et al., *MMPs are IGFBP-degrading proteinases: implications for cell proliferation and tissue growth.* Ann N Y Acad Sci, 1999. **878**: p. 696-9.
320. Schonbeck, U., F. Mach, and P. Libby, *Generation of biologically active IL-1 beta by matrix metalloproteinases: a novel caspase-1-independent pathway of IL-1 beta processing.* Journal of Immunology, 1998. **161**(7): p. 3340-3346.
321. McQuibban, G.A., et al., *Matrix metalloproteinase processing of monocyte chemoattractant proteins generates CC chemokine receptor antagonists with anti-inflammatory properties in vivo.* Blood, 2002. **100**(4): p. 1160-7.
322. Mayer, U., et al., *Sites of nidogen cleavage by proteases involved in tissue homeostasis and remodelling.* Eur J Biochem, 1993. **217**(3): p. 877-84.
323. Agnihotri, R., et al., *Osteopontin, a novel substrate for matrix metalloproteinase-3 (stromelysin-1) and matrix metalloproteinase-7 (matrilysin).* Journal Biological Chemistry, 2001. **276**(30): p. 28261-28267.
324. Whitelock, J.M., et al., *The degradation of human endothelial cell-derived perlecan and release of bound basic fibroblast growth factor by stromelysin, collagenase, plasmin, and heparanases.* J Biol Chem, 1996. **271**(17): p. 10079-86.
325. Lijnen, H.R., et al., *Generation of an angiostatin-like fragment from plasminogen by stromelysin-1 (MMP-3).* Biochemistry, 1998. **37**(14): p. 4699-702.
326. Lijnen, H.R., et al., *Inactivation of plasminogen activator inhibitor-1 by specific proteolysis with stromelysin-1 (MMP-3).* J Biol Chem, 2000. **275**(48): p. 37645-50.
327. Suzuki, K., et al., *Mechanisms of activation of tissue procollagenase by matrix metalloproteinase 3 (stromelysin).* Biochemistry, 1990. **29**(44): p. 10261-70.
328. Nagase, H., et al., *Stepwise activation mechanisms of the precursor of matrix metalloproteinase 3 (stromelysin) by proteinases and (4-aminophenyl)mercuric acetate.* Biochemistry, 1990. **29**(24): p. 5783-9.
329. Knauper, V., G. Murphy, and H. Tschesche, *Activation of human neutrophil procollagenase by stromelysin 2.* Eur J Biochem, 1996. **235**(1-2): p. 187-91.
330. Ogata, Y., J.J. Enghild, and H. Nagase, *Matrix metalloproteinase 3 (stromelysin) activates the precursor for the human matrix metalloproteinase 9.* J Biol Chem, 1992. **267**(6): p. 3581-4.
331. Gearing, A.J., et al., *Matrix metalloproteinases and processing of pro-TNF-alpha.* J Leukoc Biol, 1995. **57**(5): p. 774-7.
332. McQuibban, G.A., et al., *Matrix metalloproteinase activity inactivates the CXC chemokine stromal cell-derived factor-1.* J Biol Chem, 2001. **276**(47): p. 43503-8.
333. Stix, B., et al., *Proteolysis of AA amyloid fibril proteins by matrix metalloproteinases-1, -2, and -3.* Am J Pathol, 2001. **159**(2): p. 561-70.
334. Teahan, J., et al., *Substrate specificity of human fibroblast stromelysin. Hydrolysis of substance P and its analogues.* Biochemistry, 1989. **28**(21): p. 8497-501.
335. Ugwu, F., et al., *Proteolytic cleavage of urokinase-type plasminogen activator by stromelysin-1 (MMP-3).* Biochemistry, 1998. **37**(20): p. 7231-6.
336. Aviezer, D., et al., *Perlecan, basal lamina proteoglycan, promotes basic fibroblast growth factor-receptor binding, mitogenesis, and angiogenesis.* Cell, 1994. **79**(6): p. 1005-13.
337. Mongiat, M., et al., *Fibroblast growth factor-binding protein is a novel partner for perlecan protein core.* J Biol Chem, 2001. **276**(13): p. 10263-71.

338. Decoster, E., et al., *Generation and biological characterization of membrane-bound, uncleavable murine tumor necrosis factor.* J Biol Chem, 1995. **270**(31): p. 18473-8.
339. Tanaka, M., et al., *Downregulation of Fas ligand by shedding.* Nat Med, 1998. **4**(1): p. 31-6.
340. Tanaka, M., et al., *Expression of the functional soluble form of human fas ligand in activated lymphocytes.* EMBO J, 1995. **14**(6): p. 1129-35.
341. Vargo-Gogola, T., et al., *Identification of novel matrix metalloproteinase-7 (matrilysin) cleavage sites in murine and human Fas ligand.* Archives of Biochemistry and Biophysics, 2002. **408**(2): p. 155-161.
342. Garcia, A.J., et al., *ERalpha signaling regulates MMP3 expression to induce FasL cleavage and osteoclast apoptosis.* J Bone Miner Res, 2013. **28**(2): p. 283-90.
343. Weber, G.F. and H. Cantor, *The immunology of Eta-1/osteopontin.* Cytokine Growth Factor Rev, 1996. **7**(3): p. 241-8.
344. Denhardt, D.T., et al., *Osteopontin-induced modifications of cellular functions.* Ann N Y Acad Sci, 1995. **760**: p. 127-42.
345. Vagima, Y., et al., *Pathways implicated in stem cell migration: the SDF-1/CXCR4 axis.* Methods Mol Biol, 2011. **750**: p. 277-89.
346. Correia, A.L., et al., *The hemopexin domain of MMP3 is responsible for mammary epithelial invasion and morphogenesis through extracellular interaction with HSP90beta.* Genes Dev, 2013. **27**(7): p. 805-17.
347. Sternlicht, M.D., M.J. Bissell, and Z. Werb, *The matrix metalloproteinase stromelysin-1 acts as a natural mammary tumor promoter.* Oncogene, 2000. **19**(8): p. 1102-13.
348. Radisky, D.C., et al., *Rac1b and reactive oxygen species mediate MMP-3-induced EMT and genomic instability.* Nature, 2005. **436**(7047): p. 123-7.
349. Sternlicht, M.D., et al., *The stromal proteinase MMP3/stromelysin-1 promotes mammary carcinogenesis.* Cell, 1999. **98**(2): p. 137-46.
350. Radisky, D.C. and J.A. Przybylo, *Matrix metalloproteinase-induced fibrosis and malignancy in breast and lung.* Proc Am Thorac Soc, 2008. **5**(3): p. 316-22.
351. Robichaud, N., et al., *Phosphorylation of eIF4E promotes EMT and metastasis via translational control of SNAIL and MMP-3.* Oncogene, 2015. **34**(16): p. 2032-42.
352. Banik, D., et al., *MMP3-mediated tumor progression is controlled transcriptionally by a novel IRF8-MMP3 interaction.* Oncotarget, 2015. **6**(17): p. 15164-79.
353. Stallings-Mann, M.L., et al., *Matrix metalloproteinase induction of Rac1b, a key effector of lung cancer progression.* Sci Transl Med, 2012. **4**(142): p. 142ra95.
354. Sun, P., Y. Mu, and S. Zhang, *A novel NF-kappaB/MMP-3 signal pathway involves in the aggressivity of glioma promoted by Bmi-1.* Tumour Biol, 2014. **35**(12): p. 12721-7.
355. Pollak, M., *Insulin and insulin-like growth factor signalling in neoplasia.* Nat Rev Cancer, 2008. **8**(12): p. 915-28.
356. Heidegger, I., et al., *Oncogenic functions of IGF1R and INSR in prostate cancer include enhanced tumor growth, cell migration and angiogenesis.* Oncotarget, 2014. **5**(9): p. 2723-35.
357. Fowlkes, J.L., et al., *Insulin-like growth factor binding protein (IGFBP) substrate zymography. A new tool to identify and characterize IGFBP-degrading proteinases.* Endocrine, 1997. **7**(1): p. 33-6.
358. Cheng, K., G. Xie, and J.P. Raufman, *Matrix metalloproteinase-7-catalyzed release of HB-EGF mediates deoxycholyltaurine-induced proliferation of a human colon cancer cell line.* Biochem Pharmacol, 2007. **73**(7): p. 1001-12.
359. Kivisaari, A.K., et al., *Matrix metalloproteinase-7 activates heparin-binding epidermal growth factor-like growth factor in cutaneous squamous cell carcinoma.* Br J Dermatol, 2010. **163**(4): p. 726-35.

360. Balkwill, F., *TNF-alpha in promotion and progression of cancer.* Cancer Metastasis Rev, 2006. **25**(3): p. 409-16.
361. Kulbe, H., et al., *The inflammatory cytokine tumor necrosis factor-alpha regulates chemokine receptor expression on ovarian cancer cells.* Cancer Res, 2005. **65**(22): p. 10355-62.
362. Thiolloy, S., et al., *Osteoclast-derived matrix metalloproteinase-7, but not matrix metalloproteinase-9, contributes to tumor-induced osteolysis.* Cancer Res, 2009. **69**(16): p. 6747-55.
363. Rittling, S.R. and D.T. Denhardt, *Osteopontin function in pathology: lessons from osteopontin-deficient mice.* Exp Nephrol, 1999. **7**(2): p. 103-13.
364. McCawley, L.J., et al., *A protective role for matrix metalloproteinase-3 in squamous cell carcinoma.* Cancer Res, 2004. **64**(19): p. 6965-72.
365. Witty, J.P., et al., *Decreased tumor formation in 7,12-dimethylbenzanthracene-treated stromelysin-1 transgenic mice is associated with alterations in mammary epithelial cell apoptosis.* Cancer Res, 1995. **55**(7): p. 1401-6.
366. Farina, A.R., et al., *Inhibition of human MDA-MB-231 breast cancer cell invasion by matrix metalloproteinase 3 involves degradation of plasminogen.* Eur J Biochem, 2002. **269**(18): p. 4476-83.
367. Brummer, O., et al., *Matrix-metalloproteinases 1, 2, and 3 and their tissue inhibitors 1 and 2 in benign and malignant breast lesions: an in situ hybridization study.* Virchows Arch, 1999. **435**(6): p. 566-73.
368. Fujimoto, H., et al., *Stromal MCP-1 in mammary tumors induces tumor-associated macrophage infiltration and contributes to tumor progression.* Int J Cancer, 2009. **125**(6): p. 1276-84.
369. Ueno, T., et al., *Significance of macrophage chemoattractant protein-1 in macrophage recruitment, angiogenesis, and survival in human breast cancer.* Clin Cancer Res, 2000. **6**(8): p. 3282-9.
370. Lejeune, F.J., *Clinical use of TNF revisited: improving penetration of anti-cancer agents by increasing vascular permeability.* J Clin Invest, 2002. **110**(4): p. 433-5.
371. van Horssen, R., T.L. Ten Hagen, and A.M. Eggermont, *TNF-alpha in cancer treatment: molecular insights, antitumor effects, and clinical utility.* Oncologist, 2006. **11**(4): p. 397-408.
372. LaTulippe, E., et al., *Comprehensive gene expression analysis of prostate cancer reveals distinct transcriptional programs associated with metastatic disease.* Cancer Res, 2002. **62**(15): p. 4499-506.
373. Liu, P., et al., *Sex-determining region Y box 4 is a transforming oncogene in human prostate cancer cells.* Cancer Res, 2006. **66**(8): p. 4011-9.
374. Welsh, J.B., et al., *Analysis of gene expression identifies candidate markers and pharmacological targets in prostate cancer.* Cancer Res, 2001. **61**(16): p. 5974-8.
375. Zhu, F., et al., *Eotaxin-1 promotes prostate cancer cell invasion via activation of the CCR3-ERK pathway and upregulation of MMP-3 expression.* Oncol Rep, 2014. **31**(5): p. 2049-54.
376. Slavin, S., et al., *Estrogen receptor alpha in cancer-associated fibroblasts suppresses prostate cancer invasion via modulation of thrombospondin 2 and matrix metalloproteinase 3.* Carcinogenesis, 2014. **35**(6): p. 1301-9.
377. Pollard, M. and P.H. Luckert, *Transplantable metastasizing prostate adenocarcinomas in rats.* Journal of the National Cancer Institute, 1975. **54**(3): p. 643-9.
378. Koutsilieris, M., *PA-III rat prostate adenocarcinoma cells (review).* In Vivo, 1992. **6**(2): p. 199-203.
379. Hemers, E., et al., *Insulin-like growth factor binding protein-5 is a target of matrix metalloproteinase-7: implications for epithelial-mesenchymal signaling.* Cancer Res, 2005. **65**(16): p. 7363-9.

380. Dean, R.A., et al., *Identification of candidate angiogenic inhibitors processed by matrix metalloproteinase 2 (MMP-2) in cell-based proteomic screens: disruption of vascular endothelial growth factor (VEGF)/heparin affin regulatory peptide (pleiotrophin) and VEGF/Connective tissue growth factor angiogenic inhibitory complexes by MMP-2 proteolysis.* Mol Cell Biol, 2007. **27**(24): p. 8454-65.
381. Larsen, P.H., et al., *Myelin formation during development of the CNS is delayed in matrix metalloproteinase-9 and -12 null mice.* J Neurosci, 2006. **26**(8): p. 2207-14.
382. Heidegger, I., et al., *The insulin-like growth factor (IGF) axis as an anticancer target in prostate cancer.* Cancer Lett, 2015. **367**(2): p. 113-21.
383. Eisenach, P.A., et al., *MT1-MMP regulates VEGF-A expression through a complex with VEGFR-2 and Src.* J Cell Sci, 2010. **123**(Pt 23): p. 4182-93.
384. Yu, Q., et al., *Erythropoietin combined with granulocyte colonystimulating factor enhances MMP-2 expression in mesenchymal stem cells and promotes cell migration.* Mol Med Rep, 2011. **4**(1): p. 31-6.
385. Guntur, A.R. and C.J. Rosen, *IGF-1 regulation of key signaling pathways in bone.* Bonekey Rep, 2013. **2**: p. 437.
386. Sutherland, B.W., et al., *Conditional deletion of insulin-like growth factor-I receptor in prostate epithelium.* Cancer Res, 2008. **68**(9): p. 3495-504.
387. Guise, T.A., *The vicious cycle of bone metastases.* J Musculoskelet Neuronal Interact, 2002. **2**(6): p. 570-2.
388. Chen, Y.C., D.M. Sosnoski, and A.M. Mastro, *Breast cancer metastasis to the bone: mechanisms of bone loss.* Breast Cancer Res, 2010. **12**(6): p. 215.
389. Wu, J. and E. Yu, *Insulin-like growth factor receptor-1 (IGF-IR) as a target for prostate cancer therapy.* Cancer Metastasis Rev, 2014. **33**(2-3): p. 607-17.
390. Gupta, G.P. and J. Massague, *Cancer metastasis: building a framework.* Cell, 2006. **127**(4): p. 679-95.
391. www.cancer.gov, *Prostate Specific Antigen (PSA) Test.* National Cancer Institute, 2017.
392. Barry, M.J., *Clinical practice. Prostate-specific-antigen testing for early diagnosis of prostate cancer.* N Engl J Med, 2001. **344**(18): p. 1373-7.
393. Roy, R., J. Yang, and M.A. Moses, *Matrix metalloproteinases as novel biomarkers and potential therapeutic targets in human cancer.* J Clin Oncol, 2009. **27**(31): p. 5287-97.
394. Ranuncolo, S.M., et al., *Plasma MMP-9 (92 kDa-MMP) activity is useful in the follow-up and in the assessment of prognosis in breast cancer patients.* Int J Cancer, 2003. **106**(5): p. 745-51.
395. Selye, H., *On the stimulation of new bone formation with parathyroid extract and irradiated ergosterol.* Endocrinology, 1932. **16**(5): p. 547-558.
396. Horwitz, M.J., et al., *A comparison of parathyroid hormone-related protein (1-36) and parathyroid hormone (1-34) on markers of bone turnover and bone density in postmenopausal women: the PrOP study.* J Bone Miner Res, 2013. **28**(11): p. 2266-76.
397. Hajime, M., et al., *A case of teriparatide-induced severe hypophosphatemia and hypercalcemia.* J Bone Miner Metab, 2014. **32**(5): p. 601-4.
398. Karatoprak, C., et al., *Severe hypercalcemia due to teriparatide.* Indian J Pharmacol, 2012. **44**(2): p. 270-1.
399. Rogers, M.J., et al., *Biochemical and molecular mechanisms of action of bisphosphonates.* Bone, 2011. **49**(1): p. 34-41.
400. De Wit R, F.K., Jinga V, Efstathiou E, Fong PCC, Wirth M, Suzuki K, Moran S, Wang L, Akaza H, Nelson J, Scher HI, Dreicer R, Borgstein NG, Saad F, *Phase 3, randomized, placebo-controlled trial of orteronel (TAK-700) plus prednisone in patients with chemotherapy-naive metastatic*

castration-resistant prostate cancer (mCRPC) (ELM-PC4 trial). Journal of Clinical Oncology, 2014. **32 (suppl 5, abstr 5008)**.

401. Dreicer R, J.R., Oudard S, Efstathiou E, Saad F, De Wit R, De Bono JS, Shi Y, Tejura B, Agus DB, Borgstein NG, Bellmunt J, Fizazi K, *Results from a phase 3, randomized, double-blind, multicenter, placebo-controlled trial of orteronel (TAK-700) plus prednisone in patients with metastatic castration-resistant prostate cancer (mCRPC) that has progressed during or following docetaxel-based therapy (ELM-PC5 trial).* Journal of Clinical Oncology, 2014. **32 (suppl 4; abstr 7)**.
402. Slovin, S.F., et al., *Ipilimumab alone or in combination with radiotherapy in metastatic castration-resistant prostate cancer: results from an open-label, multicenter phase I/II study.* Ann Oncol, 2013. **24**(7): p. 1813-21.
403. Gerritsen, W.R. and P. Sharma, *Current and emerging treatment options for castration-resistant prostate cancer: a focus on immunotherapy.* J Clin Immunol, 2012. **32**(1): p. 25-35.
404. Topalian, S.L., et al., *Safety, activity, and immune correlates of anti-PD-1 antibody in cancer.* N Engl J Med, 2012. **366**(26): p. 2443-54.
405. Gulley, J.L., et al., *Immunologic and prognostic factors associated with overall survival employing a poxviral-based PSA vaccine in metastatic castrate-resistant prostate cancer.* Cancer Immunol Immunother, 2010. **59**(5): p. 663-74.
406. Smith, D.C., et al., *Cabozantinib in patients with advanced prostate cancer: results of a phase II randomized discontinuation trial.* J Clin Oncol, 2013. **31**(4): p. 412-9.
407. Osanto, S., H. van Poppel, and J. Burggraaf, *Tasquinimod: a novel drug in advanced prostate cancer.* Future Oncol, 2013. **9**(9): p. 1271-81.
408. Saad, F., et al., *Randomized phase II trial of Custirsen (OGX-011) in combination with docetaxel or mitoxantrone as second-line therapy in patients with metastatic castrate-resistant prostate cancer progressing after first-line docetaxel: CUOG trial P-06c.* Clin Cancer Res, 2011. **17**(17): p. 5765-73.

Appendices

Appendix A

RE: permission to use review article in dissertation

Nemeth, Veronica
Sent: Monday, March 13, 2017 3:14 PM
To: Frieling, Jeremy S.

That would be me & I grant you permission – of course just be sure to cite your article as the source & that permission was granted by CCJ. Roni

Veronica E. Nemeth
Editorial Coordinator
Moffitt Cancer Center

Cancer Control Journal, Intellicenter/Moffitt Business Center, 3rd Floor, 12653 Telecom Park Drive, Temple Terrace, FL 33637
| tel: 813-745-1348 **| Right Fax (direct to computer):** 813-449-8680 **| email:** Veronica.Nemeth@Moffitt.org **| Web site:** http://www.cancercontroljournal.org

From: Frieling, Jeremy S.
Sent: Monday, March 13, 2017 3:05 PM
To: Nemeth, Veronica
Subject: permission to use review article in dissertation

Dear Veronica,

I would like to use excerpts from the review article I wrote with Dr. Lynch (Current and emerging therapies for bone metastatic castration-resistant prostate cancer., January 2015 issue) in my PhD dissertation. Who would be the appropriate contact to request copyright permission to do this? Thanks for your help!

Sincerely,
Jeremy Frieling

Jeremy Frieling
Graduate Student in the Lynch Lab
Moffitt Cancer Center

12902 Magnolia Drive, Tampa, FL 33612 | **tel:** 813-745-5708| **email:** Jeremy.Frieling@moffitt.org

Appendix B

EXT: RE: permission to use our article in PhD dissertation

Journalpermissions [journalpermissions@springernature.com]
Sent: Friday, March 24, 2017 7:46 AM
To: Frieling, Jeremy S.

Dear Jeremy,

Thank you for contacting Springer Nature. As an author, you will have the right to use this manuscript and figures, as per the licence-to-publish you signed:
Ownership of copyright in the article remains with the Authors, and provided that, when reproducing the Contribution or extracts from it, the Authors acknowledge first and reference publication in the Journal, the Authors retain the following non-exclusive rights:

a) To reproduce the Contribution in whole or in part in any printed volume (book or thesis) of which they are the author(s).
b) They and any academic institution where they work at the time may reproduce the Contribution for the purpose of course teaching.
c) To post a copy of the Contribution as accepted for publication after peer review (in Word or Tex format) on the Authors' own web site or institutional repository, or the Authors' funding body's designated archive, six months after publication of the printed or online edition of the Journal, provided that they also give a hyperlink from the Contribution to the Journals web site.
d) To reuse figures or tables created by them and contained in the Contribution in other works created by them.

The above use of the term 'Contribution' refers to the author's own version, not the final version as published in the Journal.

Please note that you will have to wait until after the article is published to reuse it.

Kind regards,

Angelika Dalba
Rights Assistant

SpringerNature
The Campus, 4 Crinan Street, London N1 9XW, United Kingdom
T +44-207-014-6891

From: Frieling, Jeremy S. [mailto:Jeremy.Frieling@moffitt.org]
Sent: Wednesday, March 22, 2017 11:10 AM
To: oncogene
Subject: permission to use our article in PhD dissertation

Dear Oncogene Editorial Office,

I am writing to request permission to use excerpts from an article recently accepted to Oncogene in my PhD thesis:

"Matrix Metalloproteinase Processing of PTHrP Yields a Selective Regulator of Osteogenesis, PTHrP1-17" by Conor Lynch, Jeremy Frieling, Gemma Shay, Victoria Izumi, Sinead Aherne, Richard Saul, Mikalai Budzevich, and John Koomen [Paper #ONC-2016-02029R]

I realize that the normal procedure is to use Advanced Search and Rightslink, however our article has not been indexed yet. Is it possible to request permission directly? Thank you for your help!

Sincerely,
Jeremy Frieling

[MOFFITT_2c_RGB for signature]

Jeremy Frieling
Graduate Student in the Lynch Lab
Moffitt Cancer Center

12902 Magnolia Drive, Tampa, FL 33612 | tel: 813-745-5708| email: Jeremy.Frieling@moffitt.org

Please consider the environment before printing this email.